



Dedicated to innovation in aerospace



Rijksinstituut voor Volksgezondheid  
en Milieu  
Ministerie van Volksgezondheid,  
Welzijn en Sport

PUBLIC

NLR-CR-2021-232-RevEd-1 | July 2021

# CORSICA final report

Quantitative microbial risk assessment for aerosol transmission of SARS-CoV-2 in aircraft cabins based on measurement and simulations

CUSTOMER: Ministry of Infrastructure and Water Management

Royal NLR – Netherlands Aerospace Centre  
RIVM – National Institute for Public Health and the Environment

## CORSICA final report

### Quantitative microbial risk assessment for aerosol transmission of SARS-CoV-2 in aircraft cabins based on measurement and simulations

#### Problem area

The coronavirus pandemic is an ongoing global epidemic of coronavirus disease 2019 (COVID-19). The disease was first identified in December 2019 in Wuhan, China. The outbreak was declared a Public Health Emergency of International Concern in January 2020, and a pandemic in March 2020. As of April 2021, more than 145 million cases have been confirmed as well as more than 3 million deaths attributed to COVID-19. COVID-19 is caused by the severe acute respiratory syndrome coronavirus 2 (SARS-CoV-2).

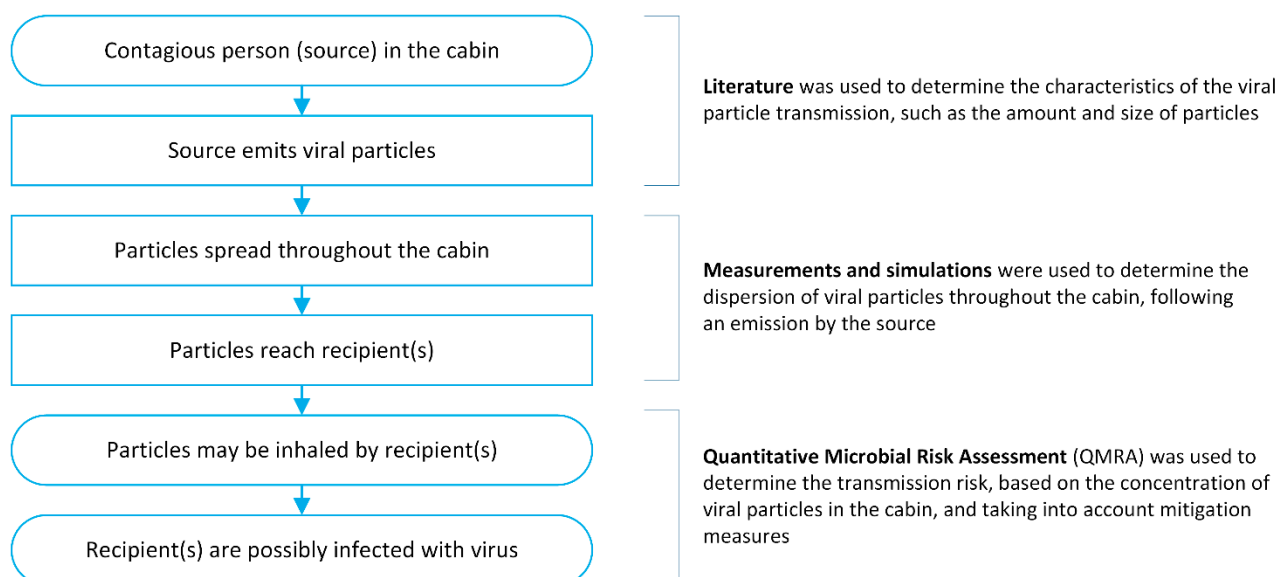
The role of modern transportation in the rapid spread of pathogens such as SARS-CoV-2 over long distances is a growing concern. However, **little is known about the transmission of SARS-CoV-2 in the cabins of aircraft**. This makes effective decision and policy making by travellers, airlines and authorities more difficult.

#### Research outline

**Tasked by the Ministry of Infrastructure and Water Management, Royal NLR – Netherlands Aerospace Centre and the National Institute for Public Health and the Environment (RIVM) have scientifically assessed the risk of illness from inhalation of aerosolised SARS-CoV-2 particles shed by an infectious passenger (referred to as index passenger) in an aircraft cabin.** Other transmission routes than transmission via inhalation of aerosolised particles with diameters from 0.5 to 20.0  $\mu\text{m}$  (after initial evaporation) have not been considered.

In the study, it was assumed that mitigation measures currently (first week of June, 2021) applied by the Dutch aviation sector are complied with. These include discouraging of unnecessary travel, a health declaration and negative coronavirus test result, more frequent aircraft cleaning, improved hand, coughing and sneezing hygiene, the use of face masks and reduced in-flight service. Similar to what holds for 99.1% of all commercial passenger flights operating to and from airports in The Netherlands, the aircraft types assessed in this study were equipped with HEPA filters.

The study was based on data from literature, particle dispersion measurements and simulations and included a quantitative microbial risk assessment (QMRA). The following figure summarises the interrelation between these parts.



**The study investigated three aircraft types commonly used at Amsterdam Airport Schiphol, in two size classes.** Two single-aisle aircraft (Airbus A320 and Boeing 737-800) were investigated, which are typically used for shorter-distance flights, such as within Europe, and seat some 200 passengers. One larger twin-aisle aircraft (Boeing 787-8) was investigated, which is operated longer on intercontinental flights, and has a higher seating capacity. Particle dispersion in these aircraft was studied using measurements in and simulations of (the latter for Airbus A320 and Boeing 787-8 only) a 7-row economy-class cabin section. **The results of the literature study highlighted the relevance of both cruise and taxi phase, thus both were investigated.** The cruise flight situation was studied by both measurements and simulations, the latter of which allowed to also investigate the effect of the seating positions of the index passenger within a row. Measurements in non-moving aircraft on the ground were conducted to evaluate the risk in a taxi scenario.

### Cabin environmental conditions

Measurements to characterise the cabin environmental conditions – temperature, relative humidity and air flow – were conducted to gather input for the simulation work. Temperature was found to vary between 19 °C and 24 °C, mostly converging to values between 21 and 22 °C over time. Relative humidity was found to be low, especially in the cruise phase, where it converged to approximately 10%. In all aircraft, a rearward flow was observed. Literature notes cabin air exchange rates between 10 and 30 times per hour.

### Source

Information from literature was used to characterise aerosolised viral emission, distinguishing between virus emission that can be considered regular or high. For a regular index passenger, the viral concentration in the mucus of the index was assumed to follow a lognormal distribution with a mean of 7.53 and standard deviation of 1.28 RNA copies / mL (i.e. an average shedding level of  $10^{7.5}$  RNA copies / mL). For a passenger who shed a high number of infectious virus particles (a so-called super shedder), emission with a concentration of  $10^{10}$  RNA copies / mL was assumed. That meant that a super shedder, on average, emitted 300 times as many RNA copies/mL as the regular shedder. Total aerosol emission volumes for breathing (assumed to occur 80% of the time) and speaking (20% of the time) were taken from literature.

In the in-cabin particle dispersion measurements, the source was represented by a manikin-mounted nozzle, connected to an aerosol pump. Artificial saliva was injected into the cabin from this nozzle. For the particle dispersion

simulations, the aerosols emitted by an index passenger were modelled to start from a 10-centimetre diameter sphere, located 10 centimetres in front of the index passenger.

## Particle dispersion

In addition to the measurements investigating cabin environmental conditions, simultaneous measurements on particle dispersion were conducted. To this effect, manikins (optionally heated, to represent normal passenger heat emission) were placed in the seats in the 7-row cabin section under investigation. Following emission of artificial saliva by the source, particle sensing equipment was used to detect aerosol particle numbers and size throughout the cabin section investigated. Particulate matter sensors were placed on all manikins and two aerodynamic particle sizers were positioned in two strategic locations. Measurements were conducted under a variety of conditions, in order to cover the impact of a large number of variables: cruise and taxi condition, use of gaspers (passenger-controlled air inlets), index passenger mask usage, manikin heating (only in taxi condition), pack setting and index location (only in Boeing 787-8). Additional manikins and particulate matter sensors, placed further away from the index passenger, were furthermore used in the single-aisle aircraft measurements to assess the possible recirculation of aerosols using the cabin ventilation system.

Dispersion of aerosols was simulated across seven rows of passengers in a ventilated aircraft cabin. A Reynolds-averaged Navier-Stokes (RANS) method was used to model the air flow and the dispersion of particles, taking into account the cabin configuration of the aircraft types studied, cabin environmental conditions, ventilation system properties and buoyancy effects due to heat sources inside the cabin. Cabin environmental conditions, air inflow, heat source and thermal conditions were modelled using a combination of measurement results, aircraft specifications and literature. Following the introduction of particles into the simulation, their trajectories were modelled, influenced by the air flow and gravity. The number, volume and residence time of particles entering a 30 × 30 × 30 centimetre 'inhalation box' was logged and subsequently used as input for the risk assessment.

Cross-checks between measurement data and simulation output of the Airbus A320 and Boeing 787-8 yielded similar aerosol dispersion per row. Both measurement and simulation data showed a predominantly rearward dispersion of aerosols, especially for the single aisle aircraft, consistent with the earlier observation of a rearward flow.

Mask usage by the index passenger was shown to clearly reduce the number and volume of aerosols detected after emission by the index. Effects of gasper settings and index location on particle dispersion were variable and limited. During the measurement runs, large quantities of aerosols were injected at the start of each run. Only very low volumes of aerosols were detected in two rows further in front of the seven-row section that was investigated. This suggests that, at least in the rear section of the economy class, **recirculation of aerosols from the HEPA-filter-equipped cabin ventilation system does not, or only to a very limited extent, occur.**

## Risk assessment

Using the experimental and simulated particle dispersion results and literature on virus shedding, dose-response (the effect a certain dose has on a person) and face mask effectiveness, a QMRA was conducted in order to estimate risk of illness. For that purpose, measured and simulated aerosol concentrations were converted to transferred fractions: the fraction of the emitted source that would be inhaled by a passenger located at a particular seat. Variability in exposure conditions was taken into account by considering distributions of exposure factors, such as inhalation rate, aerosol volume emitted by the index passenger and virus concentration in sputum. A Monte Carlo simulation was conducted based on these distributions, yielding a dose and risk of illness.

## Conclusions

For a typical cruise flight (ranging between 0.9 hour for the single-aisle Airbus A320 and 8.7 hours for the twin-aisle Boeing 787-8), **mean risk for COVID-19 due to inhalation of aerosolised SARS-CoV-2 particles were estimated to be in the range of 1/1800 to 1/120 amongst the passengers seated in the seven rows around the index passenger.** In the case of a super shedder, mean risks increased up to 1/16. **These findings were found to be in line with other model and measurement studies on in-flight illness risk. Risks increased with increasing flight duration: a flight on a single-aisle aircraft was found to result in lower risks than a flight on a twin-aisle aircraft.** Outside these seven rows the risk was not assessed, but based on decreasing risks with increasing distance to the index passenger, it was assumed that no illness occurred outside these seven rows.

**The expected number of flights to result in at least 1 case of COVID-19 due to transmission of aerosols containing the SARS-CoV-2 virus from a 'regular' virus shedding passenger was estimated to range from 2 to 44 cruise flights of durations typical for the aircraft types in the study. In case of cruise flights with longer durations, the expected number of flights ranged from 2 to 19.** The expected number of flights to result in at least 1 case of aerosol transmission from a 'super shedder' passenger was estimated to range from 1 to 9 flights (typical duration cruise) and 1 to 4 flights (longer duration cruise).

Estimates on the likelihood of one infectious passenger boarding an aircraft will be inaccurate and can change rapidly. Assuming 5% false negative results by pre-travel testing (OMT89), 5% of the number of infected persons in the Netherlands might board while shedding virus (at June 7<sup>th</sup>, 2021, that will be less than 30 per 100,000 passengers). Depending on the number of passengers per aircraft (100 – 300), every 11 – 33 flights is estimated to include an infectious passenger and less than 3% of these could be a super shedder.

Statistical analysis of the measurement data revealed that distance and angle relative to the virus shedding passenger highly significantly affected risk (i.e., decreasing risk with increasing distance, and this decrease was not the same in all directions), which is consistent with simulation results. The effect of wearing a mask by all passengers as included in the risk assessment was based on data from literature. **The experimental data suggested that a face mask reduced emission of the larger aerosols and altered the direction of the emitted aerosols. More data is required to validate these findings.**

Major sources of high variability of the risk estimates based on measurement and simulation data were the viral concentration in the aerosols and the volume of aerosol emitted by the virus shedding passenger. Their variation has an impact of over an order of magnitude ( $\times 10$  or more) on the risk. The flight duration, and the efficiency of masks to limit aerosol emission and inhalation had a direct proportional effect on the risks, but the variation resulting from these aspects was smaller than an order of magnitude (i.e., less than  $\times 10$ ).

## Applicability

The study assumed compliance with EASA and ICAO-recommended best practices, such as wearing face masks<sup>1</sup> in the cabin, except when drinking or eating (assumed to occur 10% of the time). The study addressed the risk of transmission on board of an aircraft via inhalation of virus bearing aerosols if one infectious passenger (index) was present in the cabin, based on the study of one of each of the three common aircraft types used for commercial passenger transport. **The study results cannot be used to assess the risk for a single passenger on a particular flight, and can also not be used in general to classify particular seat positions according to higher or lower levels of risk.**

<sup>1</sup> A previous version of the report incorrectly stated EASA and ICAO explicitly recommend using **non-medical** facemasks in the aircraft cabin

## CORSICA eindrapport

### Kwantitatieve microbiologische risicoschatting van verspreiding van SARS-CoV-2 via aerosolen in vliegtuigcabines op basis van metingen en simulaties

#### Probleemstelling

De coronaviruspandemie is een wereldwijde pandemie van *coronavirus disease 2019* (COVID-19). De ziekte werd voor het eerst geïdentificeerd in december 2019 in Wuhan, China. De uitbraak werd in januari 2020 geclassificeerd als internationale noodsituatie (*Public Health Emergency of International Concern*) en als pandemie in maart 2020. Sinds april 2021 zijn er meer dan 145 miljoen gevallen van COVID-19 bevestigd en zijn er meer dan 3 miljoen doden aan de ziekte toegeschreven. COVID-19 wordt veroorzaakt door het *severe acute respiratory syndrome coronavirus 2* (SARS-CoV-2).

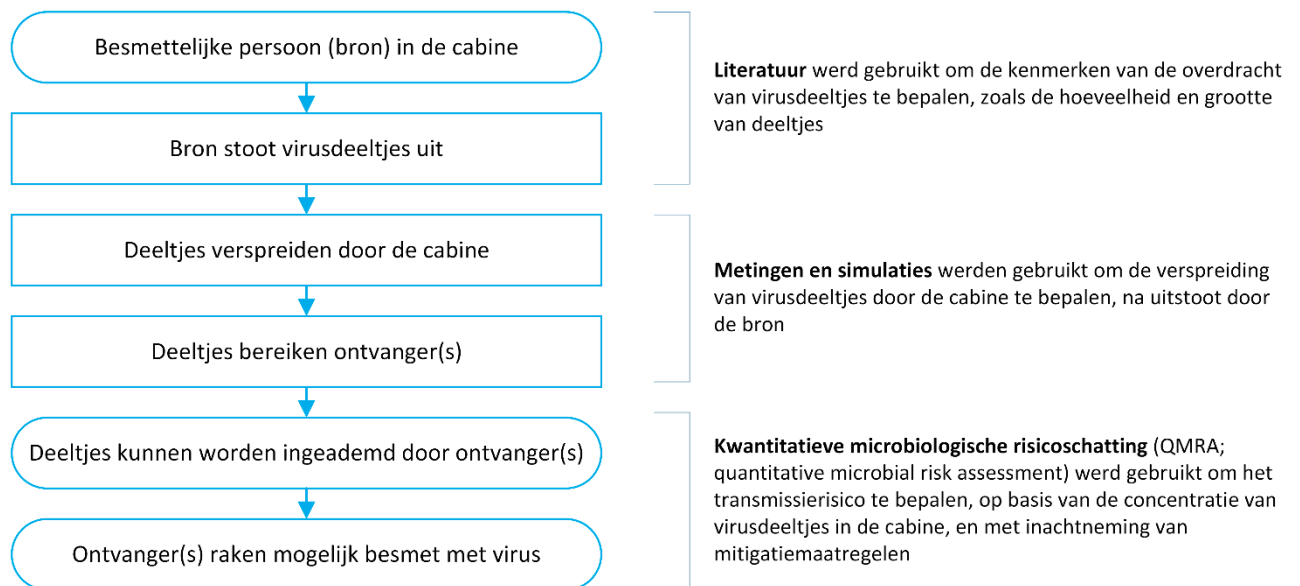
De rol van modern transport in de snelle verspreiding van ziekteverwekkers als SARS-CoV-2 over lange afstanden is een groeiende zorg. **Er is echter weinig bekend over de verspreiding van SARS-CoV-2 in vliegtuigcabines.** Dit maakt effectieve besluit- en beleidsvorming door reizigers, luchtvaartmaatschappijen en autoriteiten moeilijker.

#### Onderzoeksbeschrijving

**In opdracht van het Ministerie van Infrastructuur en Waterstaat hebben Koninklijke NLR – Nederlands Lucht- en Ruimtevaartcentrum en het Rijksinstituut voor Volksgezondheid en Milieu (RIVM) het risico op ziekte als gevolg van inademing van geaërosoliseerde SARS-CoV-2 deeltjes uitgestoten door een infectueuze passagier (hierna omschreven als indexpassagier) in een vliegtuigcabine wetenschappelijk beoordeeld.** Andere transmissieroutes dan verspreiding van geaërosoliseerde deeltjes met diameters van 0.5 tot 20.0  $\mu\text{m}$  (na initiële verdamping) zijn niet onderzocht.

In de studie is aangenomen dat mitigatiemaatregelen zoals momenteel (eerste week van juni, 2021) toegepast door de Nederlandse luchtvaartsector worden nageleefd. Dit omvat het ontmoedigen van niet-noodzakelijke reizen, het tonen van een gezondheidsverklaring en negatieve coronatestuitslag, frequentere schoonmaak van vliegtuigen, verbeterde hand-, hoest- en nieshygiëne, het gebruik van mondmaskers en verminderde dienstverlening tijdens de vlucht. Net als geldt voor 99.1% voor alle commerciële passagiersvluchten van en naar Nederlandse luchthavens, zijn in deze studie alleen toestellen onderzocht die zijn uitgerust met HEPA-filters.

De studie is gebaseerd op data uit literatuur, metingen en simulaties van deeltjesverspreiding en omvat een kwantitatieve microbiologische risicoschatting (*quantitative microbial risk assessment, QMRA*). De volgende figuur vat de samenhang van deze delen samen.



**De studie heeft drie vliegtuigtypen onderzocht die veel voorkomen op Amsterdam Airport Schiphol, in twee klassen.** Twee *single-aisles* (kleinere toestellen met een enkel gangpad; Airbus A320 en Boeing 737-800) zijn onderzocht, welke worden gebruikt voor kortere vluchten, zoals binnen Europa, en plaats bieden aan zo'n 200 passagiers. Eén *twin-aisle* (een groter toestel met twee gangpaden; Boeing 787-8) is onderzocht, welke wordt ingezet op langere, intercontinentale vluchten, en een hogere stoelcapaciteit heeft. Deeltjesverspreiding in deze toestellen is onderzocht door middel van metingen en simulaties (laatstgenoemde alleen in de Airbus A320 en Boeing 787-8) in een 7-rij cabinesectie in de *economy*-klasse. **De resultaten van de literatuurstudie toonden de relevantie van zowel de kruisvlucht- als taxifase, dus beide zijn onderzocht.** De kruisvluchtsituatie is onderzocht door middel van metingen en simulaties, waarbij de laatste is gebruikt om het effect van de zitpositie van de indexpassagier in dezelfde rij te onderzoeken. Metingen in stilstaande vliegtuigen op de grond zijn uitgevoerd om het risico in een taxiscenario te bepalen.

### Cabinecondities

Metingen van de omgevingscondities in de vliegtuigcabine – temperatuur, relatieve luchtvochtigheid en luchtstroom – werden uitgevoerd om invoergegevens te verzamelen voor de simulatiewerkzaamheden. Bij die metingen werden temperaturen tussen de 19 °C en 24 °C vastgesteld, die in het algemeen over tijd convergeerden tot waarden tussen 21 en 22 °C. De relatieve luchtvochtigheid bleek laag, in het bijzonder tijdens de kruisvlucht, met waarden die convergeerden tot ongeveer 10%. In alle vliegtuigen werd een luchtstroom naar de achterzijde van de cabine vastgesteld. Literatuur beschrijft dat de cabinelucht tussen de 10 en 30 keer per uur wordt verversd.

### Bron

Informatie uit literatuur werd gebruikt om uitscheiding van virus met aerosoldeeltjes te beschrijven. Daarbij werd onderscheid gemaakt tussen 'normaal' te verwachten uitstoot en hoge uitstoot. Voor een reguliere indexpassagier werd uitgegaan van een lognormale verdeling van virusconcentratie in het slijm van de index met een gemiddelde van 7.53 en een standaarddeviatie van 1.28 RNA-kopieën / mL (d.w.z. een gemiddelde uitscheiding van  $10^{7.5}$  RNA-kopieën / mL). Voor een passagier die een buitengewoon grote hoeveelheid infectueuze aerosolen uitscheidt (een zogenaamde superuitscheider) werd een emissie met een concentratie van  $10^{10}$  RNA-kopieën / mL aangenomen. Dat betekent dat een superverspreider gemiddeld 300 keer zoveel RNA-kopieën / mL uitscheidde als een normale indexpassagier. De totale hoeveelheid uitgestoten aerosolen tijdens ademen (aangenomen voor 80% van de tijd) en spreken (20% van de tijd) werden overgenomen uit literatuur.

Bij de deeltjesverspreidingsmetingen in de cabine is de bron nagebootst middels een op een pop gemonteerd mondstuk, verbonden met een aerosolenpomp. Kunstmatig speeksel werd via dit mondstuk in de cabine ingebracht. Bij de simulaties werd gemodelleerd dat de uitstoot van de index passagier start vanuit een bol met een diameter van 10 centimeter, op 10 centimeter afstand vóór de indexpassagier.

## Deeltjesverspreiding

Naast de metingen om de cabinecondities te onderzoeken werden deeltjesverspreidingsmetingen uitgevoerd. Hiervoor werden poppen (optioneel verwarmd, om de warmteafgifte van normale passagiers na te bootsen) geplaatst in de stoelen in de onderzochte cabinesectie van zeven rijen. Volgend op de uitstoot van kunstmatig speeksel door de bron, werden deeltjesaantallen en -volumes in de cabinesectie onderzocht via apparatuur die deeltjes detecteren. Op alle poppen werden hiertoe *particulate matter sensors* (partikelsensoren) geplaatst, en werd gebruik gemaakt van twee strategisch geplaatste *aerodynamic particle sizers*. De metingen werden onder verschillende omstandigheden uitgevoerd, om de impact van een groot aantal variabelen te onderzoeken: kruisvlucht en taxi, gebruik van *gaspers* (door passagiers instelbare inblaasopeningen), mondkmaskergebruik door de indexpassagier, popverwarming (alleen bij taxi), instellingen van het ventilatiesysteem en indexpositie (alleen in Boeing 787-8). Additionele poppen en partikelsensoren, op grotere afstand van de indexpassagier geplaatst, werden gebruikt bij de metingen in de *single-aisle* toestellen om de mogelijke recirculatie van aerosolen door het cabineventilatiesysteem te beoordelen.

In de simulaties werd verspreiding van aerosolen over zeven stoelrijen in een geventileerde vliegtuigcabine nagebootst. Een *Reynolds-averaged Navier-Stokes* (RANS) methode werd gebruikt om de luchtstroming en verspreiding van deeltjes te modelleren, rekening houdend met de cabine-indeling van de onderzochte vliegtuigtypes, cabinecondities, eigenschappen van het ventilatiesysteem en het effect van opstijgende warmte lucht als gevolg van warmtebronnen in de cabine. Cabinecondities, luchtinstroom, warmtebronnen en thermische condities werden gemodelleerd op basis van een combinatie van meetresultaten, vliegtuigspecificaties en literatuur. Na introductie van deeltjes in de simulatie werd hun pad gemodelleerd, onder invloed van luchtstroming en zwaartekracht. Het aantal, volume en de verblijfsduur van de deeltjes die in een 'inadembox' van 30 × 30 × 30 centimeter terechtkwamen werd opgeslagen en gebruikt als invoer voor de risicoschatting.

Uit vergelijkingen tussen de resultaten van metingen en simulaties van deeltjesverspreiding in de Airbus A320 en Boeing 787-8 is gebleken dat beide methoden een vergelijkbare aerosolver spreiding per rij laten zien. Zowel meet- als simulatieresultaten, in het bijzonder die van de *single-aisle* toestellen, toonden deeltjesverspreiding in overwegend achterwaartse richting, consistent met de eerder opgemerkte achterwaartse luchtstroom.

Uit verder onderzoek naar de invloed van bepaalde parameters is gebleken dat maskergebruik door de indexpassagier het aantal en volume van verspreide deeltjes duidelijk verlaagt. De effecten van de instellingen van *gaspers* en variatie in de locatie van de indexpassagier bleken gevarieerd en beperkt. Slechts zeer lage volumes aerosolen werden aangetroffen op twee rijen verder vóór de zeven-rij cabinesectie die werd onderzocht. Dit suggereert dat, ten minste in het achterste gedeelte van de *economy*-klasse, **recirculatie van aerosolen via het met HEPA-filters uitgevoerde cabineventilatiesysteem niet of slechts zeer beperkt voorkomt.**

## Risicoschatting

Op basis van meet- en simulatieresultaten van deeltjesverspreiding en literatuur over virusuitstoot, dosis-response (het effect dat een bepaalde blootstelling heeft op een persoon) en de effectiviteit van mondkmaskers werd een QMRA uitgevoerd om het risico op ziekte te schatten. Daarvoor zijn gemeten en gesimuleerde aerosolconcentraties omgerekend naar overgedragen fracties: de fractie van de uitgestoten bron die door een passagier in een bepaalde stoel zou worden ingeademd. Variatie in blootstellingscondities werd onderzocht door gebruik te maken van distributies voor blootstellingsfactoren, zoals inademsnelheid, het door de indexpassagier uitgestoten aerosolvolume

en de virusconcentratie in sputum. Op deze verdelingen werd een Monte Carlo simulatie uitgevoerd, resulterend in een dosis en risico op ziekte.

## Conclusies

Voor een typische kruisvlucht (variërend van 0,9 uur voor de *single-aisle* Airbus A320 en 8,7 voor de *twin-aisle* Boeing 787-8) werd het **gemiddelde risico op COVID-19 door inademing van geaërosoliseerde SARS-CoV-2 deeltjes bij passagiers in de zeven rijen om de indexpassagier geschat in de bandbreedte 1/1800 tot 1/120**. In het geval van een superuitscheider namen gemiddelde risico's toe tot 1/16. **Van deze uitkomsten werd bepaald dat ze in lijn zijn met andere model- en meetstudies naar het risico op ziekte tijdens de vlucht. Risico's namen toe met vluchtduur: een vlucht met een *single-aisle* toestel bleek te resulteren in lagere risico's dan een vlucht met een *twin-aisle* toestel.** Het risico buiten de onderzochte zeven rijen werd niet beoordeeld, maar gebaseerd op afnemende risico's met een toenemende afstand tot de indexpassagier werd aangenomen dat geen ziekte voorkwam buiten de vernoemde zeven rijen.

**Het verwachte aantal vluchten dat resulteerde in ten minste 1 geval van COVID-19 door de verspreiding van aerosolen die het SARS-CoV-2 virus bevatten die zijn uitgestoten door een 'reguliere' indexpassagier werd geschat tussen de 2 en 44 kruisvluchten met een voor dat toestel typische kruisvluchtduur. Bij kruisvluchten van langere duur varieerde dit verwachte aantal vluchten van 2 tot 19.** Het verwachte aantal vluchten dat resulteert in ten minste 1 geval van aerosoltransmissie door een superuitscheider is geschat op een bandbreedte van 1 tot 9 vluchten in het geval van een typische kruisvluchtduur, en op een bandbreedte van 1 tot 4 vluchten bij kruisvluchten van langere duur.

Schattingen van de waarschijnlijkheid waarmee één infectueuze passagier een vliegtuig betreedt zullen onnauwkeurig zijn en kunnen snel veranderen. Uitgaande van 5% vals-negatieve resultaten van het testen van reizigers (OMT89), zou 5% van het huidige aantal besmette personen in Nederland aan boord kunnen gaan terwijl ze het virus uitscheiden (dd. 7 juni 2021 zijn dat er minder dan 30 per 100.000 passagiers). Afhankelijk van het aantal passagiers per vliegtuig (100 – 300), zou dan elke 11 – 33 vluchten een infectueuze passagier aan boord hebben en zou minder dan 3% daarvan een superuitscheider zijn.

Statistische analyse van de meetresultaten liet zien dat afstand en hoek tot de indexpassagier het risico in alle gevallen hoog significant beïnvloedden (dat wil zeggen dat het risico afnam met toenemende afstand, en dat deze afname in risico niet gelijk was in alle richtingen), consistent met simulatieresultaten. Het effect van het dragen van een masker door alle passagiers zoals meegenomen in de risicoschatting werd gebaseerd op gegevens uit literatuur. **Meetresultaten suggereren dat een mondmasker uitstoot van grotere aerosolen beperkte en dat het de richting van uitstoot veranderde. Meer gegevens zijn nodig om die bevindingen te valideren.**

Belangrijke oorzaken van grote variabiliteit in de risicoschattingen op basis van meet- en simulatiedata waren de virusconcentratie in de aerosolen en het volume aerosolen dat werd uitgescheiden door de uitscheider. Deze varieerden over meerdere ordegrootte (factor 10 of meer). De vluchtduur en de effectiviteit van maskers op het beperken van aerosoluitstoot en -inademing hadden een direct proportioneel effect op het risico, maar de variatie ten gevolge van deze aspecten was minder dan een ordegrootte (dat wil zeggen: minder dan een factor 10).

## Toepasbaarheid

Deze studie is uitgegaan van het naleven van de door EASA en ICAO gepubliceerde *best practices*, zoals het dragen van mondmaskers<sup>2</sup> in het vliegtuig, behalve gedurende het eten of drinken (dat in 10% van de tijd is aangenomen). De

<sup>2</sup> In een eerdere versie van het rapport stond ten onrechte dat EASA en ICAO het gebruik van niet-medische mondmaskers aanraden

studie schat het risico van verspreiding aan boord van een vliegtuig door inademing van aerosolen die virusdeeltjes bevatten in het geval dat een infectueuze passagier (index) aanwezig was in de cabine, op basis van onderzoek in één van elk van drie veelvoorkomende vliegtuigen die worden gebruikt voor commercieel passagiersvervoer. **De studieresultaten kunnen niet gebruikt worden om het risico van een individuele passagier op een enkele vlucht te beoordelen en ook niet om bepaalde stoelposities in het algemeen te classificeren naar hogere of lagere risiconiveaus.**



Dedicated to innovation in aerospace



Rijksinstituut voor Volksgezondheid  
en Milieu  
Ministerie van Volksgezondheid,  
Welzijn en Sport

**PUBLIC**

NLR-CR-2021-232-RevEd-1 | July 2021

# CORSICA final report

Quantitative microbial risk assessment for aerosol transmission of SARS-CoV-2 in aircraft cabins based on measurement and simulations

**CUSTOMER:** Ministry of Infrastructure and Water Management

*The owner and/or contractor have granted permission to publish this report.  
 Content of this report may be cited on the condition that full credit is given to the owner and/or contractor.  
 Commercial use of this report is prohibited without the prior written permission of the owner and/or contractor.*

<b>CUSTOMER</b>	Ministry of Infrastructure and Water Management
<b>CONTRACT NUMBER</b>	AOEP/819/17064
<b>OWNER</b>	NLR
<b>DIVISION NLR</b>	Aerospace Operations
<b>DISTRIBUTION</b>	Unlimited
<b>CLASSIFICATION OF TITLE</b>	UNCLASSIFIED

# Contents

<b>Abbreviations and terms</b>	<b>6</b>
<b>1 Introduction</b>	<b>8</b>
1.1 The virus and transmission	8
1.2 Objective and project overview	10
1.3 Project scope and main assumptions	10
1.4 Reading guide	12
<b>2 Research approach</b>	<b>13</b>
<b>3 Cabin environmental conditions</b>	<b>17</b>
3.1 Methodology	17
3.2 Results	17
3.3 Chapter conclusions	19
<b>4 Source</b>	<b>21</b>
4.1 Methodology	21
4.1.1 Literature	21
4.1.2 Representation in measurements	22
4.1.3 Representation in simulations	23
4.2 Results	23
4.3 Chapter conclusions	24
<b>5 Particle dispersion</b>	<b>25</b>
5.1 Methodology	25
5.1.1 Measurements	25
5.1.2 Simulations	27
5.1.3 Comparison between measurements and simulations	29
5.2 Results	30
5.2.1 Comparison between measurements and simulations	30
5.2.2 Particle dispersion in different scenarios	32
5.2.3 Influence of selected variables on dispersion	33
5.2.4 Recirculation of aerosols through ventilation system	36
5.3 Chapter conclusions	37
<b>6 Risk assessment</b>	<b>38</b>
6.1 Methodology	38
6.1.1 Exposure evaluation	38
6.1.2 Estimation of risk	38
6.1.3 Scenarios and assumptions for the risk assessment	39
6.1.4 Statistical analysis	40
6.2 Results	40
6.2.1 Risk assessment per seat	40

6.2.2	Aggregated risk assessment	42
6.3	Chapter conclusions	46
<b>7</b>	<b>Discussion</b>	<b>47</b>
7.1	Applicability and scoping	47
7.1.1	Limitations and generalizing study results	47
7.1.2	Risk from other transmission routes not assessed in this study	48
7.1.3	Applicability to other aircraft types	49
7.1.4	Risk of illness per flight – extrapolation from 7-rows to full size cabin	50
7.1.5	Probability that an infectious person or super shedder boards an aircraft	51
7.2	Uncertainty and variability	52
7.2.1	In-cabin measurements	52
7.2.2	Simulations	53
7.2.3	QMRA	54
7.3	Mask effects	55
7.4	Comparison of results with other studies	56
7.4.1	Comparison with epidemiological studies in aircraft cabins	56
7.4.2	Comparison to epidemiological studies in other settings	57
7.4.3	Comparison of CORSICA with in-flight transmission studies	58
7.4.4	Comparison with estimates from computational tool <i>AirCoV2</i>	59
7.5	Current results in view of the RIVM advice with respect to air travel	60
<b>8</b>	<b>Conclusions</b>	<b>62</b>
<b>9</b>	<b>Recommendations</b>	<b>64</b>
9.1	Policy and mitigation	64
9.2	Future research	64
<b>10</b>	<b>References</b>	<b>66</b>
<b>Appendix A</b>	<b>Summary of CORSICA literature report</b>	<b>70</b>
Appendix A.1	English	70
Appendix A.2	Nederlands	71
<b>Appendix B</b>	<b>Technical appendices</b>	<b>73</b>
Appendix B.1	Research approach	73
Appendix B.1.1	Risk of illness	73
Appendix B.1.2	Drivers of variance	74
Appendix B.1.3	Description of dispersion and impact of selected variables	75
Appendix B.1.4	Cross-check measurements and simulations	76
Appendix B.2	Measurement setup	77
Appendix B.2.1	Equipment specification	77
Appendix B.2.2	Measurement grid	78
Appendix B.2.3	Measurement runs	79
Appendix B.3	Cabin environmental conditions	82
Appendix B.4	Source specification	88

Appendix B.4.1	Source used in measurements and CFD simulations (cross-check only)	88
Appendix B.4.2	Sources used in CFD simulation	89
Appendix B.5	Aerosol dispersion	91
Appendix B.5.1	Selected results of measured aerosol dispersion	91
Appendix B.5.2	Selected results of measured particle size distribution and spread	93
Appendix B.5.3	Particle size distribution in experimental setting	95
Appendix B.5.4	Selected results of simulated aerosol dispersion	95
Appendix B.6	Exposure evaluation	98
Appendix B.6.1	Exposure evaluation on the basis of transmission experiments: method	98
Appendix B.6.2	Exposure evaluation on the basis of transmission simulations: method	100
Appendix B.6.3	Simulation of exposure scenarios	100
Appendix B.6.4	Exposure evaluation on the basis of transmission experiments: parameters	101
Appendix B.7	Calculation of risk	103
Appendix B.7.1	Risk evaluation	103
Appendix B.8	Statistical analysis	104
Appendix B.8.1	Method	104
Appendix B.8.2	Results	105

## Abbreviations and terms

ACRONYM / TERM	DESCRIPTION
A320	Airbus A320, single-aisle aircraft
ACH	Air change per hour
APS	Aerodynamic Particle Sizer
APU	Auxiliary Power Unit, on-board generator powering secondary aircraft systems during flight or the ECS on the ground when no PCA is available
AR	Attack Rate
B737	Boeing 737-800, single-aisle aircraft
B787	Boeing 787-8, twin-aisle aircraft
CDC	Centers for Disease Control and Prevention
CFD	Computational Fluid Dynamics
CORSICA	<b>Contamination risk of SARS-CoV-2 in aircraft cabins</b>
COVID-19	Coronavirus disease 2019, infectious disease caused by the SARS-CoV-2 virus
<i>dose</i>	Total number of virus RNA copies to which a passenger was exposed to, over the whole period of exposure
EASA	European Aviation Safety Agency
ECDC	European Centre for Disease Prevention and Control
<i>frac</i>	Fraction of aerosol that reached a passenger
GAMM	Generalised Additive (Mixed) Model
gasper	Passenger-controlled air inlets often mounted overhead
HEPA	High Efficiency Particulate Air filter
IATA	International Air Transport Association
ICAO	International Civil Aviation Organisation
IenW	Ministry of Infrastructure and Water Management
NAAT	Nucleic Acid Amplification Test
NLR	Royal NLR - Netherlands Aerospace Centre
OMT	Outbreak Management Team
OPS	Optical Particle Sensor
PACK	Pneumatic Air Cycle Kit
PCR	Polymerase Chain Reaction
<i>p<sub>ill</sub></i>	Probability of illness, here per passenger over whole period of exposure
PM	Particulate Matter
QMRA	Quantitative microbial risk assessment
RANS	Reynolds-averaged Navier-Stokes
RAT	Rapid Antigen Test
RIVM	Dutch National Institute for Public Health and the Environment
RNA	Ribonucleic Acid

ACRONYM / TERM	DESCRIPTION
SARS-CoV-2	Severe Acute Respiratory Syndrome – Corona Virus 2, the virus that can cause the disease COVID-19

# 1 Introduction

The coronavirus pandemic is an ongoing global epidemic of coronavirus disease 2019 (COVID-19). The disease was first identified in December 2019 in Wuhan, China. The outbreak was declared as a Public Health Emergency of International Concern in January 2020, and a pandemic in March 2020. As of April 2021, more than 145 million cases have been confirmed as well as more than 3 million deaths attributed to COVID-19. COVID-19 is caused by the severe acute respiratory syndrome coronavirus 2 (SARS-CoV-2).

## 1.1 The virus and transmission

In January 2020 Severe Acute Respiratory Syndrome Coronavirus 2 (SARS-CoV-2, also known as novel Coronavirus or 2019-nCoV) was identified as the causative agent causing the disease COVID-19 (Gorbalenya, et al., 2020). The SARS-CoV-2 virus, like SARS-CoV and MERS-CoV, is a coronavirus belonging the family Coronaviridae and to the genus beta-coronavirus. It is an enveloped, positive-sense, single-stranded RNA virus of 50-200 nm in diameter, and the genome is approximately 30 kb in length. Like other coronaviruses, SARS-CoV-2 has four structural proteins, known as the S (spike), E (envelope), M (membrane), and N (nucleocapsid) proteins. The spike protein is the protein responsible for allowing the virus to attach to and fuse with the ACE2 receptor on the membrane of a host cell including the human host. By 22 January 2020, the full virus genome was affected (Zhou & et al., 2020). Since then multiple variants have been distinguished with higher binding and replication capabilities (Zhou, et al., 2021) and higher viral loads in the younger population (Volz, et al., 2021). So far data on probable differences between variants in relevance of transmission via aerosols are scarce so no distinction is made between different virus variants.

### *Transmission*

The disease spreads through exposure to respiratory fluids carrying infectious virus (CDC, 2021). This occurs via inhalation of small droplets and aerosols. The virus may also be transmitted via deposition of respiratory droplets and particles on exposed mucous membranes in the mouth, nose, or eye by direct splashes and sprays and touching of mucous membranes with hands that have been soiled either directly by virus-containing respiratory fluids or indirectly by touching contaminated surfaces. COVID-19 is a mostly respiratory disease with virus excreted in respiratory and oral secretions by coughing and sneezing and also by singing, talking and breathing. SARS-CoV-2 can also be excreted in stools and is readily inactivated by e.g. alcohol. SARS-CoV-2 infections can also occur without symptoms and the virus can be excreted in the absence, and prior to the development of symptoms. Symptomatic persons are not allowed to travel. In this study we performed a QMRA based on exposure via inhalation of SARS-CoV-2 containing very fine respiratory droplets and aerosol particles.

### *Descriptive studies*

A number of epidemiological studies concerning transmission of SARS-CoV-2 in aircraft have been published. In March, Yang et al. (2020) were the first to suggest likely in-flight SARS-CoV-2 transmission, describing 10 positive cases amongst passengers who were all infected on the same flight. Shortly after, Schwarz et al. (2020) described a case in which two COVID-19 positive passengers infected on a long-distance flight, but appeared not to have infected any other passengers. Khanh et al. (2020) described a cluster of 16 COVID-19 passengers who became infected on a 10-hour commercial flight with 217 passengers and crew. Seating proximity was strongly associated with increased infection risk (risk ratio 7.3, 95% CI 1.2–46.2), and droplet or airborne transmission were the most likely route (Khanh et al., 2020). Speake et al. (2020) described a flight on board of which 11 passengers appeared to have been infected,

a finding supported by comparison of viral gene profiles. An elevated risk was indicated for passengers in window seats (Speake, et al., 2020). Six other sources described likely transmission of SARS-CoV-2 on board an aircraft (Chen et al. , 2020; Eldin, 2020; Pavli, 2020; Hoehl, 2020; Choi, 2020; Lytras, 2020). Of these studies, Choi and Speake compared genetic sequences to support in-flight transmission of SARS-CoV-2 to two crew members. These studies suggested that acquisition of a SARS-CoV-2 infection can occur on board of an aircraft with a symptomatic or asymptomatic case. As only a small selection of flights have been examined and methodologies differed per study (with or without comparison of genetic sequencing of virus, amount of passengers traced), the available literature cannot be used to draw conclusions concerning general statistics of SARS-CoV-2 transmission risk on board of aircraft (NLR & RIVM, 2020; WHO, 2020). The descriptive studies show that in-flight transmission does occur however the numerical relevance is unclear.

#### *Studies into effectiveness of public health and social measures on board*

To estimate the number of infected passengers on board, passenger symptoms and exposure screening at the entry, a so-called triage, was considered. Entry screening aimed at assessing the presence of symptoms and/or the exposure to COVID-19 of infected passengers arriving from affected areas. Travelers that have been identified as exposed to or infected with COVID-19 should be quarantined or isolated and treated (Mouchtouri, Bogogiannidou, Dirksen-Fischer, Tsiodras, & Hadjichristodoulou, 2020; RIVM, n.d.). A number of studies on the efficiency of symptoms/exposure-based screening has been conducted (Chetty, Daniels, Ngandu, & Goga, 2020). These included modelling studies as well as observational studies. Modelling studies evaluate the probability of detection in different scenarios that typically represent different assumptions on uncertain, but highly critical factors such as the fraction of asymptomatic infected, affected and the incubation period of COVID-19. Observational studies usually use a combination of symptoms/exposure-based screening, PCR screening and monitoring during quarantine. In such retrospective studies an estimate of the efficiency of symptoms/exposure-based screening can be made by comparing screening detection with retrospective observations on the development of disease. In Line with OMT advice 89 (RIVM, 2020a) we assume that 95% of shedding persons is correctly identified by pre-boarding testing and therefore excluded from traveling.

#### *Experimental and modelling studies*

Several studies have been identified that to some extent evaluated exposure and risk of transmission in an aircraft during flight given the presence of an index passenger on board. Kinahan et al. (2021) studied the transfer of respirable aerosols in aircraft. Wang et al. (2021) evaluated risk on secondary infection on board of a flight on the basis of the transfer experiments by Kinahan et al. (2021). Marcus et al. (2021) conducted a risk assessment based on a multi-zone Markov model for the dispersion and inhalation of respirable aerosol in aircraft during flight. Sze To et al. (2009) studied dispersion of inhalable aerosol in an airplane mock-up (in a laboratory setting) after a simulated cough. In the discussion section, these studies are discussed and the results are compared with this study.

#### *RIVM advice on the prevention of SARS-CoV-2 transmission in aircraft*

The National Institute for Public Health and the Environment (RIVM) previously advised on the safety on board of aircraft in relation to SARS-CoV-2 and the associated safety protocols put in place by Dutch airlines, based on guidelines by the European Aviation Safety Agency (EASA) and the International Civil Aviation Organisation (ICAO). RIVM deemed it plausible that the ventilation system on board of aircraft, with a high air exchange rate and vertical air flows, limits possible aerogenic transmission of SARS-CoV-2 on board of aircraft (Rijksoverheid, 2020a).

## 1.2 Objective and project overview

The Ministry of Infrastructure and Water Management (IenW) assigned the Royal Netherlands Aerospace Centre (NLR) and RIVM to scientifically assess the risk of transmission of SARS-CoV-2 in aircraft cabins based on a literature review, simulations and measurements. This resulted in CORSICA (**C**ontamination risk of **S**ARS-CoV-2 in aircraft **c**abins). CORSICA follows up on the previous 'HEPA-scan' by NLR that mapped the presence of HEPA filters on board aircraft at the Dutch airports (Roosien, Peerlings, & Jabben, 2020). The current document is the final report of the CORSICA project, which builds upon on the previously published literature report (NLR & RIVM, 2020). The summary of this literature report is included as Appendix A.

The multi-disciplinary project is conducted in cooperation by the NLR and RIVM. In the project, NLR assessed the aeronautical aspects of the study and coordinated the project. RIVM assessed the virologic, bio-medical and QMRA aspects of the study. During the in-cabin measurements and with the assessment of the measurement data, NLR and RIVM were supported by the German Aerospace Center (DLR) and Medspray. For the purpose of the measurements, three aircraft were chartered from commercial operators.

The overall project ran from initiation in July 2020 until the delivery of this report in June 2021.

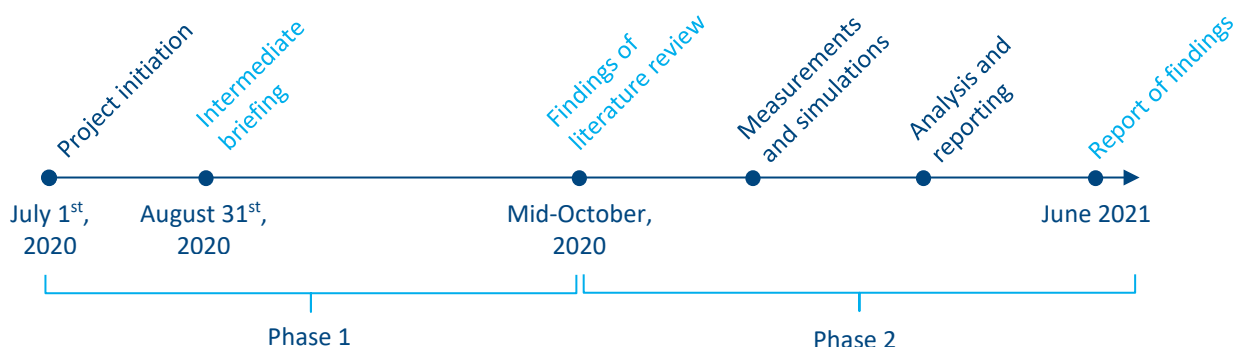


Figure 1: Project timeline, showing different phases and main deliverables

## 1.3 Project scope and main assumptions

CORSICA assessed the risk of illness due to aerosol viral transmission in the aircraft cabin in the event that one of the passengers carries the SARS-CoV-2 virus, in other words, one of the passengers was shedding SARS-CoV-2 in aerosol via the respiratory tract and other passengers inhaled the virus. The scope of this research phase is consistent with the scope and main assumptions presented in the literature report (NLR & RIVM, 2020) and the parliamentary motion supporting the assignment<sup>3</sup>.

### *A single infected passenger*

The starting point of this study is that one of the passengers (a-symptomatic, without showing symptoms) in the cabin carries and emits aerosols containing SARS-CoV-2 particles. The likelihood of such a passenger entering the cabin and the effectiveness of measures to prevent infected passengers from entering the cabin is not part of the study<sup>4</sup>.

<sup>3</sup> Kamerstuk 31936, no. 788, <https://www.tweedekamer.nl/kamerstukken/detail?id=2020Z12659&did=2020D27098>

<sup>4</sup> The discussion, specifically Section 7.1.5, provides further comments.

### *Aircraft cabin*

This study is limited to the situation inside the aircraft cabin. The airport terminal and boarding bridges are excluded. Following outcomes of the literature review, the study is focused on the taxi and cruise phases. As such, neither (de)boarding (including cabin luggage handling) and waiting before taxi nor the climb and descent phases of the flight are studied.

### *Transmission routes*

The first phase of this study was limited to three transmission routes: transmission by inhalation of aerosols<sup>5</sup>, transmission by means of larger droplets and contact transmission<sup>6</sup>. The literature review found that “the relative importance of each of these routes is not quantitatively known and difficult to investigate”, but that few cases of contact transmission were found (NLR & RIVM, 2020, p. 33). In the current phase of the study, the dispersion of aerosolised particles from 0.5 to 5 µm was measured, while the dispersion of particles up to 20.0 µm were simulated. These include the most relevant particle sizes.

### *Mitigation measures*

Unless stated otherwise, this study assumes that the mitigation measures currently applied by the Dutch aviation sector (as described by Rijksoverheid, 2020b) are complied with. A more extensive overview of these measures was presented in the literature report (NLR & RIVM, 2020). The following measures are relevant for the research documented in this report, in the manner described in Table 1.

When referred to ‘face masks’, disposable surgical (in the Netherlands known as non-medical) face masks are meant. An illustrative picture of such a mask is shown in Figure 2.



*Figure 2: Example of the type of mask that this study refers to as ‘face mask’ (NurseTogether, 2020)*

<sup>5</sup> Defined in this study as fluid droplets with a diameter less than 20 µm

<sup>6</sup> Section 1.3 of the literature report distinguished between “direct transmission either through large droplets or aerosols, transmission through recirculated air, and transmission via contact with contaminated surfaces” (NLR & RIVM, 2020, p. 9).

*Table 1: Mitigation measures relevant for the assessment of the SARS-CoV-2 transmission risk in aircraft cabins. The measures printed in italics were standard practice before the COVID-19 pandemic, but are seen as mitigation measure relevant for reducing the SARS-CoV-2 transmission risk in aircraft cabins*

Measure	Effect	Implications for current study
Prevent unnecessary travel	Reduce the number of flights and/or passengers <sup>7</sup> .	Not taken into account; study assumed fully occupied flights.
Health declaration <sup>8</sup>	Reduce the probability of having people on board the aircraft that can transmit SARS-CoV-2.	All scenarios include one (and only one) asymptotically infected passenger (who is not coughing or sneezing).
More frequent aircraft disinfection	Reduce the probability of virus particles 'migrating' from one flight to the next.	The infected passenger is the only virus source in the aircraft cabin and only inhalation of aerosolised particles is considered .
Improved personal hygiene (e.g. hand hygiene, and coughing and sneezing hygiene)	Reduce the probability of depositing virus particles on surfaces.	Contact transmission and sneezing and coughing was not included.
Wear face masks during the flight, except when consuming meals	Reduce the emission and inhalation of virus particles.	Scenarios with and without use of face masks are studied.
Reduced in-flight service	Reduce the amount of movement of and interaction between persons, and increase the time people wear surgical mouth masks.	Virus shedding by moving crew members was not considered.
<i>Filter recirculated cabin air with appropriately maintained and cleaned HEPA-filters<sup>9</sup></i>	<i>Reduce the amount of virus particles in the cabin air.</i>	<i>The infected passenger is the only virus source in the aircraft cabin.</i>

## 1.4 Reading guide

This document presents the findings from phase 2 of the project and combines findings from the literature review, in-cabin measurements, simulations and a quantitative microbial risk assessment to assess the risk of illness.

After explaining the research approach in Chapter 2, the report thematically follows the route from the contaminated passenger (the source or index passenger) in the aircraft cabin, emission of aerosolised SARS-CoV-2 particles through breathing and speaking, the distribution of these particles throughout the cabin, the exposure to SARS CoV-2 through inhalation of these particles and finally, the probability of illness in Chapters 3 to 6. Each of these chapters discusses and motivates the methodology, shows the main results and concludes how these findings are used in the study. After these thematic chapters, Chapter 7 provides a discussion of the results, addressing study limitations and sensitivities. The conclusions are presented in Chapter 8, whereas Chapter 9 lists recommendations. A list of references is provided in Chapter 10.

<sup>7</sup> Following reduced demand, aircraft operators will generally also reduce supply (i.e., flights). As such, a reduction in the amount of travellers does not automatically result in lower passenger numbers per flight. Nevertheless, load factors of flights departing Dutch airports have decreased (CBS, 2020a; CBS, 2020b).

<sup>8</sup> Currently, the Government of the Netherlands also requires travellers coming to the Netherlands from a high-risk country to provide proof that they have tested negative for COVID-19 (Government of the Netherlands, 2021). This further reduces the probability of having SARS-CoV-2 transmitting people on board.

<sup>9</sup> Previous research estimated that 99.1% of passenger flights using aircraft equipped with more than 19 seats to and from airports in The Netherlands were operated using HEPA-filter-equipped aircraft (Roosien, Peerlings, & Jabben, 2020).

## 2 Research approach

As stressed in the literature review (NLR & RIVM, 2020), the risk of in-cabin transmission of SARS-CoV-2 is a multi-disciplinary problem. It requires up-to-date knowledge of the bio-medical properties of the virus, host and recipient but also knowledge of cabin environmental conditions, aerodynamics of complex flows and the operational context of a flight. Since the majority of existing knowledge was based on other viruses or other environmental conditions, a lot of relevant data was not validated in practice or missing. Thus, it was necessary to gather new data which included the preparation, execution and analysis of the CFD simulations and (in-flight) cabin measurements; separate disciplines on their own.

This combination of distinct disciplines is reflected in the hybrid approach used for this study, combining results from literature, measurements, simulation and expert judgement to provide the clearest possible answer to the main research question: “what is the risk of SARS-CoV-2 transmission through aerosols in aircraft cabins?”.

The interrelation between literature, measurements and simulations, and quantitative microbial risk assessment (QMRA) are summarised in Figure 3 and described in more detail below.

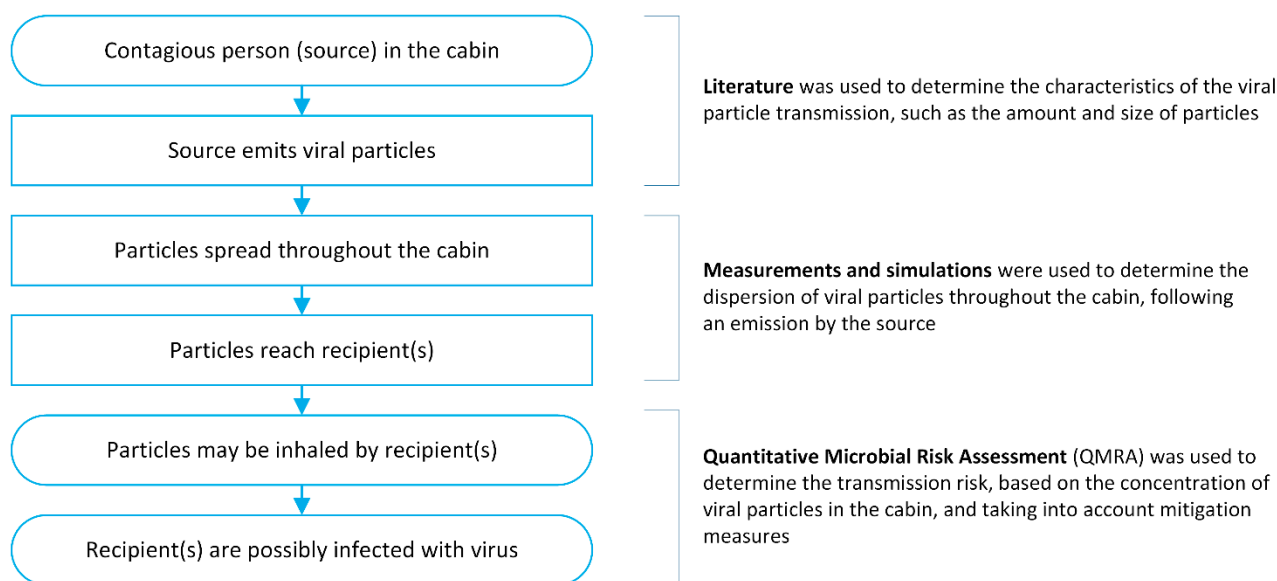


Figure 3: Overview of research approach, showing the purpose of literature (reviewed in the literature report, NLR & RIVM, 2020), measurements and simulations, and quantitative microbial risk assessment (QMRA)

### Literature

The literature review, completed in October 2020, was used to “identify the most relevant parameters for SARS-CoV-2 transmission in aircraft cabins under the current corona guidelines”, with findings to “be used as input for the measurement and simulation phase of the project” (NLR & RIVM, 2020, p. 8) and to “explicitly indicate any remaining knowledge gaps” (NLR & RIVM, 2020, p. 10). It concluded that measurements and simulations were indeed necessary to fill remaining knowledge gaps and to estimate the SARS-CoV-2 transmission risk on board of aircraft. Furthermore, the literature study noted the relevance of investigating both taxi and cruise conditions and both single and twin-aisle aircraft types.

### Measurements and simulation

The project studied two aircraft classes and a variety of parameters and outputs:

- **Aircraft classes:** single-aisle (often used on shorter, continental routes, also known as narrow-body) and twin-aisle (often used for longer, intercontinental routes, also known as wide-body) aircraft. The Airbus A320 (A320) and Boeing 787-8 (B787) were studied using measurements and simulations as relevant single- and twin-aisle aircraft. The Boeing 737-800 (B737; another single-aisle aircraft) has additionally been studied in the measurement campaign. Figure 4 shows the aircraft studied (to scale) and Figure 5 shows the seating arrangement in the cabin sections that have been investigated.
- **Parameters:** type of flight (cruise flight or ground taxi), source definition (index location, speaking or breathing, with or without mask), gasper setting<sup>10</sup>.
- **Output:** number of particles emitted, size distribution of particles emitted, number of particles sensed, size distribution of particles sensed.

A combination of aircraft and parameter setting is referred to as a ‘scenario’. All cruise-flight scenarios for the A320 and B787 have been both measured and simulated (for multiple index locations). The taxi scenario’s and the B737 scenario’s haven been measured only (for a single index location).



Figure 4: Illustrations (to scale) of the aircraft studied in this research, from left to right: Airbus A320 (A320), Boeing 737-800 (B737) and Boeing 787-8 (B787)

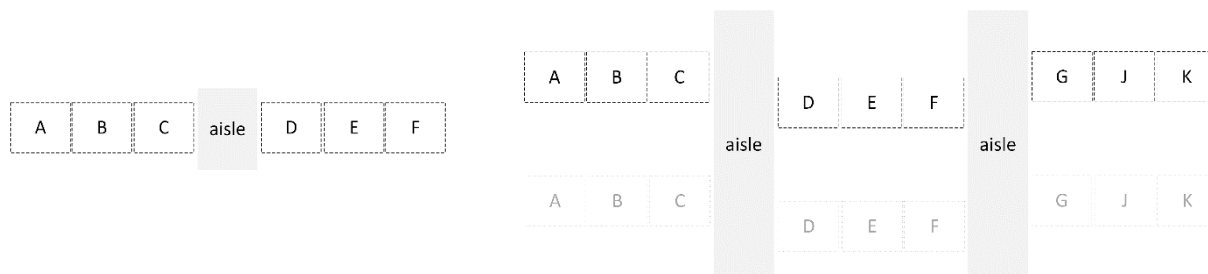


Figure 5: Seating arrangement of the single-aisle aircraft (A320 and B737; left) and twin-aisle aircraft (B787; right) sections investigated. The seat letter indicates the seat position in lateral direction. Also note how for the single-aisle aircraft, the seats are in line, whereas the seats in the twin-aisle aircraft are slightly staggered (exaggerated in figure for clarity). Row numbers are not shown but run from 1 starting with the first row from the cockpit

The measurements and simulations performed in the second phase were used to determine the total volume of aerosol particles to which passengers might be exposed to SARS CoV-2 in a particular timeframe, following emission by an index passenger. This consists of both the number and size distribution of the aerosol particles at the passengers’ seats and is relative to the number and size of particles emitted by the infected passenger. The particle volume that may be inhaled by a passenger per seat is one of the key inputs to the Quantitative Microbial Risk Assessment (QMRA) that forms the final step in assessing the risk of SARS-CoV-2 transmission and possible subsequent illness (Schijven, et al., 2021).

<sup>10</sup> Gaspers are the passenger-controlled air inlets, often mounted overhead.

In both the measurement and simulation campaigns, cabin sections with 7 rows of economy-class seats were investigated<sup>11</sup>, with a single occupant on board who is carrying the SARS-CoV-2 virus (the so-called ‘index passenger’) located in the middle row. Rows forward of the index passenger are indicated with row numbers -1, -2 and -3; rows rearward of the index passenger are labelled 1, 2 and 3. Figure 6 illustrates this.

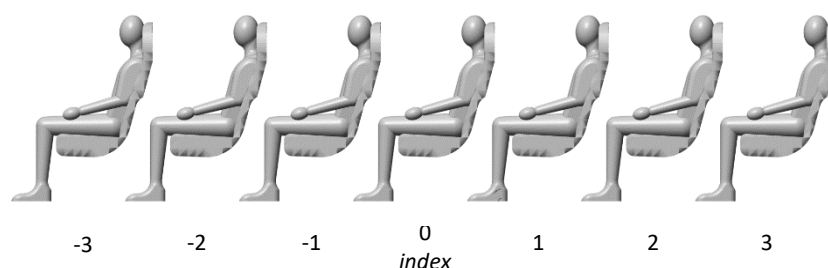


Figure 6: Schematic side-view of a 7-row economy section, illustrating the row numbering used in this report.

As both measurements and simulations come with inherent limitations, a mutually supportive and reinforcing combination was used. Because operational and technical limitations made it impossible to replicate all relevant conditions in the different aircraft types in a measurement set-up, simulations were performed in which such limitations could be overcome. The measurements conducted in the test flights, however, served three important goals that substantiate the simulation output:

- Collecting data required as input to the simulation work, such as cabin environmental parameters (temperature and humidity, for example).
- Collecting data used for validation of the simulation model, on two areas of interest:
  - Cabin air flows. These were previously identified as an important influence on transmission risk (NLR & RIVM, 2020).
  - Particle dispersion throughout the cabin (i.e.: the number of particles per seat) and particle size distribution<sup>12</sup>. For selected conditions, which could be both replicated in the measurement campaign as well as simulated, this yields data that allows for a direct comparison of the result of measurements and simulations. Based on this comparison, the simulation model was adjusted.
- Investigating the influence of selected parameters, such as the use of gaspers and the difference between two aircraft of the same class (A320 and B737), that could not be studied using simulations in the time available for this project.

Based on measured and simulated data detailing the dispersion of particles from an index passenger to the breathing zone of a seated cabin occupant, a QMRA was conducted. The QMRA estimates transmission virus from an infected index passenger to fellow passengers under realistic flight conditions, and the subsequent risk of secondary COVID-19 cases. To aid interpretation, the risk of illness was determined for typical flight durations in each of the aircraft types studied, and different scenarios of infected persons boarding the flight were considered (e.g. typical index passengers as well as a ‘super shedder’).

Figure 7 presents a schematic overview of the research approach, showing the (inter)relation between different elements of the study. Solid lines indicate an output-input relationship. The dash-dotted line (between the blocks ‘cabin environmental conditions’ and ‘source’ in the literature column) indicates source characteristics were determined for the relevant cabin environmental conditions. Dashed lines (between the blocks ‘air flow’ and ‘particle

<sup>11</sup> With a typical seat pitch of 30 to 32 inch, a 7 row section measures approximately 5,5 metres. Section 7.1.3 provides further details on the cabin configurations studied here, and how these compare to other configurations (in the same aircraft type).

<sup>12</sup> Different sizes of particles were introduced into the cabin on the measurement flights to study the effect of particle size, for example in terms of the distance they travel from the particle source before settling.

dispersion’ in the measurements and simulations columns) indicate outcomes were compared for validation purposes. With the exception of the blocks ‘source’ and ‘conclusions and recommendations’, the data gathered in each block depends on the scenario considered.

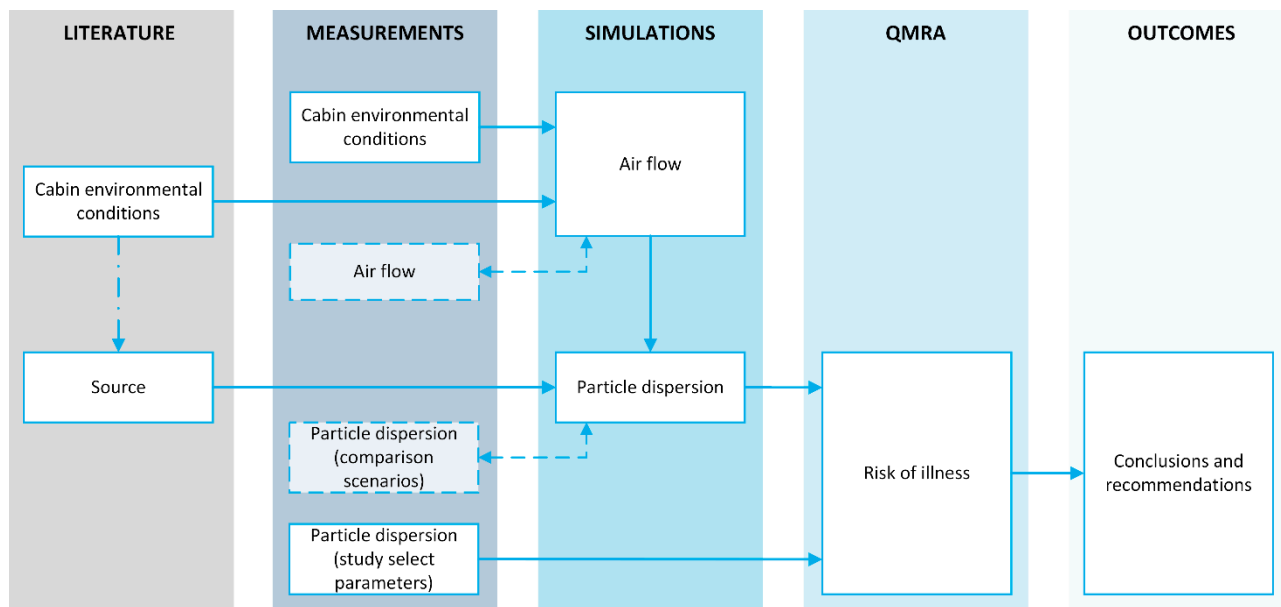


Figure 7: Overview of research approach, showing how literature (reviewed in the literature report, NLR & RIVM, 2020), measurements, simulations and quantitative microbial risk assessment (QMRA) lead to study outcomes

## 3 Cabin environmental conditions

The cabin environment – characterised by properties such as temperature and humidity – sets the scene for possible SARS-CoV-2 transmission on board of aircraft. As environmental conditions influence, among others, the flow of air throughout the cabin, these conditions are important to take into account when researching risk of illness.

This chapter further discusses the research performed into cabin environmental conditions and the implications thereof for chapters to follow. Section 3.1 discusses the methodology and Section 3.2 presents the results. Last, Section 3.3 draws partial conclusions and summarises the outcomes of this part of the study that are used in subsequent steps.

### 3.1 Methodology

A variety of measurements in aircraft cabins was performed in order to determine environmental cabin conditions for use as input for the simulation work. This was supplemented with data provided by aircraft manufacturers (OEMs) where necessary and available. Results were compared with values obtained from literature (NLR & RIVM, 2020).

For the three aircraft types studied using experiments (A320, B737 and B787), the following measurements were performed under cruise and taxi conditions:

- Temperature and relative humidity were logged at fixed positions (mounted at the seat backs of rows -3, -2, -1, 0 and 1<sup>13</sup> in front of and behind the index location). Additionally, infrared video recordings were taken of the entire cabin to examine temperature patterns.
- Air flow direction and speed in three dimensions were measured several times at various locations in the cabin (in front of and aft of the 7-row section in which particle dispersion was investigated, and between seats).

Appendix B.2.1 details the equipment used for these measurements and provides a schematic overview of the location of the different instruments.

### 3.2 Results

#### *Temperature*

During all measurements (three aircraft types, measured during cruise flight and in the taxi phase), variations in temperature were found. Temperatures mostly ranged between 19 °C and 24 °C<sup>14</sup>. Temperatures at the end of the measurements averaged around 21 °C to 22 °C, with slight variations between aircraft types and situations. Variations between rows was observed to be limited, most so in case of the B737. For illustrative purposes, Figure 8 shows the temperature measurement results in the A320 during cruise flight. Appendix B.2.2 presents the full set of results for all aircraft.

<sup>13</sup> Following the row numbering scheme shown in Figure 6, on page 20.

<sup>14</sup> An exception was found in the B787, where the environmental control system could not maintain typical cabin temperatures with gaspers closed. When gaspers were opened, cabin temperatures reduced to averages of approximately 22 °C.

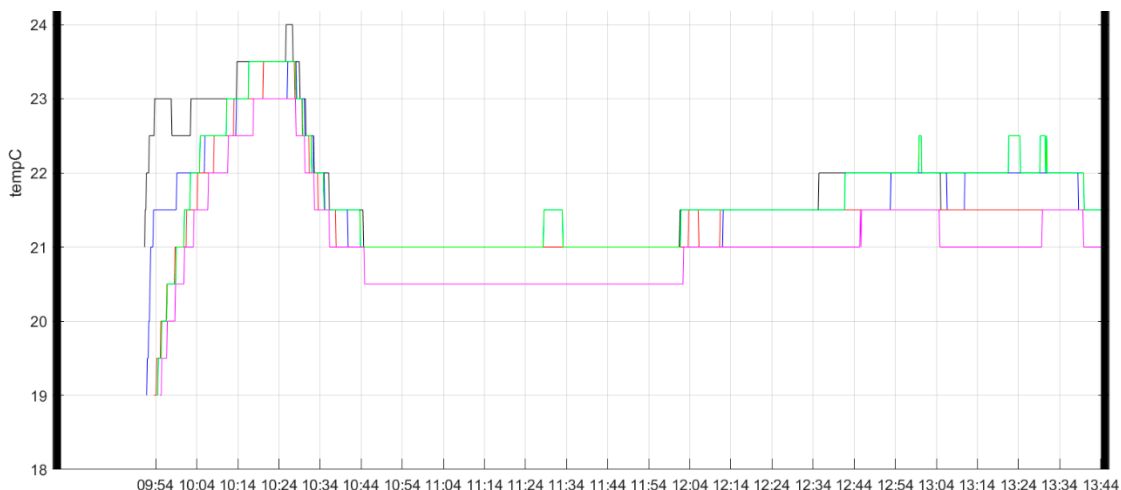


Figure 8: Temperature measurement results obtained in the A320 during cruise flight. Particle dispersion measurement runs were performed between 10:28 and 13:27. Colours indicate the different measurement positions

Temperatures found are lower than those mentioned in literature (NLR & RIVM, 2020), which indicated an average cabin temperature of  $24.4\text{ °C} \pm 2\text{ °C}$ . Except for the first few minutes (before particle dispersion measurements were started), temperatures found during measurements are within two standard deviations of the mean value obtained from literature.

Results of infrared temperature recordings showed sidewall, floor and ceiling temperatures to vary between  $17\text{ °C}$  and  $19\text{ °C}$  – a few degrees below the ambient temperature. B787 values were on the lower end of this range; A320 on the upper end.

#### Relative humidity

For all scenarios, the relative humidity decreased over the course of the measurement, as illustrated in Figure 9. Initial values mostly ranged around 40%, with initial values in the B787 notably lower (below 30%). Final values converged to values between 30 and 35% in case of the ground measurements (simulating taxi) and to approximately 10% in case of flight measurements.

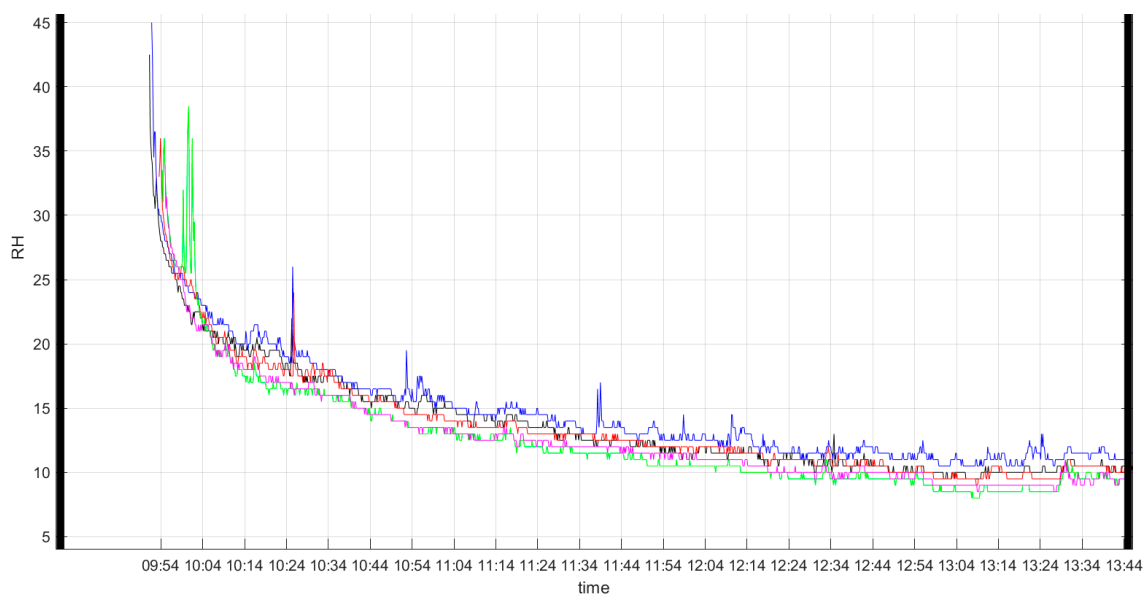


Figure 9: Relative humidity measurement results obtained in the A320 during cruise flight. Particle dispersion measurement runs were performed between 10:28 and 13:27. Colours indicate the different measurement positions

Literature reviewed in-flight values for cabin relative humidity of  $11\% \pm 5\%$  (NLR & RIVM, 2020), corresponding well with the in-flight values observed in measurement results obtained in the current study. Similarly, the reduction in relative humidity during the course of the flight is discussed in literature as well.

#### Air flow direction

A rearward flow (from the front to the aft of the measurement grid) was observed in all scenarios, with variations between aircraft types, measurement situations and measurement runs. For one case, this is illustrated in Figure 10.

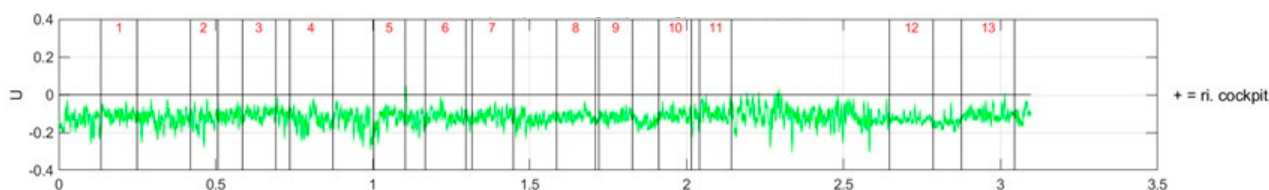


Figure 10: Longitudinal (front / back) air flow direction measurement results in metres per second obtained in the B737 during cruise flight. Positive values indicate a flow towards the front of the aircraft; negative values a flow towards the rear. The horizontal axis shows time (in hours), with the numbered vertical lines indicating particle dispersion measurement runs, conducted in parallel to the environmental measurements

#### Air exchange rate

Literature previously identified indicated that the cabin air is exchanged between 10 and 30 times per hour (NLR & RIVM, 2020). Given the large number of inlets and outlets and fluctuations over time due to changing conditions, this was difficult to measure directly with the in-cabin measurements. A proxy indicator could be the time between the instant the aerosol generators stopped emitting aerosols and the end of the measurement run. Each measurement run lasted from injection of the first aerosols until the aerosol concentration returned to the background concentration. This time varied between 3:42 and 8:12 whilst on the ground and 2:40 and 7:37 during cruise. If this is indeed indicative of the time until the cabin air is refreshed, the corresponding refresh rates would vary between 7.3 and 22.5 refresh rates per hour.

## 3.3 Chapter conclusions

Temperature was found to vary between 19 °C and 24 °C, mostly converging to values between 21 and 22 °C over time. Relative humidity was found to be low, especially in the cruise phase, where it converged to approximately 10%. In all aircraft, a rearward flow was observed. Literature notes cabin air exchange rates between 10 and 30 times per hour. Although this could not be directly measured, similar variation was observed in the measurements. The paragraphs below document how these findings were used in the remainder of the research.

#### Relative humidity

Due to the low values for relative humidity found (especially in the cruise phase), the air flow model used for studying particle dispersions using simulations (in which only the cruise phase is further studied) does not take relative humidity into account. These effects are, however, taken into account in the way the particle source is modelled. This is further treated in Chapter 4.

#### Airbus A320 (A320)

A mean cabin air temperature of 24 °C is used for the A320 simulations. This value is some 3 °C higher than the values found from measurements during the cruise phase, but was selected as it is the ambient temperature value at which air inflow values were specified in manufacturers information (used for the simulation, as described in Section 5.1.2).

A pressure difference between the front and the rear boundary of the 7-row cabin section simulated was used to replicate the rearward flow direction.

#### *Boeing 787-8 (B787)*

An ambient temperature of 22 °C is used for the B787 simulations, based on measurements. Similarly, a rearward component to the flow direction was modelled.

#### *Boeing 737-800 (B737)*

The B737 was studied in addition to the aforementioned two types, using measurements only. It was therefore unnecessary to determine cabin environmental conditions of this aircraft for use in simulations. The results show that values for temperature and relative humidity in the B737 are similar to the A320 and are in line with literature.

## 4 Source

This chapter describes the methodology and main assumptions, results and chapter conclusions related to passenger carrying the SARS-CoV-2 virus, the previously defined ‘index passenger’. It is emphasised that, by research design, the (single) index passenger is the only SARS-CoV-2 source in the cabin<sup>15</sup>.

### 4.1 Methodology

This section discusses the methodology used to represent a SARS-CoV-2 index passenger in both the measurement (Section 4.1.2) and simulation campaign (Section 4.1.3). First, Section 4.1.1, summarises knowledge obtained from literature about the characteristics of an actual source.

#### 4.1.1 Literature

In all scenarios, one passenger on board carried the SARS-CoV-2 virus. This passenger was called the ‘index passenger’. Via breathing and speaking the index passenger emitted aerosols containing viral particles. The viral concentration in the mucus of the index was assumed to follow a lognormal distribution with mean = 7.53 and sd = 1.28 RNA copies / mL (Schijven, et al., 2021). It was assumed that viral particles were emitted in an aerosol cloud during breathing (80% of the time) and speaking (20% of the time). The total volume of aerosol emitted per minute was based on Fabian et al. (2011) for breathing and Duguid (1945; 1946) and Asadi et al. (2019) for speaking, as described in Schijven et al. (2021).

A super shedder was assumed to emit the virus at a concentration in the mucus of  $10^{10}$  RNA copies / mL. RIVM data indicated that 2.7 % of the people infected with SARS-CoV-2 have concentrations of  $10^{10}$  RNA copies / mL or higher in their mucus (Schijven, et al., 2021). A super shedder or spreader is sometimes also defined as someone with above-average particle production, this was not included in the current study.

Under the influence of low humidity, as is the case in aircraft cabins, aerosolised droplets  $<60 \mu\text{m}$  quickly decrease in diameter by a factor three due to evaporation (Liu, Wei, Li, & Ooi, 2017). It was assumed that only water evaporated and that viral particles remain unaffected (Schijven, et al., 2021). When masks were worn, a particle size-independent reduction in droplet and aerosol emissions based on literature data (NLR & RIVM, 2020) was assumed. Due to lack of quantitative data, in the dose-response relation used to estimate risk of illness possible increased likelihood of infection and disease as a result of low relative humidity could not be taken into account (Courtney & Bax, 2021; Schijven, et al., 2021). The applied dose-response relation is the best current available estimate, to our knowledge (Schijven, et al., 2021).

Mask effects on both the index passenger and receiving passengers were applied as an adjustment factor based on literature values for the QMRA. This is further detailed in Section 6.1.3 and discussed in Section 7.3.

<sup>15</sup> Transmission of aerosolised SARS-CoV-2 particles from the ventilation system is not considered. Section 5.2.4 presents results to support that choice.

## 4.1.2 Representation in measurements

The measurement section of the cabin was filled with manikins representing cabin passengers during the measurement runs. At the location of the index passenger, a nozzle was mounted to the head of the manikin. This nozzle was connected to an aerosol pump that was used to inject a fixed amount of artificial saliva into the cabin in multiple puffs. Depending on the measurement run, the nozzle was either uncovered or covered by a non-medical face mask in order to replicate the effect of a face mask on the index passenger.

The nozzle connected to the aerosol generator was tweaked to emulate the particle size distribution of aerosolised droplets as produced by humans. After evaporation of liquid components, the generated particle diameters were in the range of 0.3 to 5.5  $\mu\text{m}$  (see Figure 12). Aerosol emission by humans during speaking and breathing is known to also include larger particles. For translation of the findings to the QMRA, it was assumed that the transfer of these larger particles (up to 20  $\mu\text{m}$ ) was the same as that observed for the smaller particles used in experiment. The characteristics of the injection of the fluid was validated in a laboratory setup to account for losses and initial evaporation. Table 18 in Appendix B.2.1 contains the specification of the synthetic saliva.

Note that the number of aerosols released in the cabin for measurements was exaggerated ( $\pm 7$  million) on purpose in order to obtain reliable counts for determining the fractions used in the QMRA, described in Chapter 6.

Figure 11 shows the source / index passenger, equipped with a nozzle, during the measurements inside one of the aircraft.



Figure 11: Nozzle connected to aerosol generator at index passenger location

### 4.1.3 Representation in simulations

In the simulations, the aerosol cloud was assumed to leave the mouth/nose after which it reached its starting position for the simulation. This starting position was modelled as a sphere with a diameter of 10 centimetres, located 10 centimetres in front of the index passenger. At the starting position all aerosols were uniformly distributed within the sphere. The particle size distribution at the starting position was defined by the two source definitions (breathing and speaking), described in Section 4.1.1. Any potential impact of a mask on the starting position and particle size distribution were not included in the simulation. Complementing the measurements, the particle range could be expanded to 20 micrometres in simulations (see Figure 12). Possible changes in droplet size<sup>16</sup> between emission at the mouth or nose to the starting position is not modelled, but was already accounted for in the source definitions. At the start of the simulation all initial evaporation is assumed to be complete as explained in section 4.1.1. Again, the number of aerosols inserted (1 million) was exaggerated to aid the simulation fidelity when determining the fractions used in QMRA, described in Chapter 6.

## 4.2 Results

Measurements could emulate the particle size distribution of aerosolised droplets up to 5.5  $\mu\text{m}$  in diameter due to physical nozzle constraints. With simulations, larger sized particles up to 20.0  $\mu\text{m}$  were replicated. While low in numbers, these larger particles contain a large part of the total volume emitted.

Figure 12 below provides a direct comparison of the emitted particles size distribution. Larger-size images are included in Appendix B.4.

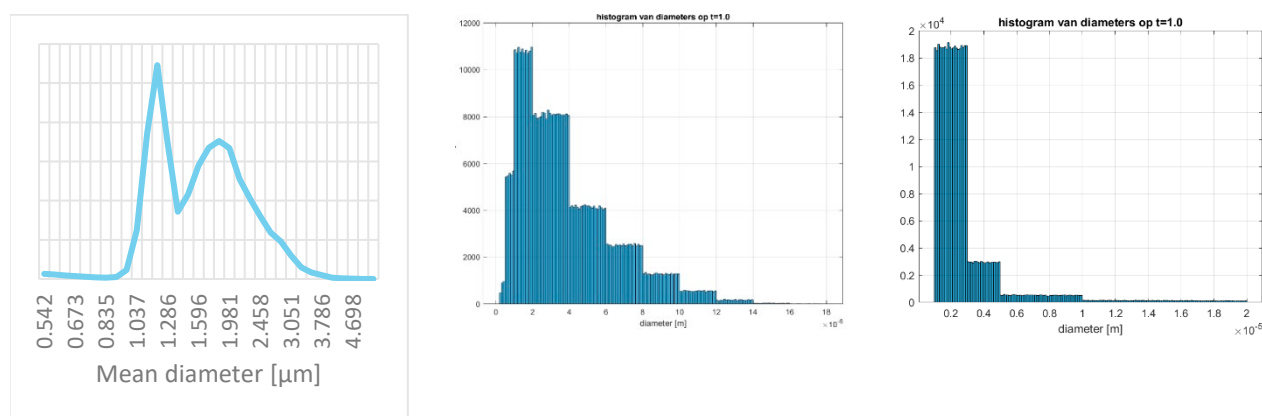


Figure 12: Direct comparison of the particle size distribution used in the measurements and CFD simulations. Please refer to Appendix B.4 for larger images

The results presented here are without a mask on the index passenger and after initial evaporation has been assumed complete. Section 5.2.3 describes the measurement observations related to a mask on the index, Section 7.3 discusses more broadly the impact of masks on aerosol dispersion.

<sup>16</sup> For example through splitting, coagulation and evaporation

## 4.3 Chapter conclusions

The emission of aerosolised droplets by the index passenger was represented in both measurements and simulations. In measurements, particle sizes ranged between 0.3 and 5.5  $\mu\text{m}$ , distributed as such to represent human speech. In simulations, particle size distributions representative of both speaking (0.25 – 18  $\mu\text{m}$ ) and breathing (1.0 – 20  $\mu\text{m}$ ) were used, allowing to model the dispersion of larger droplets, carrying a larger dose of viral particles. Initial droplet evaporation was not modelled<sup>17</sup>, but taken into account in the definition of the initial cloud of particles emitted.

For the viral load of the index passenger, two situations have been defined. In addition to the normal variation in viral load (following a lognormal distribution with mean = 7.53 and sd = 1.28 RNA copies / mL), a super shedder was defined with a viral load of  $10^{10}$  RNA copies / mL.

Mask effects on both the index passenger and receiving passengers were applied as an adjustment factor based on literature values for the QMRA. This is further detailed in Section 6.1.3 and discussed in Section 7.3.

---

<sup>17</sup> This occurs in the first brief moments after exhalation (Morawska, 2006).

## 5 Particle dispersion

Following the description of cabin environmental conditions and source properties in Chapters 3 and 4, this chapter presents the methodology and findings related to the dispersion of aerosols through the cabin. Research methodology is discussed in Section 5.1 and main findings are presented in Section 5.2. Section 5.3 presents chapter conclusions, summarising the outcomes of this part of the study for use in subsequent steps.

### 5.1 Methodology

This section describes the methods employed for investigating particle dispersion on board of aircraft cabins, in both the measurement and simulation campaigns.

#### 5.1.1 Measurements

The goal of the measurement campaign was to collect data on the dispersion of emitted particles by the index passenger amidst seven rows of passengers and to assess the impact of certain selected parameters that were not assessed with simulations, such as mask wear and gasper setting. Within the time for the measurements, priority was given to cover the impact of a large number of variables over repetition of identical scenarios. The measurements were performed during taxi and cruise flight conditions.

Taxi measurements were performed at a remote location at the airport where the aircraft could remain stationary with the main engines running and powering the environmental control system and the Auxiliary Power Unit (APU) switched off. This set-up replicated regular taxi conditions. In-flight measurements were performed at cruise altitude under normal operating conditions, in level and steady flight. These measurements were instrumental to account for the large pressure difference between the atmosphere at cruise altitude and the pressurised cabin, which would be difficult to replicate on the ground.

As indicated in Chapter 2, all measurements were performed in the rear economy-class section, with the index passenger positioned in the middle row of a 7-row measurement grid (row '0' in Figure 6, page 15). In the single-aisle aircraft, the index passenger was located in seat E (the middle seat in the right block of three seats, also see Figure 5 on page 14). In most of the twin-aisle measurements, the index passenger was located in seat E (the middle seat in the centre block), but index locations in seats B and C were also studied. More detailed schematic representations of the measurement grids are included in Appendix B.2.2.

Lifesize manikins were placed on the seats inside the grid to replicate the physical presence of the passengers. Electric heating blankets were placed on the manikins during ground testing<sup>18</sup> to replicate the heat signature of human passengers. One seat behind-and-to-the-left of the index passenger was left empty for the operator of the aerosol generator<sup>19</sup>. Figure 13 below shows the manikins without blankets prior to a ground measurement. Appendix B.2.2 shows the measurement grids and equipment positions.

---

<sup>18</sup> Due to safety restrictions these blankets could only be powered whilst on the ground.

<sup>19</sup> As the operator was wearing a face mask and the aerosol emission from the index passenger was exaggerated substantially in comparison to a normal person (as indicated in Section 4.1.2), it is unlikely for the operator to have significantly affected measurement results.



Figure 13: Measurement section including manikins ready for ground measurements

### Particle sensing

To detect aerosol particle number and size distribution per seat, sixty particulate matter (PM) sensors and two Aerodynamic Particle Sizer (APS) sensors were used (see Appendix B.2.1 for specifications). PM sensors were placed on all manikins inside the measurement grid. In case of the single-aisles, additional manikins positioned in two rows in front of the measurement grid (separated by two empty rows), were also equipped with PM sensors. One APS sensor was placed right next to the source with the inhalation tube tilted towards the source. The other APS sensor was placed two rows in front of the source.

The PM sensors had a native measurement range of 0.3 to 2.5  $\mu\text{m}^{20}$  and were used to measure the particle concentration (number / volume) in each seating location. The APS sensors had a native measurement range of 0.5 to 20.0  $\mu\text{m}$  and were used to determine the size distribution of the particles. For the determination of the particle dispersion in number and sizes of the particles, measurements from both sensors were combined as shown in Table 2.

Table 2: Methodology for determining particle distribution combining PM and APS sensor readings

Variable	Description	Method
$f_{0.5-2.5}$	Percentage of particles 0.5 to 2.5 $\mu\text{m}$	Direct reading from APS sensor next to source as measured during cruise
$f_{0.5-1.0}$	Percentage of particles 0.5 to 1.0 $\mu\text{m}$	Direct reading from APS sensor next to source as measured during cruise
$f_{1.0-2.5}$	Percentage of particles 1.0 to 2.5 $\mu\text{m}$	Direct reading from APS sensor next to source as measured during cruise
$f_{2.5-4}$	Percentage of particles 2.5 to 4.0 $\mu\text{m}$	Direct reading from APS sensor next to source as measured during cruise
$f_{4-10}$	Percentage of particles 4.0 to 10.0 $\mu\text{m}$	Direct reading from APS sensor next to source as measured during cruise
$N_{\text{TOT}}$	Number of particles 0.5 to 10.0 $\mu\text{m}$	$(N_{0.5-1.0} + N_{1.0-2.5}) / f_{0.5-2.5}$
$N_{0.5-2.5}$	Number of particles 0.5 to 2.5 $\mu\text{m}$	Direct reading from PM sensor at seat
$N_{0.5-1.0}$	Number of particles 0.5 to 1.0 $\mu\text{m}$	$N_{\text{TOT}} \times f_{0.5-1.0}$
$N_{1.0-2.5}$	Number of particles 1.0 to 2.5 $\mu\text{m}$	$N_{\text{TOT}} \times f_{1.0-2.5}$
$N_{2.5-4}$	Number of particles 2.5 to 4.0 $\mu\text{m}$	$N_{\text{TOT}} \times f_{2.5-4}$
$N_{4-10}$	Number of particles 4.0 to 10.0 $\mu\text{m}$	$N_{\text{TOT}} \times f_{4-10}$

<sup>20</sup> The native range is also the range where the sensor provides the most accurate readings

### Measurement conditions

Under predetermined conditions and for a set time, aerosol particles were emitted from the index location. The spread of these particles through the cabin was monitored for several minutes, until all sensors measured only background concentrations. Table 3 shows the conditions which were varied within the experiments to gauge the effect of certain conditions on particle dispersion.

Table 3: Conditions varied in particle dispersion runs

Parameter	Single-aisle	Twin-aisle	Rationale
Phase of flight	Cruise, taxi	Cruise, taxi	Two phases of interest, due to different cabin air pressure levels
Gaspers settings	All closed, middle open, all open	Middle gaspers open	Possible (local) effect on dispersion, easy to manipulate
Mask on index	New mask, reused mask, no mask	New mask, reused mask, no mask	Assess the effect of a face mask on particle dispersion in an aircraft
Heated blankets on manikins	On, off	On, off	Simulate heat coming from passengers, which changes air flow in the aircraft.
Pack settings	Normal, high	Normal	Possible (cabin) effect on dispersion
Location of index	Seat E	Seats E, B, C	Effect of location infected passenger on particle distribution

The results from (comparing) different measurement conditions provide an indication of the influence of selected parameters on particle dispersion:

- Mask usage on index (no mask, new mask, re-used mask)
- Gasper setting (all gaspers closed, middle gaspers open, all gaspers open)

## 5.1.2 Simulations

Dispersion of aerosols was simulated across seven rows of passengers in a ventilated aircraft cabin. A Reynolds-averaged Navier-Stokes (RANS) method was used to model the air flow and the dispersion of particles in the aircraft cabin (NLR & RIVM, 2020). This takes into account the cabin configuration of the aircraft types studied, cabin environmental conditions and ventilation system properties. Buoyancy effects due to heat sources inside the cabin (cabin occupants, primarily) were modelled using the Boussinesq approximation (Boussinesq, 1897). As indicated in Chapter 2, only the A320 and B787 were studied using simulations.

### Cabin configuration

A fully occupied 7-row economy class cabin section was modelled<sup>21</sup>. Passengers were modelled according to Tanabe et al. (2002), unmoving and in a seated and forward-looking position. Seats were positioned in their upright position with tray-tables stowed away and all luggage was assumed to be stored in luggage bins.

<sup>21</sup> Periodic boundary conditions were set at both ends of the cabin (following, e.g., Gupta, Lin, & Chen, 2011; Davis, Menard, Clark, Cummins, & Olson, 2021; Davis, et al., 2021), which allow air to flow through the cabin in a longitudinal direction without prescribing a velocity.

### *Cabin environmental conditions and air inflow*

Stable cabin environmental conditions were used: a constant pressure and constant cabin temperatures, the latter specified as in Chapter 3.

Inflow of air was modelled through side, ceiling and (only for the B787) gasper inlets. For the A320, cruise-flight manufacturer specifications were used. For the B787, the inflow rates per inlet (side, ceiling and gasper) were selected such as to limit differences between measurement and simulation results (based on the comparisons described in Sections 5.1.3 and 5.2.1). For both aircraft, the inflow temperature was set such to maintain a constant cabin temperature.

### *Heat sources and thermal conditions*

Based on measurement results (described in Chapter 3), surfaces inside the cabin (the seats, the luggage bins, the floor<sup>22</sup> and the roof<sup>23</sup>) were treated as adiabatic, whereas for the sidewalls, fixed temperatures were set (varying between 17° and 19°C). Although measurement results showed variations, constant temperatures were used in the simulations – as is common practice (e.g. Gupta, Lin, & Chen, 2011; Davis, Menard, Clark, Cummins, & Olson, 2021; Davis, et al., 2021). Temperature and heat emission of cabin occupants was modelled according to Tanabe et al. (2002).

### *Particle trajectory modelling*

Following the introduction of particles into the simulation as described in Section 4.1.3, their trajectories were modelled. The influence of air flow (in turn, influenced by e.g. inflow and outflow and buoyancy effects due to cabin occupants emitting heat) and gravity on droplet trajectories is modelled, whereas the possible influence of inhalation and exhalation by or movement of cabin occupants was not included. Lacking knowledge on the behaviour of droplets upon coming in contact with the aircraft cabin surfaces, droplets were conservatively modelled to bounce back rather than to stick to the surface<sup>24</sup>. Interactions between droplets were not modelled and the size of droplets was modelled to remain fixed during their movement through the cabin.

In each simulation run, various quantities were logged to derive the input for the QMRA described in Chapter 6. These quantities were determined for inhalation boxes, defined as 30 × 30 × 30-centimetre cubes, centred at the nose of other cabin occupants, based on Gupta et al. (2011). These boxes are illustrated in the schematic representation shown in Figure 14. The inputs to the QMRA model were:

- The residence time of each particle that entered an inhalation box. Particles with the same residence time were grouped. The total volume of aerosol particles and the corresponding residence time, at a one-second resolution, was exported as input for the QMRA.
- The number and volume of droplets per size (diameter) bin in each inhalation box.

<sup>22</sup> Only for the A320. A fixed floor temperature was set for the B787.

<sup>23</sup> Only for the B787. A fixed roof temperature was set for the A320.

<sup>24</sup> In case modelling droplets bouncing back was not feasible, due to limitations with respect to computational effort, (partial) stick was modelled.

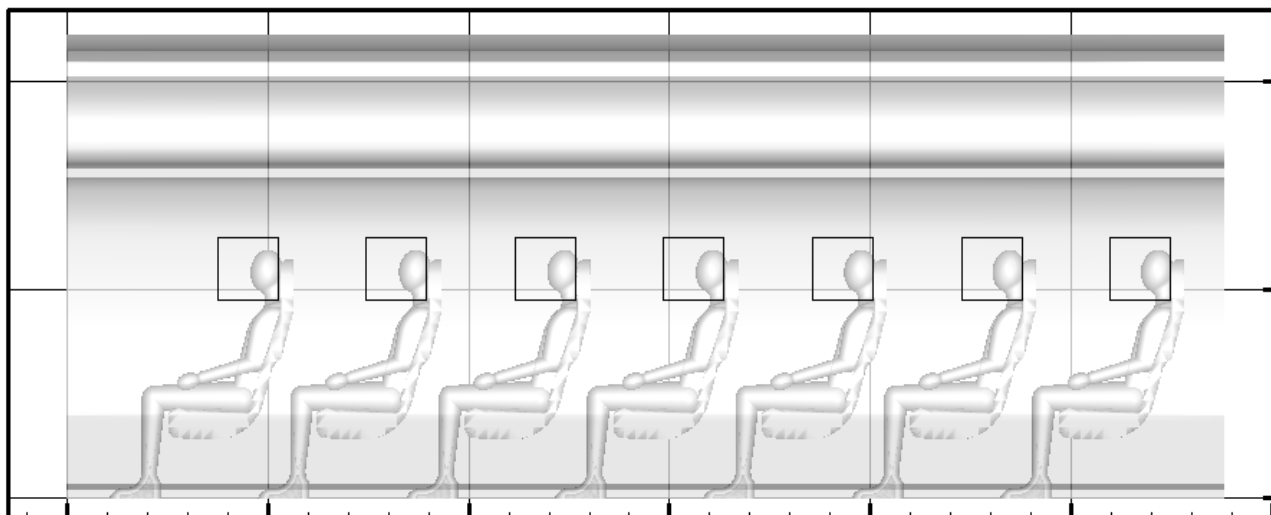


Figure 14: Schematic representation of the 7-row cabin section modelled in the simulations, viewed from the side, showing the 30 × 30 × 30-centimetre inhalation boxes, centred at the nose of the cabin occupants

As the influence of inhalation and exhalation on cabin air flow has not been included in the model, possible impacts of a mask on the direction and speed of air inhaled and exhaled are not modelled either. Following inconclusive literature on the subject, the filter efficiency of the mask is assumed to hold for all particle sizes, such that the mask does not alter the size distribution of particles exhaled.

The model has been used to evaluate particle dispersion in a number of different scenarios in order to gather the required input for the QMRA, described in Chapter 6. These are defined in Table 4.

Table 4: Definition of scenarios used for simulations, providing input to the QMRA

#	Scenario	Aircraft type	Situation		
			Flight phase	Gasper use	Source characteristics
1	A320-Flight-Breathe	A320	Cruise flight	Closed	Breathing
2	A320-Flight-Speak	A320	Cruise flight	Closed	Speaking
3	B787-Flight-Breathe	B787	Cruise flight	Middle gaspers open	Breathing
4	B787-Flight-Speak	B787	Cruise flight	Middle gaspers open	Speaking

Mask effects were not included in the simulation model but were applied as an adjustment factor based on literature values in the QMRA. This is further detailed in Section 6.1.3. All scenarios listed above are therefore without mask.

In addition to the scenario results (presented in Section 5.2.2), simulations were used to investigate the effect of index passenger location. These results are presented as part of Section 5.2.3.

### 5.1.3 Comparison between measurements and simulations

To improve the quality of the findings based on measurements and simulations, both were compared in similar scenarios. To ensure an accurate comparison, environmental conditions and other input parameters used for the simulations were matched to those observed during the measurements. The comparison was done based on the total number of particles counted by each sensor, per one million particles simulated. In the experimental campaign, the sensor was formed by the measuring equipment (specifically the PM sensors, described in Section 5.1.1). For the

simulations, a separate sensing model was used<sup>25</sup>, with a flow rate identical to the flow rate of the equipment used for the experiments.

Results from measurements and simulations were compared for two scenarios, based on the opportunity to replicate these accurately in both the measurement and simulation campaign. Table 5 shows which scenarios have been compared.

Table 5: Definition of scenarios used for model validation

Parameter	Value in comparison scenario 1	Value in comparison scenario 2
Aircraft type	Airbus A320 (A320)	Boeing 787-8 (B787)
Flight phase	Cruise	Cruise
Pack settings	Normal	Normal
Gasper settings	Closed	All gaspers above middle seats <sup>26</sup> open, pointing straight downwards
Cabin occupant heat emission	None	None

## 5.2 Results

Using both in-cabin measurements and simulations, the study assessed how the cabin flow conditions disperse the aerosols emitted by the index through the cabin. This section shows the main results from both the in-cabin measurements and particle dispersion simulations, presenting the outcome of the comparison between measurements and simulations (Section 5.2.1), the results of cruise flight and taxi particle dispersion results (Section 5.2.2), the influence of select variables (Section 5.2.3) and recirculation of aerosols through the ventilation system (Section 5.2.4).

All results are expressed in number of particles or volume of particles per one million particles emitted by the index passenger for the situation without masks, gaspers closed and normal pack settings, unless stated otherwise. Appendix B.5 includes samples of the data discussed in this section.

### 5.2.1 Comparison between measurements and simulations

Table 6 shows the differences (in the total number of droplets observed per seat, per one million particles emitted by the index passenger) between the measurement and simulation results for each of the two comparison scenarios defined in Section 5.1.3, averaged over all seats – with exception of the index location and operator seat – in the 7-row cabin model studied. On average, the simulation results show 50% (A320) or 70% (B787) more particles per seat compared to the measurement results.

<sup>25</sup> This sensing model models inhalation by a continuous inflow at a specified rate. Assuming equal dispersion of particles over the inhalation box, the particle concentration in 'inhaled' air is equal to the particle concentration in the inhalation box – even though the volume inhaled is a fraction of the volume of the inhalation box.

<sup>26</sup> The gaspers mounted in overhead panels were positioned rather to the centre of each set of (three) seats. Sets of three gaspers were positioned above seats B and J (the seats directly adjacent to the window seats on both sides of the cabin), of which the middle ones were opened. A set of four gaspers was positioned above seat E (in the middle of the cabin), of which the 2<sup>nd</sup> gasper (counting from left to right) was opened. Seat lettering referred to is defined in Figure 6, shown on page 20.

Table 6: Differences in the averaged total number of particles observed per seat in 7-row section, per one million particles emitted by the index passenger, between the measurement and simulation results for the two comparison scenarios

Comparison scenario (aircraft type)	Measurement result	Simulation result	Difference
1 (A320)	20	30	10 (50%)
2 (B787)	11	19	8 (70%)

A possible explanation for higher mean particle counts is the conservative choice to model droplets bouncing back from the surfaces they come into contact with, rather than having them (partially) stick to the surface. Due to this modelling choice, the number of particles that flow through the cabin remained larger<sup>27</sup>, yielding higher concentrations.

Figure 15 shows the differences between the dispersion of all observed particles over rows for both comparison scenarios. Note that, as the dispersion of particles is shown normalised to all observed particles in that situation (measurement or simulation), the absolute differences shown in Table 6 is not shown in these figures.

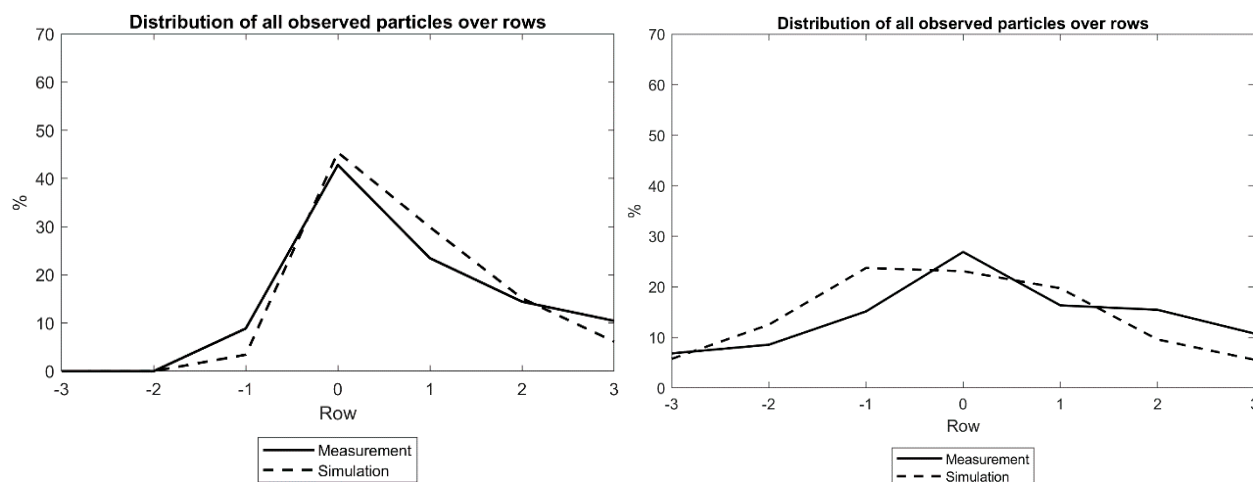


Figure 15: Dispersion of all observed particles over rows in numbers for measurement and simulation in comparison scenario 1 (A320; left) and 2 (B787; right). The sum of the values over the rows is normalised to 100%

For both aircraft, the dispersion over rows and row groups determined using the simulation model is judged to up to a factor 2 in the above figures on row level to these same results obtained from measurements. As comparisons between measurement and simulation results showed large variations in particle distribution along the lateral axis (left / right), the simulation model was found to be unsuitable for seat-by-seat comparisons.

More detailed comparisons and additional simulations performed to better understand differences and their possible causes furthermore identified a number of parameters that can have a noticeable effect on particle counts at seat level:

- initial particle cloud position;
- empty seats, or seats occupied by measurement equipment;
- gasper location and direction; and
- local air flow pattern

<sup>27</sup> If a particle would stick to the surface, it would be effectively removed from the cabin air, lowering the total number of particles flowing through the cabin.

Overall, the comparison between results obtained from measurements and simulations shows that, based on the average particle count over all seats in the 7-row cabin section, the simulations indicate a higher number of particles. The observed difference is larger for the B787 than for the A320. The dispersion over rows is judged to compare to these same results obtained from measurements in a similar way as for the A320. As such, the simulation model is concluded to be suitable for modelling conservatively the dispersion of particles for determining the risk of illness through transmission of aerosolised SARS-CoV-2 on board of aircraft.

## 5.2.2 Particle dispersion in different scenarios

This section presents the results from the particle dispersion measurements and simulations for a number of scenarios. As the QMRA (described in Chapter 6) will model the effects of mask usage based on literature, the results of the scenarios presented here are for the situation without masks. Results speaking to the effects of mask usage, as studied using measurements, are presented in Section 5.2.3.

### *Cruise conditions – without mask*

Without a mask on the aerosol generator at the index location, open gaspers and normal pack flow settings the measurements showed a consistent dispersion pattern during most measurement runs in cruise conditions. Peak concentrations appear at the same locations for most runs but the magnitude of the peaks can vary in between runs by a factor of 2 to 3. This could be due to minor variations in cabin flow, gasper attitude or external disturbances.

The two single-aisle aircraft showed similar dispersion patterns with most aerosol volume dispersing towards the rear, due to a rearward cabin flow. The majority of aerosol volume remained on the same side of the aisle as the index location (seats D-E-F). This effect was most prominent in measurements with gaspers open. In the twin-aisle aircraft, a significant share of the aerosol volume was observed in the row in front of the index location (row -1). With the exception of two runs, the index location was in the mid-middle seat of the row (seat E, as indicated in Figure 5). The majority of aerosol volume dispersed with a slight skew to left (seats A-B-C and D-E-F).

Cruise conditions without a mask were also replicated using simulations. As indicated in Section 5.2.1, this resulted in similar volume dispersion per row, but with higher volumes.

### *Taxi conditions – without mask*

In the taxi situation, the two single-aisle aircraft (with gaspers closed) showed a similar aerosol volume distribution per row. Compared to cruise conditions, the distribution is shifted towards the front. For the A320 a rearward skew was still evident, but less pronounced than under cruise conditions. In terms of mean aerosol volume per seat, the two single aisles diverged. While both types displayed mean volumes of the same order of magnitude, the volume observed in the A320 was approximately 2 times less during taxi (total volume for 7 rows), compared to cruise conditions). However, a lot of variation was observed in the statistical analysis. The B737 measurements recorded between 3 and 6 times more aerosol volume per seat (total volume for 7 rows), compared to cruise conditions, depending on gasper configuration.

The twin-aisle showed a similar volume dispersion distribution as during cruise conditions. In terms of mean aerosol volume per seat, the total volume for the 7 rows that were assessed was about 2 times less than under cruise conditions.

Taxi conditions were not assessed using simulations.

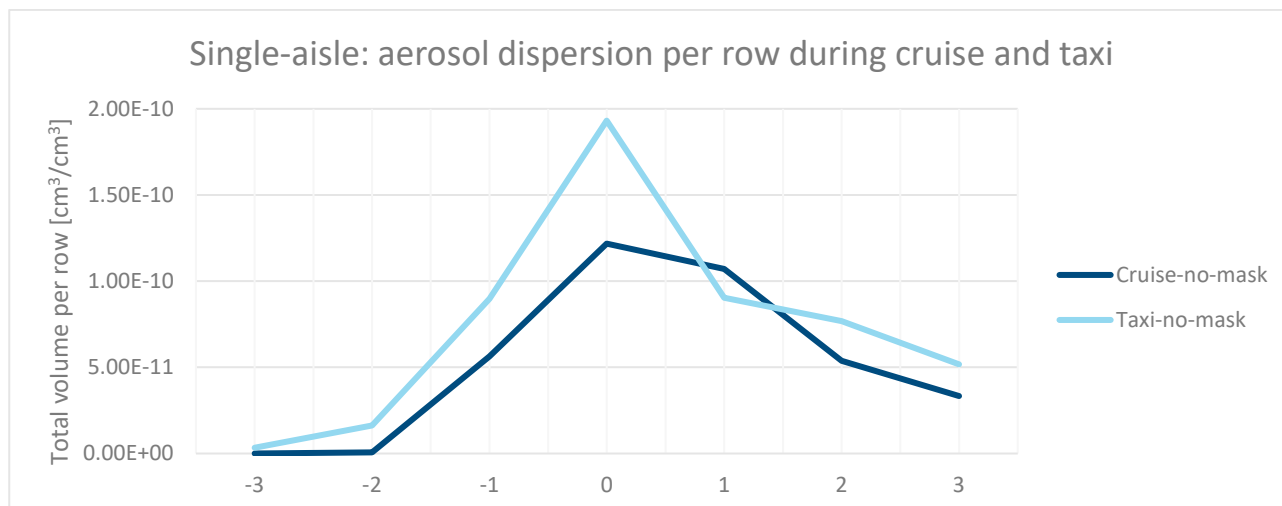


Figure 16: Averaged aerosol volumes per row for all single-aisle measurements without mask (open gaspers during cruise, closed gaspers during taxi)

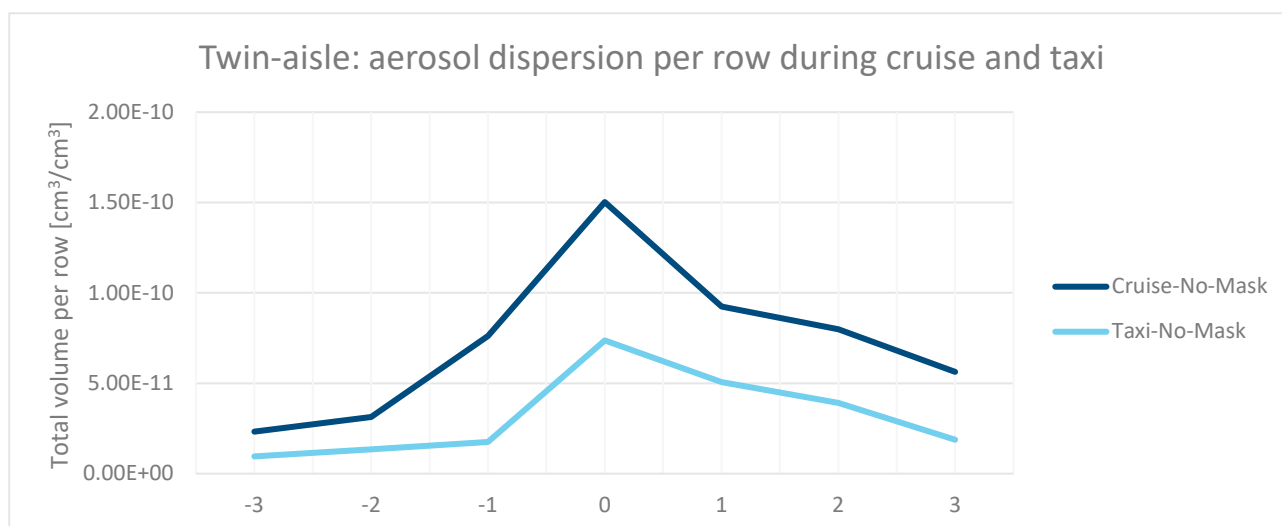


Figure 17: Averaged aerosol volumes per row for all twin-aisle measurements without mask

### 5.2.3 Influence of selected variables on dispersion

#### Mask usage on index

With a mask on the aerosol generator at the index location, open gaspers and normal pack flow settings in cruise flight, the measurements showed a consistent dispersion pattern during most measurement runs. As shown in Figures 18 and 19, concentrations were highest in row 0, which is the row where the index passenger was located. The magnitude of the peaks varied less between runs when the index passenger wore a mask than between runs when not. Compared to the runs without a mask, the mean number of particles was reduced throughout in runs with a mask. For all aircraft types studied, results showed that the mask reduced the number of particles measured in the measurement grid. The reduction in numbers of particles per seat varied through the aircraft. Reduction factors were highest in front of the index row ( $\pm 1.2 - 1.5$  times less compared to runs without a mask) in relative terms. However, since aerosol concentrations were already lower in front of the index passenger, the largest reductions were found aft of the index passenger and in the same row as the index passenger. The comparison between a new and a reused mask shows no substantial differences in number of particles measured.

For both single-aisle aircraft, measurement runs with a mask showed peak aerosol concentrations of the same order of magnitude. It was observed that for those measurement runs with a mask on the aerosol generator, the mean aerosol volume over all seats in the 7-row measurement grid dropped substantially both during cruise and during taxi. Within this study it could not be determined as to why the observed reduction is stronger than found in literature. Section 7.3 further discusses mask effects.

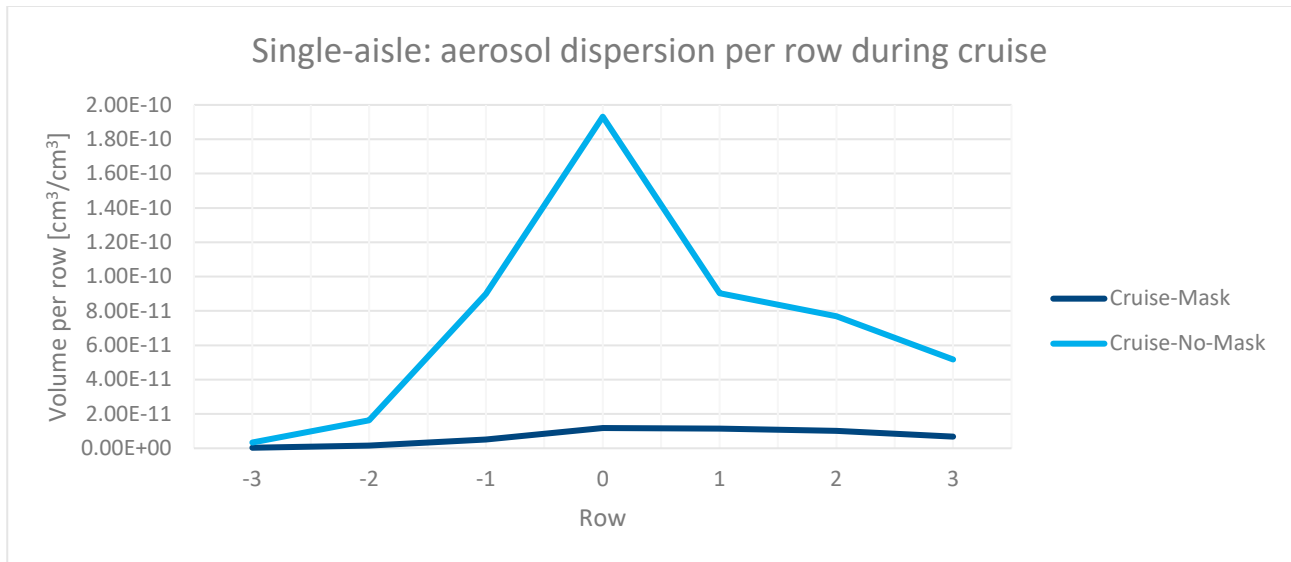


Figure 18: Averaged particle volumes per row for all single-aisle cruise measurements (open gaspers)

For the twin-aisle, it was observed that for those measurement runs with a mask on the aerosol generator the mean aerosol volume over all seats in the 7-row measurement section again dropped significantly both during cruise and during taxi. The effect is less pronounced for the second and third row in front of the index where particle volumes are already lower. Within this study it could not be determined as to why the observed reduction is stronger than found in literature or as to why the impact is stronger in the twin-aisle aircraft. Section 7.3 further discusses mask effects.

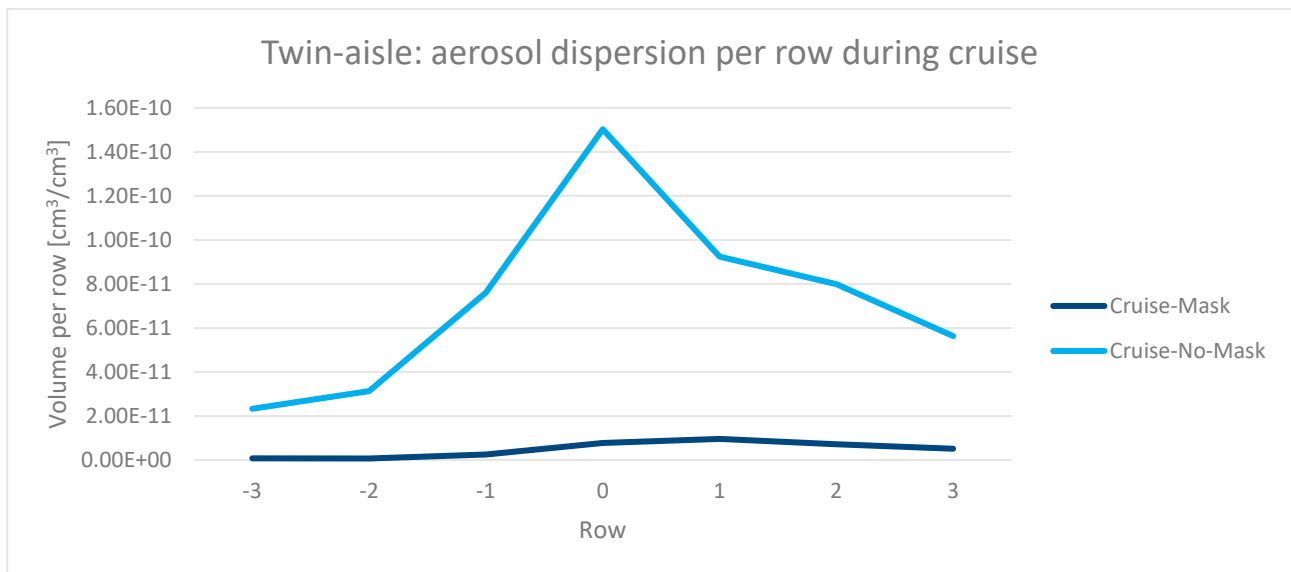


Figure 19: Averaged particle volumes per row for all twin-aisle cruise measurements (open gaspers)

Based on results from APS measurements, the mask was also found to affect the size distribution of particles. In experiments without a mask, a constant particle size distribution was found throughout the cabin that corresponded

well with the particle size distribution at the source and to the particle size distribution as validated in a laboratory setting. In experimental runs with a mask on the aerosol generator, the share of larger particles (1.5 - 4  $\mu\text{m}$ ) was observed to be lower relative to smaller ones (0.5-1.5  $\mu\text{m}$ ). No substantial differences were observed between new masks and masks that had been used for multiple runs. It is possible the mask could have; blocked larger particles more efficiently, absorbed fluid when particles are pushed through, or slowed down aerosols and thus taking them longer to reach the sensors, leaving more time for evaporation to take place. This is further discussed in Section 7.3. Supplementary data is provided in Appendix B.5.2 (aerosol distribution per row) and Appendix B.5.3 (particle size distribution).

#### Gasper setting

Gasper setting (on/off) was varied during measurement runs of the single-aisle aircraft. In the twin-aisle, by instruction from the flight crew, the gasper setting remained open after the first two measurement runs. As such the impact of gaspers on dispersion could only be assessed for the single-aisle aircraft.

The measured aerosol concentrations suggest open gaspers prohibit aerosols from traversing the aisle. On the index' side of the aisle (i.e., seats D, E, and F) and aft of the index, aerosol volumes are sometimes increased by as much as a factor 2. On the opposite side of the aisle (i.e., seats A, B, and C) and aft of the index aerosol concentrations were lowered by as much as a factor 5. Due to aircraft limitations, only two measurements with gaspers closed could be performed in the B787, with the other measurements being conducted with middle gaspers open. In this (limited) comparison, no effect of the gasper could be found.

#### Index location

The index location was varied using simulations for the single-aisle A320 and twin-aisle B787. For the single-aisle, aerosol volume distributions per row with an index in seats D (aisle) and F (window) were highly similar both in case of breathing and speaking. In both seats the index passenger creates a volume distribution skewed to the rear. With an index in seat E (middle seat), the volume distribution is more even but still skewed to the rear.

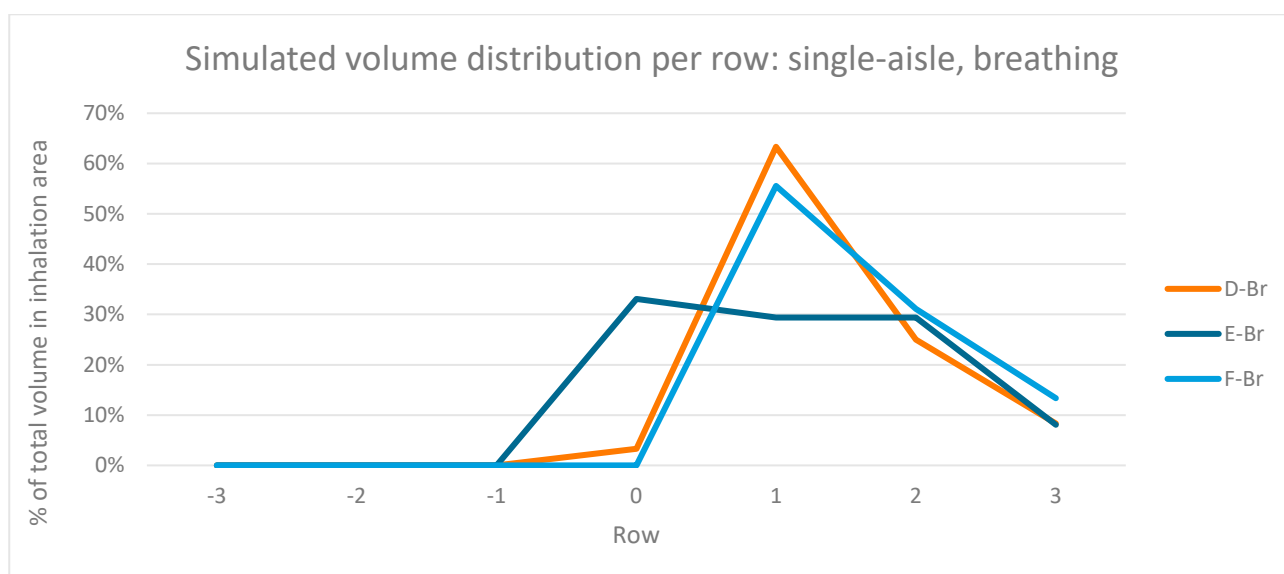


Figure 20: Simulated volume distribution per row for breathing relative to total volume in inhalation area

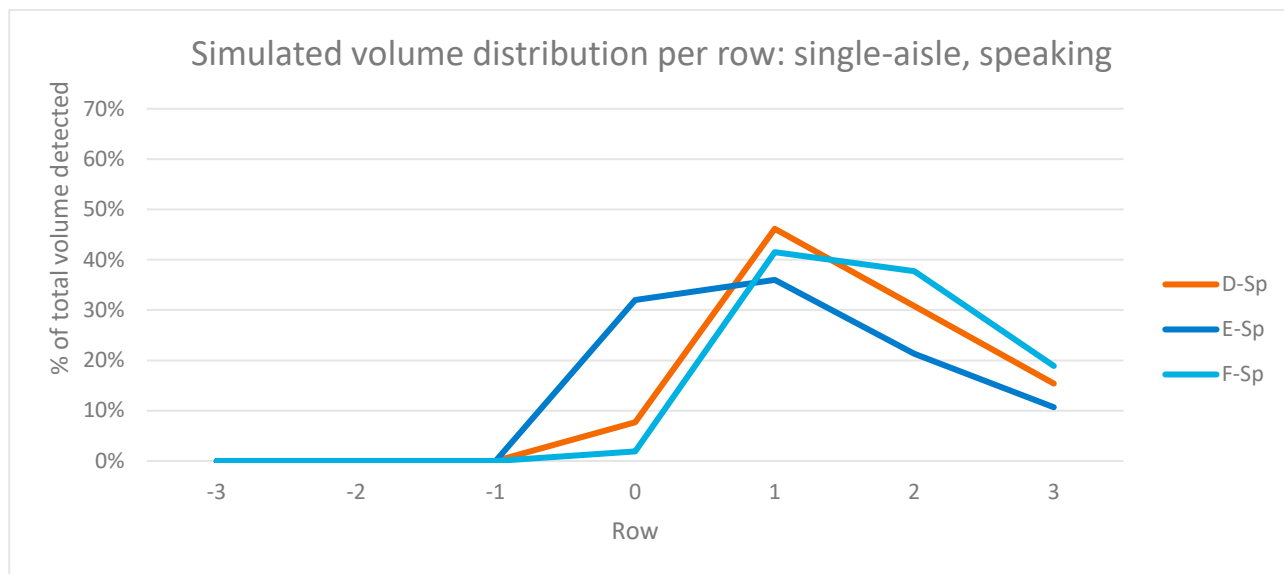


Figure 21: Simulated volume distribution per row for speaking in inhalation area

For the twin-aisle, aerosol volume distributions per row all index locations were highly similar between breathing and speaking. An index directly below an open gasper (seats B and E) showed less dispersion to rows further away from the index (in front of row -1 and aft of row 1) compared to the other index locations.

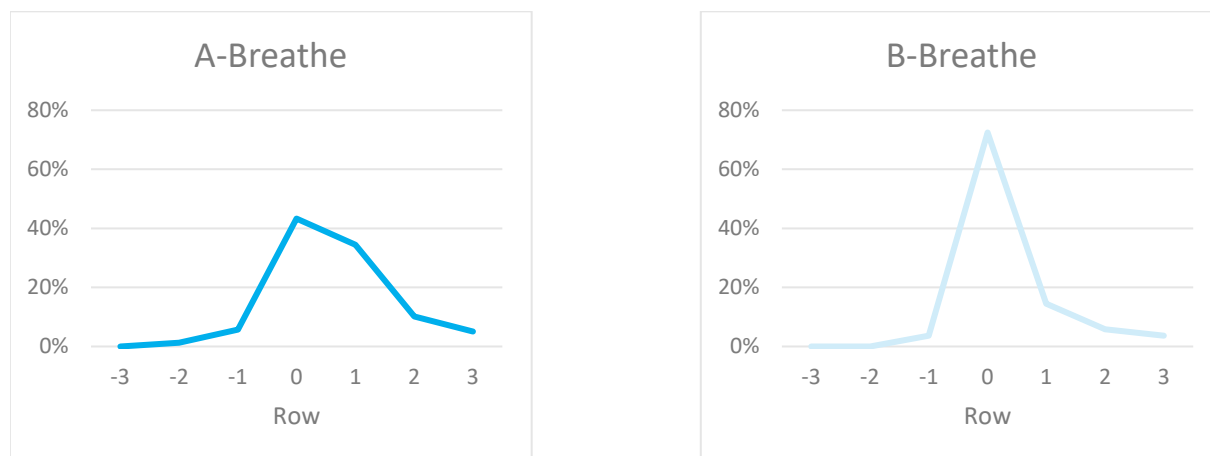


Figure 22: Simulated volume distribution per row for breathing for index location A and B

## 5.2.4 Recirculation of aerosols through ventilation system

During the measurement runs, large quantities of aerosols were injected at the start of each run. The measurements continued until the concentration of aerosols matched the background concentration. Concentrations remained low for all seats in the measurement grid between measurement runs. Also, only very low volumes of aerosols were detected in the two rows in front of the measurement grids (within the same order of magnitude as the uncertainty margin of the PM sensors used). This suggests that, at least in the rear section of the economy class, no detectable volumes of aerosol recirculate from the HEPA-filter-equipped cabin ventilation system<sup>28</sup>. It is uncertain what exact share of air volume is recirculated or discharged by the ventilation system at the specific location in the aircraft cabin.

<sup>28</sup> The environmental control system used in aircraft was described in the literature review (NLR & RIVM, 2020).

## 5.3 Chapter conclusions

Measurement and simulation results on counts of particles dispersed in a 7-row section of a ventilated aircraft cabin showed comparable results at cabin- and row-level. Particle counts from simulations were found to be higher than counts found in the measurements, possibly due to (more) conservative modelling choices. Additional simulations varying particle cloud position, seat occupancy, gasper location and direction and local air flow were found to noticeably affect particle counts at seat level.

In the cruise flight scenario, particle dispersion measurements showed consistent results. The largest fraction of volume was found in the index row and the rows behind the index passenger, mostly so in case of the single-aisle aircraft, and consistent with the rearward flow described in Chapter 3. The rearward skew was less pronounced in the taxi scenario than in the cruise flight scenario, but still evident.

Measurements and simulations were used to study the influence of select parameters: mask usage, gasper setting and index passenger position. Measurement results showed mask usage on the index passenger substantially reduced the number and volume of aerosolised particles observed throughout the cabin. The more emphasised rearward spread that was observed in measurements without the use of a mask, was also seen in with-mask runs. Gasper settings were found to affect the airflow, although with effects varying per aircraft. Lateral spreading of particles in measurements with gaspers on was found to be reduced compared to gasper closed measurements. Simulations with different index positions revealed comparable volume distributions per row, although less variation per row was observed with an index on a middle seat than for indices located at a window or aisle seat.

The detection of very low aerosol volumes in locations further away from the index passengers (but still in the rearward economy section) suggests that recirculation of aerosol particles that might carry SARS-CoV-2 particles from the HEPA-filter-equipped cabin ventilation system is unlikely. It is uncertain what exact share of air volume is recirculated or discharged by the ventilation system at the specific location in the aircraft cabin.

## 6 Risk assessment

This chapter presents the methodology (Section 6.1) and the results (Section 6.2) of the quantitative microbial risk assessment (QMRA).

### 6.1 Methodology

The methodology used for the QMRA is described in this section. It treats exposure evaluation (Section 6.1.1) and risk estimation (Section 6.1.2) methods, defines scenarios and states assumptions (Section 6.1.3) and provides detail on the statistical modelling and analysis performed (Section 6.1.4).

#### 6.1.1 Exposure evaluation

Exposure to SARS-Cov-2 of aircraft passengers during a flight was determined on the basis of the aerosol transmission experiments as well as the simulations.

For the purpose of risk assessment, aerosol concentrations were converted to transfer fractions (referred to as '*frac*'): the fraction of the emitted source that would be inhaled by a passenger located at a particular seat. Extrapolation to different, realistic exposure scenarios was done by assuming that the transfer fractions under real flight conditions are identical to those in experiment. Aerosol exposure of passengers during flight was estimated as the inhaled volume dose, by multiplying the transfer fractions with the aerosol volume emitted through breathing and speaking by an index passenger on board of the flight.

Similarly, simulated aerosol transmissions from the computational fluid dynamics (CFD) simulations (Section 5.1.2) were converted to transfer fractions ('*frac*') at different seats. Transfer fractions obtained from the simulations were used in analogous fashion to the experimentally determined transfer fractions to simulate exposure under realistic flight conditions.

From the inhaled aerosol estimated in flight scenarios, virus dose was estimated by assuming that emitted aerosol initially has a virus concentration similar to that found in human sputum of infected persons (Schijven, et al., 2021). Effects of passengers wearing a standard surgical mask (in the Netherlands known as non-medical mask) were included by assuming fixed removal efficiencies for inhalation (30%) and exhalation (60%).

#### 6.1.2 Estimation of risk

To estimate risk, a dose-response model was used to estimate the probability of illness,  $p_{ill}$  due to inhalation of aerosol contaminated with the virus dose by each passenger (Schijven, et al., 2021). In the evaluation of inhaled aerosol in the exposure scenarios, variability in exposure conditions was accounted for by considering distributions of exposure factors such as inhalation rate, aerosol volume emitted by the index, virus concentration in sputum. On the basis of the distributions of these exposure factors, a Monte Carlo simulation was conducted, drawing 10 000 samples from

the distributions and evaluating the number of virus particles inhaled, the dose, and the risk  $p_{III}$  at a seat, for each sample. This resulted in 10 000 doses and  $p_{III}$  estimates per seat in the 7 rows considered.

As a measure of risk, the mean of  $p_{III}$  was determined over all the Monte Carlo samples for all the seats in the experiment or the simulations. The 95<sup>th</sup> percentile of  $p_{III}$  was also determined as a measure of the variation in the risk evaluation.

A full description of the methods can be found in Appendix B.6.

### 6.1.3 Scenarios and assumptions for the risk assessment

Risk of SARS-CoV-2 illness per person,  $p_{III}$  was calculated for a range of scenarios. Assumptions for these scenarios included:

- One index passenger was present in the aircraft. The index passenger emitted aerosol droplets based on the particle emission profiles for breathing 80% of the time and speaking 20% of the time.
- The results pertained to the passengers seated on the 7 rows surrounding the index passenger; as this was the area investigated during the measurements and simulations. The typical capacity for the types of A320, B737 and B787 investigated is 180, 185 and 280 (including business class) passengers, respectively.
- Conditions during cruise flight were modelled, excluding the climb and descend phases. Average cruise flight duration is 0.9 hours for A320, 1.4 hours for B737 and 8.7 hours for B787. High (95<sup>th</sup> percentile) cruise flight duration is 2.5 hours for A320, 3.6 hours for B737 and 11.1 hours for B787. These values are based on flights operated to and from Amsterdam Airport Schiphol in 2019<sup>29</sup>.
- Average taxi duration was estimated at 10 minutes, high taxi duration was estimated at 20 minutes. This refers to the time the engines are running and does not include boarding or disembarking time at the gate. These values are typical for the situation at Amsterdam Airport Schiphol. Average worldwide taxi durations are slightly shorter (EUROCONTROL, 2019a; EUROCONTROL, 2019b).
- The typical time duration that masks are not worn (due to consumption of drinks, snacks and meals on board) was estimated to be 10% of the flight duration.
- Representativeness of the measurement runs that included a mask covering the source for realistic mask wearing was deemed highly uncertain. Therefore, for the risk assessment, mask efficiency was based on literature (assuming 60% removal for the emission source, and 30% removal for inhalation by the receiver, so the fraction of aerosol passing the masks of both the shedder and the exposed person was  $(1-0.6) \times (1-0.3) = 0.28$ ).
- Assessments based on experimental data were also aggregated by taking the mean of all runs that fit the scenario conditions. Assessments based on the simulation data were aggregated by pooling all simulations with different index passenger locations and taking mean and 95<sup>th</sup> percentile estimates of the estimated transmission of all simulated seats.

<sup>29</sup> Great circle distance, reduced by  $2 \times 40$  nautical miles for climb and descent phases, at an average cruise speed of 850 km/h.

## 6.1.4 Statistical modelling and analysis

The risk of illness,  $p_{ill}$ , was subjected to statistical analysis in order to evaluate the effects of the index person wearing a mask, heating of the blankets that the manikins were wearing, the use of gaspers, distance and angle relative to the index passenger. To that aim, a Generalized Additive (Mixed) Model was fitted using R to the data for the single and twin aisle aircraft in ground and cruise conditions.

A full description of the methods can be found in Appendix B.8.

## 6.2 Results

This section presents the results of the risk assessment.

### 6.2.1 Risk assessment per seat

Here, estimates of  $frac$ ,  $dose$  and  $p_{ill}$  are presented per seat for the risk assessment based on the measurements. The CFD simulation results were found to be unsuitable for seat-by-seat comparisons, as discussed in Section 5.2.1. Instead, for the assessment based on the CFD simulation, only generalized information on the distribution of  $frac$  over all seats is given, without reference to individual seat locations.

#### *Summary of measurement data*

The fraction of aerosol emitted by an infectious person that reached other persons in the aircraft,  $frac$  was computed using the measured particle air concentrations. For one aircraft, this is illustrated in Figure 23. The figure consists of three parts: on each seat, the mean and 95-percentile values of  $frac$  (top left), the  $dose$  (top right) and risk  $p_{ill}$  (bottom) are given. The background colour is scaled along the entire range of values for each quantity (i.e. is a relative scale). This specific set of figures represents the result of a single measurement run during cruise flight, in which the index was not equipped with a mask and with opened gaspers. For that case,  $frac$  was found to range from  $2 \times 10^{-6}$  to 0.007, dose from 0.03 to 110, and the risk  $p_{ill}$  from  $2 \times 10^{-5}$  to 0.026.

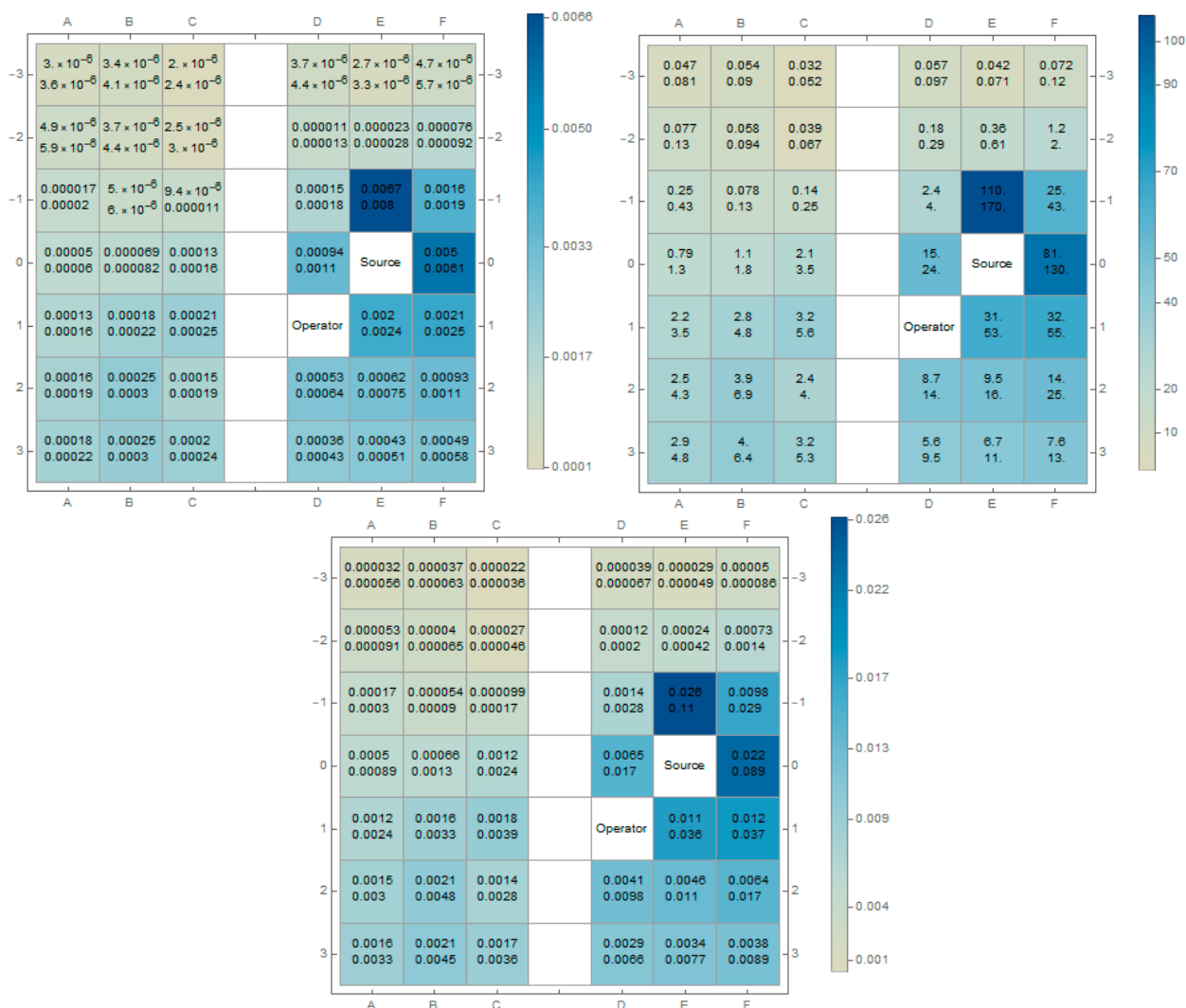


Figure 23: Illustration of seat-level risk assessment, showing mean and 95-percentile values of the fraction (frac; top left) of aerosols that reached other persons in the airplane, dose (top right) and risk  $p_{III}$  (bottom)

Summary of simulation data

On the basis of the CFD simulation, *frac* was calculated in a Monte Carlo simulation. Simulations with different index passenger locations were combined into one data set. The resulting distribution among seats was summarized in Table 7 for each aircraft class. A distinction was made between the aerosol emission from breathing and that from speaking. For each aircraft and emission type, the distribution among seats was summarized as the mean over the seats and different quantiles of the distribution.

In this calculation, the effects of the wearing of a mask were not included.

Table 7: Distribution of *frac* derived from CFD simulation of aerosol transport. Note that only the mean values of the *frac* have been validated with the measurement data as described in Section 5.2.1

	Mean	Quantiles				
		0.25	0.5	0.75	0.95	0.99
Single-aisle Breathing	0.00080	0.0	$6.32 \times 10^{-6}$	0.00011	0.0049	0.014
Single-aisle Speaking	0.00040	0.0	$8.1 \times 10^{-6}$	0.00025	0.0021	0.0046
Twin-aisle Breathing	0.00015	$6.14 \times 10^{-6}$	0.000020	0.000082	0.00072	0.0022

	Mean	Quantiles				
		0.25	0.5	0.75	0.95	0.99
Twin-aisle Speaking	0.00029	0.000016	0.000055	0.00019	0.0014	0.0032

From *frac*, the dose and risk of illness  $p_{ill}$  are evaluated using assumptions on the emitted volume of aerosol by the index passenger, the effect of mask wearing, the viral load of the emitted particles and the exposure duration. These assumptions varied between scenarios.

### Statistical modelling and analysis

Overall, risks were reduced by a factor of 3.7 when the index passenger wore a mask. Temperature and relative humidity also significantly affected risks. Generally, risks increased with increasing cabin air temperature and increasing humidity. In ground conditions, the overall effect of opening gaspers was an increase in risks by a factor of 1.5; that of heating the blankets that were covering the passengers to mimic body heat decreased risks by a factor of 1.7. Analysis of particle dispersion data, as described in Section 5.2.3, shows the impact of mask usage and gasper setting on particle dispersion to depend on the location.

## 6.2.2 Aggregated risk assessment

Overall transmission risk on board was determined from the  $p_{ill}$  per seat as determined from the measurements by taking the mean and 95<sup>th</sup> percentile of the risk of passengers seated on the 7 rows surrounding the index passenger; as this was the area investigated during the measurements. Average values of  $p_{ill}$  over all seats were determined from the CFD simulations. These were used to check the central tendency of the risks assessed on basis of the measurements. The 95<sup>th</sup> percentiles of  $p_{ill}$  estimated from the CFD simulations were also included in the risk assessment. Although the variation in aerosol exposure among seats was not validated with measurements (as described in Section 5.2.1), the estimated risks were found to be consistent with the risk assessment based on the measurement data.

### What was the estimated risk of SARS-CoV-2 transmission via aerosols during typical cruise flight conditions?

Risk calculations based on measurements and simulations for the two single-aisle aircraft studied showed that on average between 1 in 1800 and 1 in 710 passengers will get ill. For the twin-aisle aircraft this probability ranged from about 1 in 230 and 1 in 120, respectively. The risk was highest for the twin-aisle aircraft mainly due to the longer typical flight duration of this aircraft.

*Table 8: Lower and upper estimates of mean and 95<sup>th</sup> percentile individual risk of illness for typical cruise flight conditions for all aircraft. Lower and upper estimates here represent the variation observed between the simulations and measurements in the various aircraft*

Scenario		Lower	Upper
Cruise flight or taxi conditions		Cruise	
Transfer fraction based on measurements or simulations		Both	
Duration		Typical cruise flight duration	
Mask use		Typical mask use	
Viral load of infectious person (RNA copies / mL)		Variable	
Probability of illness (mean)	Single aisle	1/1754	1/712
	Twin aisle	1/228	1/118
Probability of illness (95 <sup>th</sup> percentile)	Single aisle	1/1119	1/599
	Twin aisle	1/131	1/44

*What if a super shedder was on board?*

In the case that a super shedder was on board, risk of SARS-CoV-2 transmission was on average about 7 times higher than in the case of an ‘average shedder’. The estimated mean probability was that 1 in 370 up to 1 in 16 passengers will get ill.

*Table 9: Lower and upper estimates of mean and 95<sup>th</sup> percentile individual risk of illness for typical cruise flight conditions for all aircraft in case of a super shedder index. Lower and upper estimates here represent the variation observed between the simulations and measurements in the various aircraft*

Scenario		Lower	Upper
Cruise flight or taxi conditions		Cruise	
Transfer fraction based on measurements or simulations		Both	
Duration		Typical cruise flight duration	
Mask use		Typical mask use	
Viral load of infectious person (RNA copies / mL)		Super shedder	
Probability of illness (mean)	Single aisle	1/372	1/108
	Twin aisle	1/31	1/16
Probability of illness (95 <sup>th</sup> percentile)	Single aisle	1/129	1/24
	Twin aisle	1/6	1/5

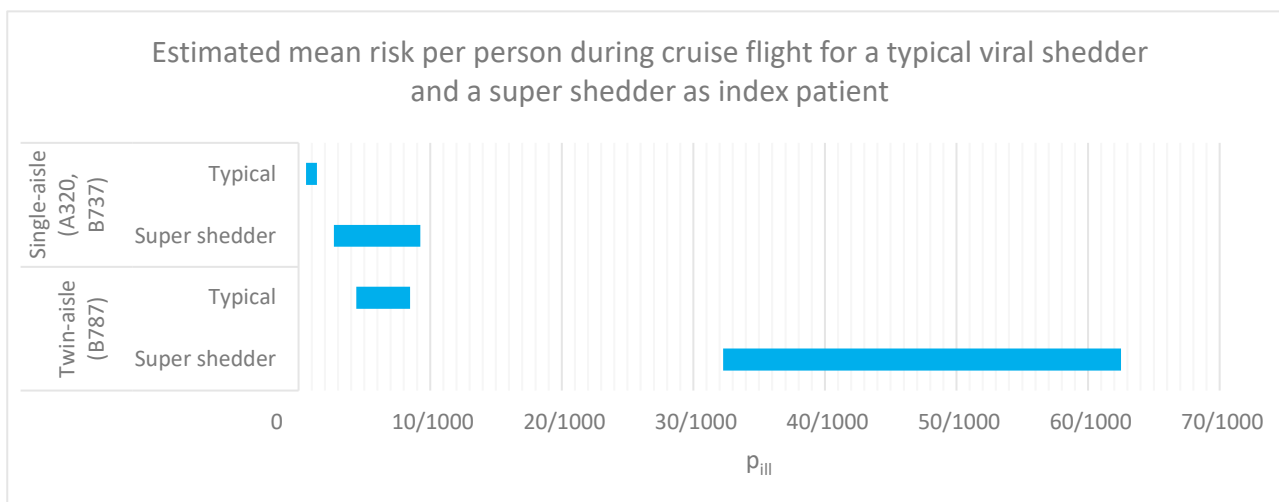


*Figure 24: Estimated mean risk per person during cruise flight for a typical viral shedder and a super shedder as index passenger*

*What was the effect of flight duration?*

During longer flights, the risks increased as *dose* increased proportionally with flight duration. The mean individual risk of illness on board the single aisle aircraft performing a longer flight was found to lie between about 1 in 760 and 1 and 330 (between 1 in 150 and 1 in 43 in case of a super shedder index). For a longer twin aisle flight, the mean individual risk varied from 1 in 190 to approximately 1 in 100, increasing to values between 1 in 50 and 1 in 9 when a super shedder index is on board.

Table 10: Lower and upper estimates of mean and 95<sup>th</sup> percentile individual risk of illness for long flight duration during cruise flight conditions for all aircraft. Lower and upper estimates here represent the variation observed between the simulations and measurements in the various aircraft

Scenario		Lower	Upper	Lower	Upper
Cruise flight or taxi conditions		Cruise			
Transfer fraction based on measurements or simulations		Both			
Duration		High cruise flight duration			
Mask use		Typical mask use			
Viral load of infectious person (RNA copies / mL)		Variable		Super shedder	
Probability of illness (mean)	Single aisle	1/757	1/329	1/148	1/43
	Twin aisle	1/192	1/99	1/25	1/13
Probability of illness (95 <sup>th</sup> percentile)	Single aisle	1/432	1/216	1/50	1/9
	Twin aisle	1/103	1/34	1/5	¼

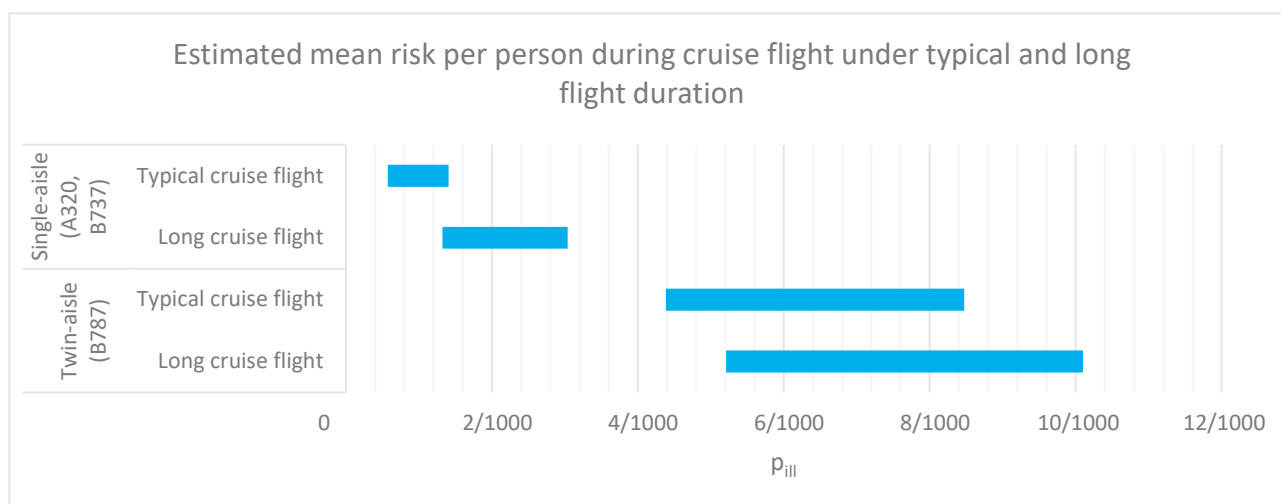


Figure 25: Estimated mean risk per person during cruise flight under typical and long flight duration

**What was the effect of mask usage on board?**

Risk during continuous mask wearing was estimated to be approximately a factor three lower than risk without any mask wearing, based on literature data. For a one-hour cruise flight, the mean individual risk of illness in the two single aisle aircraft was approximately between 1 in 3000 and 1 in 790, assuming continuous mask usage. For the twin aisle aircraft, the mean risk ranged from 1 in about 1400 to 760 – in line with the single aisle aircraft results. Without masks, the mean risk of illness on board the single aisle aircraft was 1 in 930 to 1 in 300. Again, the mean risk on board the twin aisle aircraft studied (1/510 to 1/270) is mostly in line with these results.

Table 11: Lower and upper estimates of mean and 95<sup>th</sup> percentile individual risk of illness per hour with and without mask wearing during cruise flight conditions for all aircraft. Lower and upper estimates here represent the variation observed between the simulations and measurements in the various aircraft

Scenario		Lower	Upper	Lower	Upper
Cruise flight or taxi conditions		Cruise			
Transfer fraction based on measurements or simulations		Both			
Duration		1 hour			
Mask use		Continuous		None	
Viral load of infectious person (RNA copies / mL)		Variable			

Scenario		Lower	Upper	Lower	Upper
Probability of illness (mean)	Single aisle	1/2959	1/785	1/930	1/299
	Twin aisle	1/1401	1/756	1/509	1/273
Probability of illness (95 <sup>th</sup> percentile)	Single aisle	1/1960	1/677	1/549	1/191
	Twin aisle	1/1365	1/472	1/383	1/133

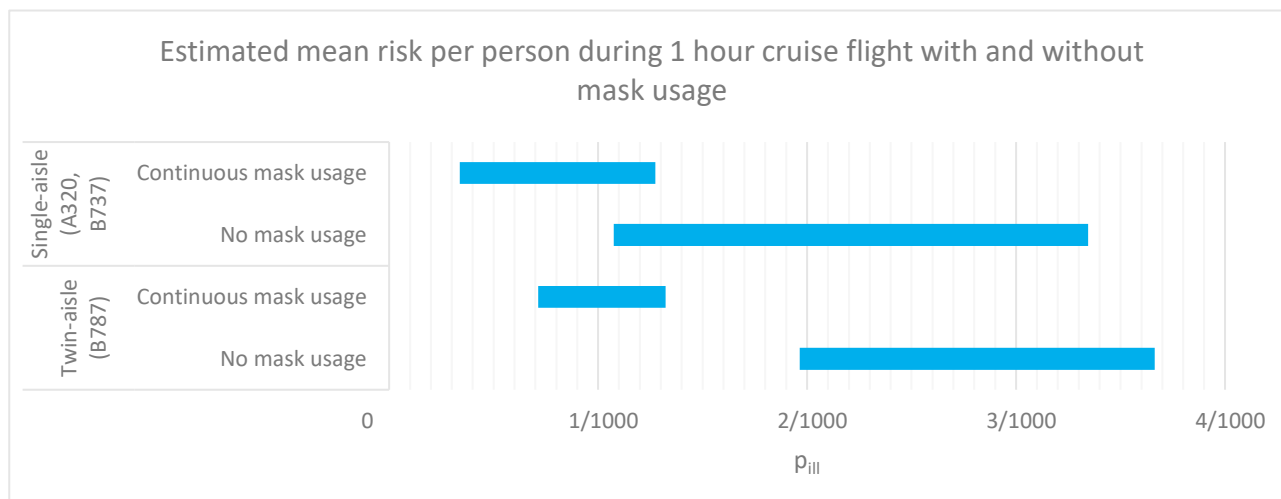


Figure 26: Estimated mean risk per person during 1-hour flight with continuous and without mask wearing

**What was the risk during taxiing?**

During taxi, the mean individual risk of illness for passengers varied with taxi duration. For typical taxi times, the mean risk on board the single aisle aircraft was between 1 in 5400 and 1 in 1700; for longer taxi times, these values increased to about 1 in 3100 and 1 in 910. Twin aisle results fall within these ranges, at 1/3700 for a typical taxi period and 1/1900 for a longer taxi duration.

Table 12: Lower and upper estimates of mean and 95<sup>th</sup> percentile individual risk of illness for taxi conditions for all aircraft. Lower and upper estimates here represent the variation in mean risk observed between the measurements in the two single aisle aircraft

Scenario		Lower	Upper	Lower	Upper
Cruise flight or taxi conditions		Taxi			
Transfer fraction based on measurements or simulations		Measurements			
Duration		Typical taxi duration		Long taxi duration	
Mask use		Continuous			
Viral load of infectious person (RNA copies / mL)		Variable			
Probability of illness (mean)	Single aisle	1/5388	1/1688	1/3056	1/905
	Twin aisle	1/3650		1/1920	
Probability of illness (95 <sup>th</sup> percentile)	Single aisle	1/12188	1/1114	1/6084	1/557
	Twin aisle	1/2644		1/1320	

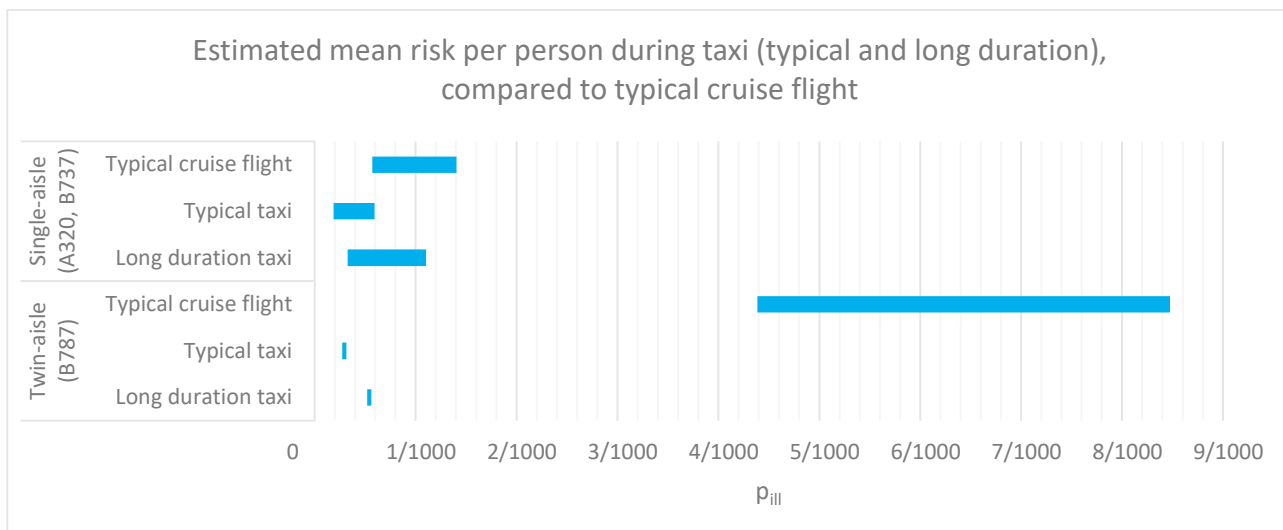


Figure 27: Estimated mean risk per person during typical cruise flight versus taxiing (average and long duration)

### 6.3 Chapter conclusions

Among the three aircraft types studied, the mean individual risk of illness for a one-hour cruise flight with continuous mask usage was found to range from about 1 in 3000 to 1 in 760 (95<sup>th</sup> percentile: 1/2000 – 1/470), increasing to 1/930 – 1/270 (95<sup>th</sup> percentile: 1/550 – 1/130) with no mask usage. Mean risk during taxi (typical duration, equal for all aircraft types) was found to vary approximately between 1/5400 and 1/1700 (95<sup>th</sup> percentile: 1/12000 – 1/1100).

Due to variations in the typical duration of flight length with aircraft types (shorter for single aisle aircraft; longer for twin aisle aircraft), differences in mean individual risk of illness were found when evaluating a typical cruise duration. For the two single aisle aircraft, risks between 1/1800 and 1/710 were found (95<sup>th</sup> percentile: 1/1100 – 1/600), whereas for the twin aisle aircraft studied in this project, higher values of 1/230 to 1/120 (95<sup>th</sup> percentile: 1/130 to 1/44) were found. Risks were found to increase with longer flights and when a super shedder index passenger was on board, with mean risk up to 1/16.

## 7 Discussion

This section discusses the main limitations and approximations of the study, and thus provides context on the fidelity and applicability of the findings. Furthermore, the section discusses pointers for mitigation measures.

### 7.1 Applicability and scoping

#### 7.1.1 Limitations and generalizing study results

This work was limited in a number of aspects. First, the QMRA considered only the transmission of aerosol particles with diameters up to 20  $\mu\text{m}$  as carrier of virus particles. This class of particles is expected to have the highest potential of transporting virus over larger distances. Transmission via larger particles or droplets was not considered. Second, both the experimental work as well as the CFD simulations conducted in this work studied only the transport of aerosol particles in an area of seven rows around the index passenger. It was found that transfer of particles decreased strongly with the distance from the index passenger. The risks evaluated on the basis of the transport study results were also limited to seven rows around the index passenger. Reported mean risks therefore refer to this subset of seats only. The risk for passengers outside the considered area will be lower, but may not be zero. This is further discussed in section 7.1.4. Also not considered in this work was the contribution to the risk via direct contact with an infected subject or indirect contact, through hand-mediated transfer of the virus from contaminated fomites to the mouth, nose, or eyes. This direct contact route is also considered a primary transmission pathway (La Rosa, Bonadonna, Lucentini, Kenmoe, & Suffredini, 2020). Finally, this study considered emission from breathing and speaking by an index passenger but did not consider the several orders of magnitude higher emission from coughing and sneezing. This was out of scope, as this study specifically considered the situation with guidelines in place that do not allow symptomatic people to board aircraft.

Three aircraft were measured in this study, and two were also simulated. Some variation in estimated risks between aircraft was observed. This variation stems partly from differences in indoor aircraft conditions that lead to different aerosol transport and exposure. For another part, the variation resulted from the differences in flight durations that were assigned to each aircraft in the QMRA scenarios. Here, it was assumed that the same aircraft will not be used on flights of other durations. Finally, variation in estimated exposure potential may also result from variation in the maintenance state of the selected aircraft.

Comparing the estimated transmission risk for typical flight durations of each aircraft (Table 8) with the risk per hour cruise flight (Table 10), demonstrated that differences in assumed flight duration made the largest contribution in the inter-aircraft variation. Considering the risks per hour flight, the maximum difference between aircraft was about a factor of 4. Furthermore, transfer fractions determined for two additional aircraft in (Kinahan, 2021), the Boeing 767-300 and Boeing 777-200 respectively, were on average between the Single aisle and Twin aisle determined in this study. This provided some indication that differences in the conditions that govern transmission between aircraft may be limited and that the transfer fractions determined in this work, combined with those of (Kinahan, 2021) could provide a plausible basis to generalize the exposure and risk assessment to other aircraft, combining transfer fractions with representative flight durations.

Another limitation was that this study considered only a static source, bound to a specific seat, to represent the index. Risk was evaluated as an average probability of illness among exposed fellow passengers. In the case of a moving index (e.g. an infected crew member), one could assume that the viral emission would be similar. This would mean that the same quantity of virions would be dispersed over a larger group of passengers. This would likely lead to a larger group of passengers being exposed to lower virus doses per person. Under the assumption that the transport of virus as determined in this study does not depend on the location in the aircraft, but represented e.g. the entire economy class, it is expected that the mean transmission risk in the scenario of a moving index would be very similar to that evaluated for the static index passenger considered here. The maximum individual risk on the other hand, is expected to be lower in the case of a moving index, as exposed passengers will be in the proximity of the index for much shorter times, and therefore receive a lower cumulative virus dose.

Since late 2020 introduction of new variants of SARS-CoV-2 raises concern over changes in transmissibility, clinical presentation and severity, and impact on public health and social measures (PHSM) (World Health Organization, 2021). With increasing numbers of infections, variations in the virus such as mutations and deletions accumulate. These are carefully monitored to identify so-called Variants of Interest (World Health Organization, 2021). So-called Variants of Concern (VOC) include the British, Brazilian and South-African variants. Variants of High Consequence have not been identified until now (June 7, 2021). One can assume that air travel plays a role in the introduction of new variants for SARS-CoV-2 as was shown for other viruses, and restrictions were put into effect on flights coming from India for fear of introductions of the Delta variant B.1.617. PHSM remain critical to curb the spread of SARS-CoV-2 and its variants. Even though variability among variants may result in differences in transmissibility and infectivity, differences between variants were outside the scope of this study. Given the relative short time between emission and exposure in aircraft, that was typically less than 10 minutes, possible differences in stability of virus variants in aerosol particles was not expected to lead to differences in transmission. In effect, therefore, the findings in this study may be generalized to other variants by considering changes in the dose-response only. Currently, a specific dose-response relation for SARS CoV-2 is not available, however. Generalizing the QMRA performed here to other variants of the virus would first and foremost require specific dose-response information for SARS-CoV-2 and its variants.

### 7.1.2 Risk from other transmission routes not assessed in this study

In this work, the risk of illness of SARS-CoV-2 with aerosol particles with diameters up to 20  $\mu\text{m}$  was assessed. SARS-CoV-2 can also be transmitted via larger aerosol particles or via droplets. Such large droplets can be produced during coughing and sneezing, and to a lesser extent during breathing and speaking. Larger droplets fall ballistically under the influence of gravity, typically within a distance of 1.5 meters from the index. The effect of airflows on droplets larger than 20  $\mu\text{m}$  is limited. Susceptible individuals can be exposed to the virus directly when such droplets end up on mucosa (mouth, nose, eyes). Typically, the largest volume of the aerosol particles generated during coughing and sneezing will be in the larger droplets, rather than in the droplets with diameters smaller than 20  $\mu\text{m}$  (Duguid J. P., 1945; Schijven, et al., 2021). This means that most viral particles will likely be in the large (ballistic) droplet fraction. However, symptomatically infected persons should not travel and adequate sneezing and coughing hygiene should be applied (i.e. the number of coughing and sneezing persons should be very low). Additionally, the surface area available for direct transmission in the recipients' face is estimated at only 15  $\text{cm}^2$ , indicating that the chance that a droplet directly hits the mucosa might not be very high (Chen, Zhang, Wei, Yen, & Li, 2020). Transmission might also occur indirectly via hand-mucosa contact. Hands can become contaminated by (ballistic) droplets directly or indirectly via fomites. The probability of hand-mediated transfer is dependent on factors such as hand hygiene, the persistence of infectivity of the virus, transfer rates, hand-mouth/nose/eye contact and cleaning and disinfection practices in the airplane/cabin.

In general, for SARS-CoV-2 and other respiratory infectious diseases, the relative importance of the different transmission routes is subject of discussion (NLR & RIVM, 2020; Kampf, et al., 2020).

### 7.1.3 Applicability to other aircraft types

The goal of the study was to estimate the risk of transmission in aircraft cabins irrespective of aircraft type, rather than comparing particular types. Based on results from the literature review (NLR & RIVM, 2020), both small (single-aisle) and large (twin-aisle) aircraft were considered<sup>30</sup>. Specific aircraft models were selected based on their prevalence at Amsterdam Airport Schiphol and the desire to include types from both large manufacturers (Airbus and Boeing). As such, the single-aisle Airbus A320 and Boeing 737-800 and the twin-aisle Boeing 787-8 were studied.

Single aisle aircraft were used for over 80% of flights to and from Amsterdam Airport Schiphol in 2019<sup>31</sup>, producing over 70% of all available seats and 25% of available seat kilometres<sup>32</sup>. Within this class, the Boeing 737 Next Generation family<sup>33</sup> was found most relevant, followed by the Airbus A320 family<sup>34</sup>. Combined, they were used for more than half of single-aisle flights and produced approximately 75% of seats and 85% of ASK. Within these families of aircraft, the Boeing 737-800 and Airbus A320 were found to produce most seats at 74% and 57% of their family total.

The remainder of flights to and from Amsterdam Airport Schiphol was operated using twin aisle aircraft. In that class, the most relevant aircraft families were found to be the Airbus A330 (based on number of flights) and the Boeing 777 (based on seats and ASK). As the former is foreseen to largely retire in the next years and the latter was unavailable for study in this project, the Boeing 787 (specifically, the Boeing 787-8) was selected.

Overall, the aircraft subtypes studied in CORSICA were used in 35% of flights to and from Schiphol, producing 25% of seats and 20% of ASK. If other subtypes of families are included, these numbers rise to over 55%, 60% and almost 40%.

The specific aircraft configurations used for measurements and simulations were found to compare rather well with typical configurations used by other operators of these aircraft subtypes. Compared to configurations by other airlines at Amsterdam Airport Schiphol that operate the same aircraft subtypes, typical economy class seat counts were found to be between 1 and 5% lower than studied here. Seat pitch and width were compared to global averages for the aircraft subtypes studied. Compared to the configurations studied in CORSICA (29 or 30 pitch and 17- or 18-inch width), economy class seat pitch was found to be between 7 and 9% higher and economy seat width was found to be 1% smaller to 3% larger (SeatGuru, 2020b; SeatGuru, 2020a).

The aircraft cabin remains a complex environment with a large number of complex shapes and variability due to the presence of passengers and small possible changes to the ventilation system (e.g. passenger adjustable gaspers or minor variations between aircraft types). Individual aircraft of the same type can perform differently and even over the course of a single flight the dispersion of particles could change. The number of measurements and simulation

<sup>30</sup> Business jets have not been considered in this project.

<sup>31</sup> Consistent with earlier work (Roosien, Peerlings, & Jabben, 2020), cargo and governmental aircraft were largely excluded, as were flights operated by airlines that have ceased operations in 2019 or 2020.

<sup>32</sup> The number of available seat kilometres (ASK) is found by multiplying the distance covered by a flight with the amount of seats available on that flight.

<sup>33</sup> Spanning the Boeing 737-600, -700, -800 and -900 subtypes. These aircraft share their fuselage diameter, but vary mainly in fuselage length.

<sup>34</sup> Airbus A318, A319, A320 and A321. These aircraft share their fuselage diameter, but vary mainly in fuselage length.

scenarios is too small to statistically prove the effect of all individual variations. Differences observed between aircraft were found to be substantially less than the largest drivers of variance: viral load, flight duration, and mask usage.

### 7.1.4 Risk of illness per flight – extrapolation from 7-rows to full size cabin

The QMRA evaluated risk of illness on the basis exposure information for a limited set of seats (i.e. in seven rows surrounding the index passenger). The risks presented thus far apply strictly only to passengers seated in the proximity of an index (assuming one is on board). To relate the risk to the entire aircraft, it was assumed that for passengers seated outside the seven-row section, the risk of illness was negligible. The expected number of new cases in the seven-row section can, in that case assumed to be equal to the expected number of cases of illness  $E(\text{cases})$  in the entire aircraft. Under this assumption  $E(\text{cases})$  was calculated as the number of passengers in the seven rows surrounding the index times the average risk of illness.

In most scenarios the expected number of new cases was less than one. Therefore, also the number of flights that was expected to result in at least one case of illness was also calculated. This was determined as  $1/E(\text{cases})$ . For the most relevant scenarios, both the expected number of cases and the expected number of flights to result in (at least) one case are given in Table 13. The risks per flight presented here are still under the condition that an infectious index passenger has boarded the flight. Furthermore, transmission routes other than aerosol transmission (e.g. via larger droplets or fomites), are ignored. Moreover, these numbers pertain only to the cruise flight conditions that were studied, whereas possible transmission during transit, boarding, taxiing etc. is not taken into account. Actual risk per flight is therefore likely higher.

*Table 13: Risk per cruise flight from aerosol transmission, under the assumption that the risk outside the seven rows studied is negligible. Expected number of cases per flight and expected number of flights that result in at least one case. Risks for the flight are under the condition that one infectious index is on board of the aircraft and that aerosol transmission is the only transmission route*

Scenario		lower	upper	lower	upper	lower	upper	lower	upper
Cruise flight or taxi conditions		Cruise							
Transfer fraction based on measurements or simulations		Both							
Duration		Typical cruise flight duration				High cruise flight duration			
Mask use		Typical mask use							
Viral load of infectious person (RNA copies / mL)		Variable		Super shedder		Variable		Super shedder	
Expected number of cases per flight, based on mean risk	Single aisle	0.02	0.06	0.11	0.37	0.05	0.12	0.27	0.93
	Twin aisle	0.26	0.50	1.9	3.7	0.31	0.60	2.4	4.5
Expected number of flights to result in at least 1 case, based on mean risk	Single aisle	44	18	9	3	19	8	4	1
	Twin aisle	4	2	1	1	3	2	1	1

### 7.1.5 Probability that an infectious person or super shedder boards an aircraft

Ren et al. (2021) found 3100 SARS-CoV-2 positive people in their study among 19 million international travellers entering China during the period 16 April – 12 October 2020. The probability that a (highly) infectious person boards an aircraft is dependent on the current epidemiological situation in the originating country, as well as on the measures taken to prevent infectious people from boarding. This study focused on the situation with pre-boarding measures as currently in place in the Netherlands: triage and pre-boarding testing. Triage is targeted at preventing symptomatic people from boarding aircraft. However, people with a pre- or asymptomatic SARS-CoV-2 infection can also spread the disease. Oran & Topol (2021) concluded in their systematic review that at least one third of SARS-CoV-2 infections were asymptomatic, meaning that triage alone would not prevent all infectious people from boarding.

Testing of people before they board an aircraft can prevent a large part of a- and pre-symptomatic people from boarding. For testing before admission to events, the Dutch Outbreak Management Team recommends that rapid antigen tests are valid when administered within 24 hours before the end of the event (RIVM, 2021b). The current policy (June 2021) for air travel to the Netherlands is that travellers should be able to show a negative NAAT-test (PCR) with a sampling date no longer than 24 h before boarding, or both a negative NAAT-test with a sampling date no longer than 72 h before arrival in the Netherlands and a negative rapid antigen test (RAT) with a sampling date no longer than 24 h before boarding of the aircraft (Rijksoverheid, 2021). In the case of long flights, this could lead to a significantly longer period than 24 hours before disembarking. The PCR test has a sensitivity of 95%, and the RAT of around 80% (RIVM, 2020b) (dependent on a.o. specific RAT used), meaning around 5 and 20% respectively will receive a false negative result. Moreover, the rapid increase in viral load at the onset of a SARS-CoV-2 infection (RIVM, 2021b) means that some people, after testing negatively 72 and 24 hours before boarding, could become positive in the meantime. How high this probability is exactly, is unknown. For super shedders specifically, this is also unknown. A person with a high viral load might be less likely to test negatively 24 hours in advance than an 'average shedder', but this is uncertain. Further research on this topic is necessary, not only in the context of air travel but for the effectiveness of preventive testing in general.

The probability of an active SARS-CoV-2 shedder entering an airplane is hard to estimate. The current (early June 2021) prevalence in The Netherlands is less than 600/100,000 persons infected with SARS-CoV-2. A part of these people will be symptomatic and in quarantine, this number can be thought of as an upper estimate of prevalence in the population that can board an aircraft. Estimates by the OMT assumes that 95% of the infected persons will be detected by pre-flight screening. This would indicate that less than 30/100,000 persons boarding an airplane may be shedding SARS-CoV-2. This is in the same order of magnitude as the findings by Ren et al. (2021) described above. Depending on the number of passengers per aircraft (100 – 300), every 11 - 33 flights could carry an infectious passenger. The probability of a super shedder entering an airplane is even smaller since only 2.7% of those infected are possibly a super shedder (Schijven, et al., 2021) and high-level shedders are more likely to be detected by the pre-screening RAT-tests (RIVM, 2021). Less than 2.7% of 30 / 100,000 would mean less than 0.8 / 100,000 people boarding an aircraft may be a super shedder. It should be noted that our definition of super shedder has only considered viral load. It is known that people also differ in the amount of aerosol droplets they produce. A person with an average viral load but very high droplet production, could potentially also spread the virus easily.

## 7.2 Uncertainty and variability

### 7.2.1 In-cabin measurements

In the limited time-frame available to perform the in-cabin measurements, the measurement plan gave priority to collect data on a large number of variables instead of repetition of identical scenarios in order to complete the simulation models and fill the knowledge gaps identified by the literature review. The measurement campaign succeeded in collecting large amounts of previously unknown data. Priority was given to collecting a variety of data over repetition of identical scenarios, this made it more difficult to statistically prove the effect of all individual variations.

#### *Systemic errors*

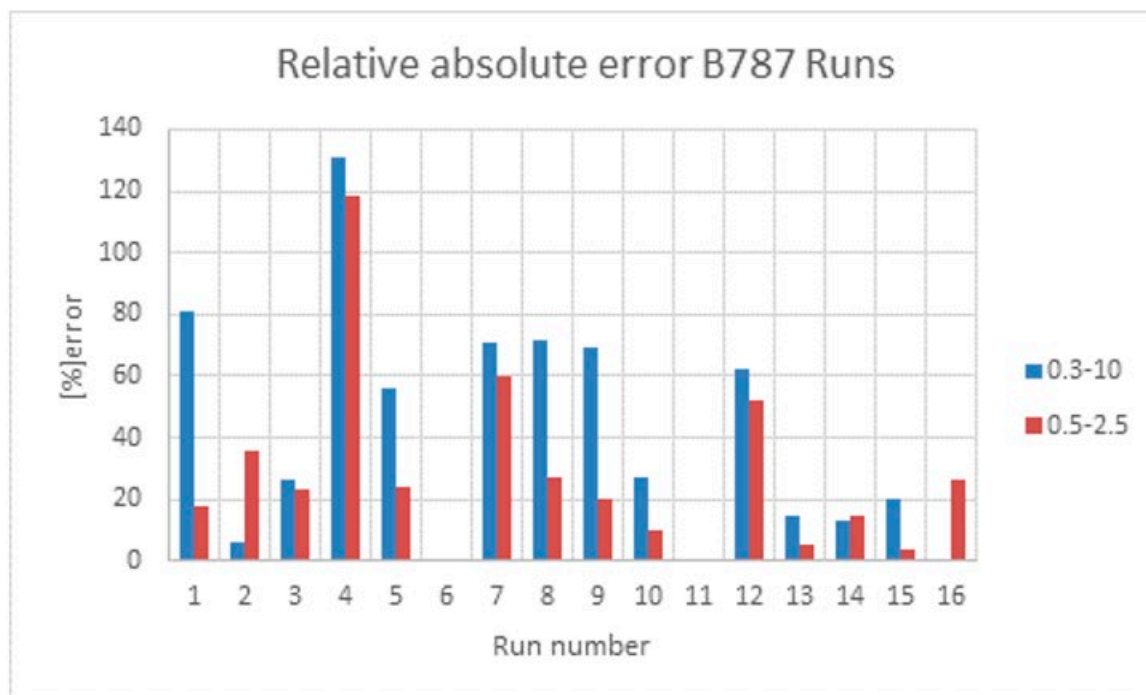
During a small number of runs some PM sensors had temporary failures. The readings of these sensors have been excluded from the analysis. Due to the large number of PM sensors, the impact of these failures was deemed low.

As discussed in Section 5.2, the measurement runs with a mask showed a significantly lower number of sensed particles compared to the runs without a mask. In addition, the runs with a mask showed a different dispersion pattern with a stronger backward flow compared to the runs without a mask. Also, the mask appeared to reduce the number of larger particles more than the smaller particles. Due to the limited number of runs and the possibility of changes in fitment of the mask, these effects could not be statistically proven. In reality, these changes in fitment are also expected to occur.

Similarly, the exact gasper configuration in terms of flow and direction of flow could not be kept constant in between runs and aircraft types. Minor changes in gasper location and flow near the index location could have altered the particle dispersion to an unknown degree. In reality, these variations are also expected to occur.

#### *APS-PM sensor*

A comparison between the APS and PM sensors showed that particle counts do not correspond exactly. This is due to a combination of the operation of the PM sensors that calculates bins  $> 2.5$  microns instead of measuring them. In contrast, the bin  $< 0.5$  micron is not measured with the APS. During the measurements the APS showed timing problems at different moments. Due to this timing problem, particle counts cannot be summed. During the B787 flight measurements, the timing problem of the APS did not occur, so it can be used well for comparisons of absolute particle counts. When we compare the mutual bins (e.g. PM sensors 0.5-1 vs. APS 0.5-1), we initially see very large (non-constant) deviations of the bin totals within a run. In a first comparison between APS and PM sensors of the sum of all bins (0.5-10 micron) we determined the deviations. The average of this deviation over all runs is 46%. When we consider only the range of bins measured by both devices (0.5-2.5 micron), we see that the mean absolute deviation falls to 31%. In the figure below, we see that the deviation between APS and PM sensors is  $\pm 80\%$  of the runs is greater with the 0.3-10 than with the 0.5-2.5.



Based on this comparison, it was proposed to use the total number of particles within the 0.5-2.5-micron range as a reference to determine the total number of particles of 0.5-10 microns per run and per seat. This is done as follows: initially you look at bin 0.5-2.5 of the PM sensors. From this the total number of particles in these bins is determined. Then the particle size distribution is taken and can be used to determine the number of particles within the bins (0.5-1, 1-2.5, 2.5-4 and 4-10 microns) for each seat within each run. The fidelity of the PM sensor in the range 0.5-2.5  $\mu\text{m}$  was later validated by DLR in a laboratory setting using a highly accurate Optical Particle Sensor (OPS).

## 7.2.2 Simulations

Particle dispersion was modelled using a state-of-the-art stationary RANS method, as further described in Section 5.1.1. This section discusses some relevant uncertainties and variabilities. Overall, where known and possible, assumptions and choice were typically taken on the conservative side, as further discussed below.

### *Droplet interaction with surfaces*

When droplets come into contact with a surface, they can stick to the surface or bounce back – completely or partially. Lacking information on this behaviour, the modelling has conservatively assumed droplets to bounce back. This means they remain flowing through the cabin for a longer period of time than would have been the case if they were modelled to stick, which is the modelling applied by e.g. Davis et al. (2021).

In case of the B787 simulations, limitations with respect to computational effort made it impossible to model all droplets to bounce back. In that situation, particles larger than 10  $\mu\text{m}$  were modelled to stick when coming into contact with seats and passengers' clothes. Separate analyses have shown this resulted in significantly lower volume fractions (almost a factor two for the index row).

Lacking knowledge on the realistic behaviour of droplets interacting with surfaces, the extent to which the choice to model droplets to bounce is conservative with respect to reality could not be established. Similarly, it could not be determined whether the 'partial stick'-situation modelled in the B787 is still conservative with respect to reality.

### *Double counting of particles*

In the simulation, droplets were modelled to be able to travel from one inhalation box to another. In that case, they contribute multiple times to the (expected) aerosol volume that may be inhaled by passengers. In reality, that would not be possible: a droplet inhaled by one passenger, cannot be inhaled again by another passenger. To mitigate this issue the residence time of each particle in an inhalation box is also calculated, in order to use it as a weighting factor for determining the chance of actual inhalation of the particle.

### *Differences between measurements and simulations*

The results from measurements and simulations have been compared in order to improve the quality of the results and to refine and improve the simulation model, as described in Section 5.1.3. As also indicated in the description of the results of that comparison (Section 5.2.1), differences exist, and can possibly be explained by the choices with regard to droplet-surface interaction discussed before. Additional simulations identified parameters that can have a noticeable effect on particle dispersion. One of these factors was the initial particle cloud position, which was modelled at 10 centimetres in front of the index passenger. Compared to real-life variability in passenger position, behaviour and characteristics, this is a simplified approach.

## 7.2.3 QMRA

The QMRA as conducted in this work was subject to various sources of uncertainty and variability. Most important sources for uncertainty include:

- The extent to which the experiments and simulations on aerosol transport in aircraft represent realistic conditions of passenger exposure during flight
- The dose-response model used to estimate risk of illness from the inhaled virus dose

The quantitative impact of these uncertainties on the results of the risk assessment could not be assessed. As explained by Schijven et al. (2021), the fraction of RNA virus copies that were able to infect a cell was assumed to be 1/80, which may be seen as a conservative estimate. The recommendation of Haas (2020) was followed to use the dose-response data for human coronavirus 229E as representative for SARS-CoV-2. For human coronavirus 229E, it was found that each plaque forming unit (PFU) has a probability of  $r = 1/18$  of causing illness. This implied that, on average, 1440 virus RNA copies were needed to cause illness, which matches really well with the number of viral genomes needed to initiate infection on average 1000 (1-5000) as reported by Popa et al. (2020) based on a transmission network with thirty-nine transmission events. Dose-response data are often from studies with healthy volunteers. It is possible that for specific susceptible populations, dose-response behaviour is different. This was not considered as no data are available.

Furthermore, the QMRA involved multiple sources of variability.

- Risks were found to vary between aircraft. The variation was partly due to differences in aircraft indoor conditions, but mostly due to different flight durations. The study found a variation in estimated risk of about 9 times between maximum and minimum risk. True inter-aircraft variability may be larger, as only a very small sample of aircraft was considered.
- Variation in exposure and risk between seats. On the basis of the simulations the range between the mean and maximum transfer was found to vary between aircraft, but to be around 1 order of magnitude. Virus load varies widely among contagious persons, spanning a range of  $10^2$ - $10^{11}$  RNA copies/ml (Schijven, et al., 2021).
- Inhalation rates vary per person. In this work, a distribution was assumed with a 5%-95% inter-quantile range of 5.6-8.2 l/min.

- The volume of aerosol particles generated was assumed to vary among contagious persons. The 5%-95% inter-quantile range of the distribution used in this work was [0.11 – 120] pL/[20 minutes] for breathing and [86.-880] pL/[20 minutes] for speaking.

The inhaled virus dose is proportional to variations in each of these factors. Overall, the largest source of variability in the QMRA was the virus load in the sputum of contagious persons. This was followed by the variability in aerosol emission volume of an index passenger during breathing.

## 7.3 Mask effects

ICAO and EASA recommend that face masks<sup>35</sup> are worn by passengers and crew during the entire flight except when eating or drinking. Mask wearing works in two ways, by preventing infected subjects from spreading droplets and aerosols, and by limiting exposure through inhalation. Filtering efficiency of masks will depend on the material of which the mask is made, fitting of the mask on the face, whether inhalation (exposure) or exhalation (emission) is considered and on the size of the emitted or inhaled particles or droplets.

The wearing of masks by the index passenger will limit the number of aerosol particles emitted during breathing or speaking. In addition, the removal efficiency of the mask may depend on the diameter of the aerosol particle. A review of the literature (NLR & RIVM, 2020) found a wide variability in reported overall mask removal efficiency, as well as particle diameter dependence of the mask's filter efficiency.

The QMRA in this work was, therefore, based on simplified assumptions of a particle size independent removal efficiency of 60% of the emitted virus particles by the index passenger during the time the mask was worn. Mask wearing by an index passenger will also affect the distance over which particles are emitted during speech or breathing. These aspects of particle emission were not considered in this work.

In the experimental study, additional experimental runs were conducted in which the artificial emission source was covered by a mask. According to the statistical analysis of the experimental data (Appendix B.8.2), risks were generally reduced when the source wore a mask: the overall effect, independent of aircraft, was highly significant and amounted to a risk reduction factor of 3.7. This indicates a higher effect than assumed on the basis of literature (section 6.1). Nevertheless, to what extent the experimental setup was representative of mask wearing by a human index passenger wearing a mask remained uncertain.

The removal efficiency of a mask worn by a susceptible passenger was set at 30%, assuming here also no dependency of the particle diameter on the removal efficiency (NLR & RIVM, 2020). In the scenarios, masks were always considered to be either worn or off for all passengers simultaneously. The period that masks were off represented situations in which a meal or drink was served. Effects of alternating mask removal by e.g. spreading meal serving across groups of passengers, may result in some risk reduction, but is not investigated in this study). The overall reduction in the assessed risk when all passengers wear a mask was about 70% as based on literature.

<sup>35</sup> A previous version of the report incorrectly stated EASA and ICAO explicitly recommend using **non-medical** facemasks in the aircraft cabin

## 7.4 Comparison of results with other studies

### 7.4.1 Comparison with epidemiological studies in aircraft cabins

Different epidemiological studies were carried out as described in the phase 1 literature study (NLR & RIVM, 2020). From Khanh et al. (2020), it is clear that passengers can become infected within a short distance of a symptomatic passenger and in absence of intervention measures on board. The flight from Hanoi to London took place at the beginning of March 2020 before interventions were in place. During the flight one passenger experienced complaints such as a sore throat and cough. In the cabin 20 passengers were seated which amounted to a 75% seat occupancy. Out of these 20 business class passengers 12 tested positive after the flight. They were seated within 2 meters of the index passenger. In economy class at least 2 out of the other 180 passengers became positive. From (Khanh et al., 2020), a maximum attack rate in the absence of PHSM of 62% in one area can be inferred. This was much higher than in the QMRA presented in this work. Seating proximity was strongly associated with increased risk. For the whole aircraft, the attack rate was much lower in the descriptive study by Khanh et al. (2020), and more in line with this study. It should be noted that risks evaluated from Khanh et al. (2020) most likely stem from transmission via both ballistic droplets and airborne aerosol transmission, whereas in our study transmission via aerosols only was considered. One other important consideration in the interpretation of the results of Khanh et al. (2020), was that transmission between 1<sup>st</sup> class passengers or 2<sup>nd</sup> class passengers may have occurred during lounge stay, immigration passage or baggage claim.

Another study described a 7.5h flight to Ireland with a seat occupancy of 17% (49/283 seats) and 12 crew (Murphy, 2020). Thirteen cases were identified on this flight. Each of these passengers had been transferred via a large international airport, flying into Europe from one of three different continents. The inferred maximum attack rate (AR) for this flight would be 12 of 48 or 1/4. This attack rate is higher than the highest predicted mean transmission risks from aerosol transmission in this study; the predicted mean risks for the super shedder scenarios under typical flight conditions varied between 1/370 to 1/16, but close to the 95-percentile estimates for the super shedder scenario (up to 1 / 5) (Table 9). Reviewing the epidemiology of the Murphy study (2020), an AR of 17.8% via was plausible if eight of 45 contracted COVID-19 in-flight. In other words: four of these flight cases were not seated next to any other positive case, had no contact in the transit lounge, wore face masks in-flight and would not be deemed close contacts under current guidance from the European Centre for Disease Prevention and Control (ECDC), rendering aerosol transmission a plausible route. Findings were confirmed by phylogeny of virus variants.

Bae et al. (2020) researched virus transmission by asymptomatic passengers on a 11-hour evacuation flight carrying 310 passengers from Milan, Italy, to South-Korea. When the passengers arrived at the Milan airport for departure, medical staff performed physical examinations, medical interviews, and body temperature checks outside the airport before boarding, and 11 symptomatic passengers were removed from the flight. Most passengers wore N95 respirators except at mealtimes and when using the toilet during the flight. After the flight, 6 out of 299 passengers had a confirmed positive result for SARS-CoV-2 on quarantine day 1, and on day 8 another passenger seated 3 rows apart from the 6 asymptomatic passengers. Prior to the flight this passenger was quarantined for 3 weeks. None of the crew had a positive test. Overall, one infection originating from one of six asymptomatic sources yielding a 0.2% (1/500) transmission probability comparable to the risk of transmission during typical flight durations (1/1800 - 1/120) as estimated in this study (Table 8) which however, a risk of illness and not of infection. Noteworthy is the low average age of the passengers at 30.0 years.

Transmission via/during air travel has also been described for other pathogens<sup>36</sup>. For instance, during the SARS-epidemic in 2003, aircraft transmission has also been documented (Olsen, et al., 2003). Olsen et al. noted that illness in passengers was related to the physical proximity to the index passenger. Illness was observed in 8 of the 23 persons who were seated in the three rows (a distance of 2.3 meter) in front of the index passenger, as compared with 10 of the 88 persons who were seated elsewhere. Olsen et al. offer airborne transmission as a possible explanation for the observed pattern. (Hertzberg & Weiss, 2016), looking at 7 studies on aircraft transmission of SARS, influenza and measles, found a 6% (1/17) risk to passengers seated within two rows of an infectious individual and a 2% (1/50) risk to passengers seated beyond two rows from an infectious individual.

## 7.4.2 Comparison to epidemiological studies in other settings

Relevant other settings to compare the results to are indoor settings where people 1) spend a limited amount of time (in the order of hours), 2) in the company of a group of people they do not meet frequently, 3) keeping 1.5-meter distance is not always possible, and 4) seats are assigned. This applies mostly to public transport (buses and trains), and for instance to restaurants (depending on the local policies).

Hu et al. (2021) quantified an attack rate of COVID 19 for high speed train passengers using epidemiological data from 2,334 index passengers and 72,093 contacts who travelled together for 0 to 8 hours from December 2019 to March 2020 in China. They found that the attack rate among train passengers on seats within a distance of 3 rows and 5 columns from the index passenger varied from 0 to 10.3% with a mean of 0.32% (1/312). This attack rate is comparable to the transmission risk estimated in this study for the typical flight scenario and conditions (Table 8). It was somewhat higher than the estimated mean risk for the two single-aisle aircraft that varied from 1/1800 to 1/710, and a bit lower than the mean risk estimated for the twin-aisle (1/230 to 1/120). The attack rate decreased with increasing distance and increased with increasing co-travel time. Travellers adjacent to the index passenger had the highest attack rate, with a mean of 3.5%.

Several case studies of very high attack rates in buses and restaurants have been described in the literature. Luo et al. (2020) describe a case study of an index passenger who took two bus trips, causing an attack rate of 15% (1/7) among 60 co-travellers, most of whom were seated more than 2 meters away from the index passenger. Directional air flow caused by a single exhaust fan may have contributed to transporting aerosol droplets through the bus. Similarly, Shen et al. (2020) describe an attack rate of 35% (1/3) among 68 passengers on a 100-minute round-trip bus ride. Lu et al. (2020) describe a case study of a very high attack rate in a restaurant outbreak, where 10 of 83 (1/8) customers became ill with COVID-19. All cases were seated at three tables that were in the circulating air flow of the same air conditioner. When looking at the people seated at these tables only the attack rate was 10 out of 21 (1/2) people. This is anecdotal evidence only, but such high attack rates are higher than the highest predicted mean transmission risks in this study; the predicted mean risks for the super shedder scenarios under typical flight conditions varied between 1/370 to 1/16 (Table 9).

---

<sup>36</sup> Infectious agent.

### 7.4.3 Comparison of CORSICA with in-flight transmission studies

Several studies have been identified that to some extent evaluated exposure and risk of transmission in an aircraft during flight given the presence of an index passenger on board.

Here, the studies were briefly summarized, and the results were compared to the CORSICA findings. Kinahan et al. (2021) studied the transfer of respirable aerosols in aircraft. This study is known as the TRANSCOM study. A well-defined number of artificial aerosol particles in sizes 1-3  $\mu\text{m}$  of fluorescent and DNA labelled particles was released in aircraft during flight. Transfers were determined as (potentially) inhaled doses at each seat in 7 rows of an aircraft during flight, normalized by the emitted volume ('transfer fraction'). The study included 2 different aircraft: Boeing B767 and B777. Transfer fractions determined in (Kinahan, 2021) were directly comparable to transfer fractions determined in this work. For comparison with the CORSICA study, the reported mean and maximum transfer fractions of (Kinahan, 2021) were compared to the same measures calculated from the CORSICA CFD simulation.

*Table 14: Comparison of the transfer fractions measured in (Kinahan, 2021). With the transfer fractions calculated on the basis of the CORSICA CFD simulation. Mean transfer refers to the average over all seats in the 7-rows measured in (Kinahan, 2021) and the 7 simulated rows in CORSICA CFD respectively. The maximum transfer fraction refers to the single seat with the highest transfer in both measurement and simulation*

Study	Aircraft	mean	max
Kinahan (2021)	Boeing 767-300	0.000176	0.000947
	Boeing 777-200	0.000262	0.00461
CORSICA	Single-aisle	0.000388	0.00343
	Twin-aisle	0.000173	0.00307

Mean values correspond reasonably well between the two studies. The variance in maximum transfer is somewhat larger, but still the studies seem in agreement.

Sze To et al. (2009) studied dispersion of inhalable aerosol in an airplane mock-up (in a laboratory setting) after a simulated cough. Artificial saliva was injected at different index locations, translocation to seats on 3 rows in a mock-up cabin was measured for particle diameters 0.3-20  $\mu\text{m}$ . Different ventilation regimes were considered: 11 and 23 air changes per hour (ACH), respectively. Humidity was kept at 5% RH. Transfer fractions calculated from the reported doses at different seats in different measurement scenarios ranged from [0.002 – 0.042]. These were a factor 10-100 higher than averages reported in (Kinahan, 2021) and in the present study. It should be noted, however, that (Sze To G. N., 2009) reported the aerosol dose on only three rows around the index passenger, whereas the other studies report the mean transfers over 7 rows. As the transfer strongly declines with the distance from the source, this may account for the observed discrepancy. Also, (Sze To G. N., 2009) simulated emission of a cough in experiment whereas this study evaluated transmission after speaking or breathing.

Wang et al. (2021) evaluated risk on secondary infection on board of a flight on the basis of the transfer experiments by Kinahan et al. (2021). A Wells-Riley approach (Sze To & Chao, 2010) was used to characterize emission. Mild, medium and severe emission scenarios were quantified using quantum emission rates (in the Wells-Riley terminology) of 5q/h, 20q/h and 100 q/h resp. The effect of masks was evaluated in scenarios covering different assumptions for mask filtering efficiency and duration of mask wearing.

For a 12-hour flight during which as mask was worn for 11 hours (Wang, Galea, Grandison, Ewer, & Jia, 2021) reported for the mean risk of infection. In comparing the results of the assessment of (Wang, Galea, Grandison, Ewer, & Jia,

2021) with the present work, it should be noted that in this work, the risk of illness is estimated, which is different from risk of infection.

*Table 15. Risk of infection (mean and maximum individual) during a 12-hour flight as estimated by Wang et al. (2021). Different scenarios for mask removal efficiency and emission strength were evaluated*

Statistic	Mask removal efficiency (%)	Mild emission scenario	Medium emission scenario	Severe emission scenario
Mean	31.0	1/227 (0.44%)	1/63 (1.6%)	1/15 (6.5%)
	65.6	1/625 (0.16%)	1/156 (0.64%)	1/36 (2.8%)
Maximum (individual)	31.0	1/7.5 (13.4%)	1/2.3 (43.7%)	1/1.1 (94.3%)
	65.6	1/19 (5.2%)	1/5.2 (19.1%)	1/1.5 (65.3%)

Marcus et al. (2021) conducted a risk assessment based on a multi-zone Markov model for the dispersion and inhalation of respirable aerosol in aircraft during flight. The model represented a subsection of the economy cabin in a Boeing 737-900 with 36 seats, six rows of six seats each. The results of the simulation of aerosol dispersion were evaluated against CFD simulations from Boeing and Airbus as well as to the experimental findings of the USTRANSCOM study by (Kinahan, 2021) and found to be in 'general agreement' with these studies. Emission expressed in Wells-Riley terminology as quanta per hour, assuming different scenarios: 'low' (14 q/h), 'medium' (48 q/h) and 'high' (100 q/h). The latter was taken to be representative of a high extreme, 'super shedder' situation. Masks were assumed to have a combined efficiency of 80% (60% emitter, 50% receiver). and found to be in 'general agreement' with these studies. Emission expressed in Wells-Riley terminology as quanta per hour, assuming different scenarios: 'low' (14 q/h), 'medium' (48 q/h) and 'high' (100 q/h). The latter was taken to be representative of a high extreme, 'super shedder' situation. Masks were assumed to have a combined efficiency of 80% (60% emitter, 50% receiver).

Risks were expressed as expected flight hours until infection. For comparison, these were converted to a risk of infection per hour flight duration. To extrapolate these estimates to longer flight durations, the numbers should be multiplied with the expected flight duration.

*Table 16. Risk of infection per hour flight as evaluated in Marcus et al. (2021). Different scenarios of emission (quantified by the quanta emission rate) were evaluated*

Emission scenario	Quanta emission rate	Risk of infection per hour of flight
Low	14	1/238
Medium	48	1/70
High	100	1/34

#### 7.4.4 Comparison with estimates from computational tool *AirCoV2*

Model *AirCoV2* (Schijven, et al., 2021) was used to estimate the risk assuming that the air in the room was well mixed. For comparison with the risk estimates for the airplanes, the tool was applied to two rooms with volumes of 31 and 64 m<sup>3</sup>, estimated to be roughly the same as taken in by 7 passenger rows in the single-aisle and twin-aisle aircraft studied. Three different air exchange rates per hour were applied: 30, 10 and 0.

The aircraft scenario without mask and 1 hour of exposure time (Table 11) was compared with scenarios 1 and 7 in Table 17. The mean risk of scenario 1 in Table 17 of 0.0036 (1/280), was found to lie in the range of the risks for the single aisle aircraft with one hour exposure time and no mask wearing (Figure 26). The mean risk of scenario 7 in Table

17 of 0.0019 (1/530) was found to be within the range of the risk for the twin-aisle aircraft (Figure 26). The aircraft scenario with typical mask use and long flight duration was compared with scenarios 4 and 10 in Table 17. The mean risk of scenario 4 in Table 17 of 0.0038 (1/260) was above the range of mean risks for the single-aisle aircraft for long flight duration in Figure 25. The mean risk of scenario 10 in Table 17 of 0.0053 (1/190) was found to be in the range of the risk for the twin-aisle aircraft for long flight duration, and in the range of the risks for average flight duration (Figure 25).

To conclude, the risk estimates from tool *AirCoV2* were, apparently, similar to those from the corresponding scenarios based on measured data in the airplanes. This suggests that the assumption of well mixed air in a room was acceptable. But note that the tool did not account for spatial effects such the dependence of distance from the source. Risks near the index passenger may be three orders in magnitude higher than farther away from the index passenger (Figure 23).

In addition, the tool indicated that by having an air exchange rate of 30 per hour compared to no ventilation, risks are reduced 20 – 30 times in such rooms. With the *AirCoV2* tool, further comparisons can be made with rooms of similar size and various extents of ventilation that are occupied for up to several hours with relatively large numbers of persons.

Table 17: Risk estimates in rooms of roughly similar size as 7 rows in an airplane (e.g. a bus, train) using computational tool *AirCoV2* (Schijven, et al., 2021)

Scenario <i>AirCoV2</i>	1.	2.	3.	4.	5.	6.	7.	8.	9.	10.	11.	12.
Length, m	5.6	5.6	5.6	5.6	5.6	5.6	5.6	5.6	5.6	5.6	5.6	5.6
Width, m	2.8	2.8	2.8	2.8	2.8	2.8	5.7	5.7	5.7	5.7	5.7	5.7
Height, m	2.	2.	2.	2.	2.	2.	2.	2.	2.	2.	2.	2.
Volume, m <sup>3</sup>	31.	31.	31.	31.	31.	31.	64.	64.	64.	64.	64.	64.
Number of persons	42.	42.	42.	42.	42.	42.	63.	63.	63.	63.	63.	63.
Air exchanges/h	30.	6.	0.	30.	6.	0.	30.	6.	0.	30.	6.	0.
Ventilation, m <sup>3</sup> /h	930.	190.	0.	930.	190.	0.	1900.	390.	0.	1900.	390.	0.
Ventilation, L/sec/person	6.2	1.2	0.	6.2	1.2	0.	8.5	1.7	0.	8.5	1.7	0.
Mask effect	1.	1.	1.	0.35	0.35	0.35	1.	1.	1.	0.35	0.35	0.35
Exposure time, h	1.	1.	1.	3.	3.	3.	1.	1.	1.	9.	9.	9.
Mean risk	0.0036	0.012	0.063	0.0038	0.013	0.065	0.0019	0.0074	0.05	0.0053	0.017	0.095

## 7.5 Current results in view of the RIVM advice with respect to air travel

In June 2020 the RIVM presented an advise on the prevention of SARS-CoV-2 transmission in aircraft (Rijksoverheid, 2020a), in which it refers to the EASA/ECDC protocols. The advice included social distancing, a health check (current practice is a negative SARS-CoV-2 test), limited movements through the cabin and use of face masks for passengers and crew, in addition to “an optimized use of filter- and ventilation systems”. Generic guidelines as refraining from travel when symptomatic, and complying to good hand hygiene apply as much too air travel as any other form of public transport (RIVM, 2021a; Rijksoverheid, n.d.). The current policy (June 2021) for air travel to the Netherlands is that travellers should be able to show a negative NAAT (PCR) test from a sample taken within 24 h prior to boarding, or within 72 h prior to boarding together with a negative rapid antigen test (RAT) from a sample taken within 24 h prior to boarding (Rijksoverheid, 2021).

ECDC states the following: COVID-19 can be transmitted through close contact with infected persons and/or with surfaces or objects that have been contaminated by the secretions of infected persons. Any activity or situation that

involves the gathering together of people poses a risk for the transmission of infection. Thus, all forms of transport that bring people into close proximity, particularly in closed/indoor spaces, pose an increased risk for transmission. Such forms of transport include buses, trains, airplanes and ships. Measures advised include to maintain appropriate physical distancing and avoidance of contact with contaminated surfaces, together with strict hand hygiene and cough/sneeze etiquette. Hygiene will decrease the risk of transmission, but some risk will remain (ECDC, 2020).

In line with the ECDC statement the Director of the RIVM Centre for Infectious Diseases Jaap van Dissel has stated that the risk of being infected with SARS-CoV-2 during a flight is small but not zero and that airplane operators need to implement measures to limit the risk as much as possible.

## 8 Conclusions

With increasing globalisation, the role of modern transportation in the rapid spread of pathogens such as SARS-CoV-2 over long distances is a growing concern. However, little is known about the transmission of SARS-CoV-2 in the cabins of aircraft. The study aimed to assess the risk of illness from inhalation of aerosolised SARS-CoV-2 particles shed by an infectious passenger (referred to as index passenger) in an aircraft cabin using data from literature, measurements and simulations. Furthermore, the study assumed compliance with EASA and ICAO-recommended best practices, such as wearing face masks<sup>37</sup>, except when drinking or eating.

Because little was known about the specific risk of SARS-CoV-2 aerosol transmission in aircraft cabins, the study started with a literature review to identify knowledge gaps and to collect data for setting up experiments and simulations as the basis for a risk assessment. The likely number of particles and particle size distribution expelled by a breathing and speaking infected passenger in a low humidity environment were defined from literature. This artificial source was replicated in an in-cabin experimental set-up (with droplets having diameters up to 5.5 µm) and in a simulation model (with droplets having diameters up to 20.0 µm). The experiment measured the aerosol dispersion in a 7-row grid around the index passenger in the rear economy section of two aircraft frequently seen at Schiphol and other international airports, a single-aisle (Airbus A320) and a twin-aisle (Boeing 787-8) aircraft. To assess the wider applicability of the results, another common single-aisle aircraft (Boeing 737-800) was added to the measurement campaign. The primary goal of the experiment was to measure the volume of aerosol particles that disperse from the index passenger to the other passengers in the measurement grid under both taxi and cruise flight conditions. Additionally, the effects of mask wearing by the index passenger, gasper settings, temperature, relative humidity, distance and angle relative to the index on the aerosol dispersion were studied. Finally, input parameters were collected for the computational fluid dynamics (CFD) model during the experiment. The results from measurement in the Airbus A320 and Boeing 787-8 were compared to results from CFD simulations. The findings were used to simulate the aerosol dispersion over the same 7 rows of the economy cabin originating from different index seat locations. Based on the experimental and simulated aerosol data and literature data on levels of virus shedding and dose-response, a quantitative microbial risk assessment (QMRA) was conducted in order to estimate risk of illness.

The measurements and simulations resulted in valuable data about aerosol dispersion in aircraft cabins of a relevant selection of commonly used aircraft. Cross-checks between measurement data and simulation output of the Airbus A320 and Boeing 787 yielded similar aerosol dispersion per row but the lateral (left-right) differences as measured per seat could not be replicated in the simulations. Since in real-life the index position is unknown this had no impact on the overall findings. Both measurement and simulation data showed a predominantly rearward dispersion of aerosols, especially for the single-aisle aircraft. Based on the simulations, the particle size after evaporation appeared to have little impact on dispersion, at least up to diameters of 8 µm. Simulations showed size-dependent effects for aerosols larger than 8 µm. Masks were shown to clearly reduce the number and volume of aerosols detected after emission by the index. Effects of gasper settings and index location on particle dispersion were variable and limited. Only very low volumes of aerosols were detected in two rows further in front of the seven-row section that was investigated. This suggests that, at least at the measurement location, recirculation of aerosols from the HEPA-filter-equipped cabin ventilation system does not, or only to a very limited extent, occur.

For a typical cruise flight (ranging between 0.9 hour for the Airbus A320 and 8.7 for the Boeing 787), mean risk for COVID-19 due to inhalation of aerosolised SARS-CoV-2 particles were estimated to be in the range of 1/1800 to 1/120 amongst the passengers seated in the seven rows around the index passenger. In the case of a passenger who sheds

<sup>37</sup> A previous version of the report incorrectly stated EASA and ICAO explicitly recommend using **non-medical** facemasks in the aircraft cabin

an extraordinary amount of infectious aerosol particles (a so-called super shedder), mean risks increased up to 1/16. These findings were found to be in line with other model and measurement studies on in-flight illness risk as a result of inhalation of virus bearing aerosols. Risks assessed in other studies varied between 1/625-1/227 for modest or mild emission by an index (compared to 1/1800 – 1/120 in the current study), to around 1/35 for a high emission index (compared to 1/370 – 1/16 for the super-shedder scenarios in the present work). Risk estimates for aerosol transmission in aircraft were very similar to estimated risks in a roughly similarly sized, well-mixed room with a ventilation comparable to aircraft cruise conditions. Further analysis with a well-mixed air room model demonstrated that risks may be reduced 30-20 times for ventilation rates of 30 air changes per hour (ACH) as compared with unventilated rooms. Risks determined in this work (1/1800 – 1/120) for typical flight conditions) were similar to attack rates observed in a study on SARS-CoV-2 transmission on board of high-speed trains (1/312). Targeted studies on very high attack rates in buses and restaurants on the other hand, indicated risks as high as 1/8 – 1/2, i.e. significantly higher than this study estimated for the scenario in which a super shedder boarded the aircraft (1/370 – 1/16).

The results from the seven rows around the index passenger were also extrapolated to a fully occupied aircraft cabin in order to estimate the expected number of cruise flights with an infectious passenger on board required for at least one COVID-19 case as a result of SARS-CoV-2 transmission via aerosols. The expected number of cruise flights to result in at least 1 case of aerosol transmission from a 'regular' virus shedding index passenger was estimated to range from 2 to 44 cruise flights of durations typical for the aircraft types in the study. In case of longer durations cruise flights, the expected number of flights ranged from 2 to 19. The expected number of cruise flights to result in at least 1 case of aerosol transmission from a 'super shedder' index passenger was estimated to range from 1 to 9 flights (typical duration cruise) and 1 to 4 flights (longer duration cruise).

The study addressed the risk of transmission on board of an aircraft via inhalation of virus bearing aerosols if one index passenger was present in the cabin. Control measures such as triage and testing that are targeted at preventing infectious people from boarding an aircraft are essential. However, these measures are likely not 100% effective. Public health and social measures on board should be in compliance with national and sectoral procedures. Estimates on the likelihood of one infectious passenger boarding an aircraft are hard to validate but an upper limit of 5% of the current prevalence (June 7, 2021) in the Netherlands would indicate less than 30/100.000 passengers. Depending on the number of passengers per aircraft (100 – 300), every 11 – 33 flights could carry an infectious passenger and less than 3% of these could be a super shedder. Complying to all (non-pharmaceutical) mitigation strategies in place, such as good hygiene and mask wearing, will decrease the risk of transmission, although some risk will remain.

Statistical analysis of the measurement data revealed that distance and angle relative to the virus shedding passenger was highly significant in all cases. The effect of wearing a mask by all passengers as included in the risk assessment was based on data from literature. The experimental data suggested that a face mask reduced emission of the larger aerosols and altered the direction of the emitted aerosols. More data is required to validate these findings.

Major sources of the high variability of the risk estimates based on measurement and simulation data were the viral concentration in the aerosols and the volume of aerosol emitted by the virus shedding passenger. Their variation has an impact of over an order of magnitude on the risk. The flight duration, and the efficiency of masks to limit aerosol emission and inhalation had a direct proportional effect on the risks, but the variation resulting from these aspects was smaller than an order of magnitude.

## 9 Recommendations

Following the conclusions drawn in Chapter 8, the study led to a number of recommendations. Policy-related recommendations are described in Section 9.1 and recommendations for future research are described in Section 9.2.

It is emphasised that the current study assesses the risk of illness and does not evaluate or comment on the acceptability of such risks.

### 9.1 Policy and mitigation

The study concludes that there is a risk of in-cabin SARS-CoV-2 transmission via aerosols, but it is relatively low, assuming that mitigation measures as described in Section 1.4 that minimise the probability of contagious passengers entering the cabin are in place, and masks are worn throughout the flight. It should be noted that the risks presented in the study are based on an assessment of a small set of aircraft under set conditions and can vary among aircraft types. Also, the risks assessment presented here, expressed risks as averages over (parts of) the aircraft. An individual passenger's risk will vary strongly with their seat location in relation to the index passenger. It is thus recommended to continue existing efforts to minimise the likelihood of an infected passenger entering the aircraft. Based on literature mask efficiencies of 30% (inhalation) and 60% (emission) were assumed throughout the QMRA. In-cabin measurements showed an even larger reduction on emission. The reduction in emitted particles directly translates to a lower dose and risk of illness. This stresses the relevance of the recommendation to wear a mask as much as possible as long as passengers might be infectious. Although that scenario has not been investigated specifically, this could be particularly relevant for longer flight durations during which (hot) meals are served and consumed.

### 9.2 Future research

This study has added to the growing body of knowledge available on the transmission risk of SARS-CoV-2 in aircraft cabins by investigating the risk of illness following transmission of virus bearing aerosols in two aircraft size classes and three aircraft types under a variety of conditions using a mutually supportive and reinforcing combinations of particle dispersion measurements and simulations and an extensive quantitative microbial risk assessment. Recommendations for future research exists in two primary directions – widening or deepening understanding.

In the former direction – studying SARS-CoV-2 transmission in aircraft cabins in different situations and different circumstances – other often-used aircraft types and classes can be studied. Smaller aircraft, such as regional jets, seem to have received the lowest attention up to now – although the shorter routes these are used for, inherently limit the transmission risk by reducing the time occupants are exposed. Scenarios where passengers board and deboard the aircraft and move and interact with each other and where the aircraft ventilation system is powered by its APU or ground systems, is another suggested area of interest. Besides regional aircraft, single aisle types might be prioritised here, given the attention already paid to twin aisle aircraft in a terminal jetway in earlier work (Kinahan, 2021). Independent of the flight phase, study of the effects of passenger or crew movement on transmission risk, forms an interesting path. Due to the limited time aircraft spend in the take-off, climb, descent and landing phases (reducing the risk by reducing exposure time), evaluating transmission risk there seem of lower interest. All future studies are

recommended to, in addition to presenting risk for typical situations, also document risks per hour, allowing studies to be compared more easily.

Besides studying other aircraft types and situations, the study of other transmission routes is a key recommendation. The previous literature review noted that the relative importance of different routes was unknown. Studies that help determine precisely that, can help in the design and implementation of the most relevant and effective mitigation measures. Of course, that also holds for situations and locations different than the aircraft cabins investigated in this study.

Attempts to deepen understanding of the situations studied in this work exist in multiple fields. Due to uncertainty about the representativeness of measurements runs with a face mask, the risk assessments presented here were based on conservative assumptions of mask efficiency based on values from literature. Analysis of the results from measurement runs in which the index was equipped with a face mask suggest that mask effectiveness may, in cases, be higher. This is also suggested by data on mask efficiency reported in literature, which shows large variation in efficiency based on mask type, mask wearing and aerosol size. Similarly, by using no-mask particle dispersion results and applying a knock-down factor afterwards, the effects of masks on the particle distribution and air flow have not been taken into account. Opportunities for refinement exist, also in including the influence of in and exhalation by other passengers on airflow as modelled using simulations. Replicating the in-flight particle dispersion measurements with heated manikins, which was not possible in the current study, could be another refinement.

In addition to better studying the effects of mouth masks on aerosol dispersion in an aircraft cabin environment, more research could go out to the influence of specific parameters. Possibly relevant examples are seat and tray table position, further variation in gasper use, and other ventilation system settings.

## 10 References

- Asadi, S., Wexler, A. S., Cappa, C. D., Barreda, S., Bouvier, N. M., & Ristenpart, W. D. (2019). Aerosol emission and superemission during human speech increase with voice loudness. *Nature Scientific Reports*.
- Bae, S. S. (2020). Asymptomatic Transmission of SARS-CoV-2 on Evacuation Flight. *Emerging Infectious Diseases*, 26(11), 2705-2708. doi:10.3201/eid2611.203353
- Boussinesq, J. (1897). *Théorie de l'écoulement tourbillonnant et tumultueux des liquides dans les lits rectilignes a grande section*. Paris: Gauthier-Villars et fils.
- CBS. (2020a, June 29). *Nauwelijks beweging in de luchtvaart in mei*. Retrieved from <https://www.cbs.nl/nl-nl/nieuws/2020/27/nauwelijks-beweging-in-de-luchtvaart-in-mei>
- CBS. (2020b, November 2). *Derde kwartaal ruim drie kwart minder luchtvaartpassagiers dan jaar eerder*. Retrieved from <https://www.cbs.nl/nl-nl/nieuws/2020/45/derde-kwartaal-ruim-drie-kwart-minder-luchtvaartpassagiers-dan-jaar-eerder>
- CDC. (2021, May 7). *Scientific Brief: SARS-CoV-2 Transmission*. Retrieved from <https://www.cdc.gov/coronavirus/2019-ncov/science/science-briefs/sars-cov-2-transmission.html>
- Chen et al. . (2020). Potential transmission of SARS-CoV-2 on a flight from Singapore to Hangzhou, China: An epidemiological investigation. *Elsevier Public Health Emergency Collection*.
- Chen, W., Zhang, N., Wei, J., Yen, H.-L., & Li, Y. (2020). Short-range airborne route dominates exposure of respiratory infection during close contact. *Building and Environment*, 176, 106859.
- Chetty, T., Daniels, B., Ngandu, N., & Goga, A. (2020, October 12). A rapid review of the effectiveness of screening practices at airports, land borders and ports to reduce the transmission of respiratory infectious diseases such as COVID-19. *South African Medical Journal*, 110(11), 1105-1109.
- Choi, E. M. (2020). In-Flight Transmission of Severe Acute Respiratory Syndrome Coronavirus 2. *Emerging Infectious Diseases*.
- Courtney, J., & Bax, A. (2021, March 16). Hydrating the respiratory tract: An alternative explanation why masks lower severity of COVID-19. *Biophysical Journal*, 120(6), 994-1000.
- Davis, A. C., Zee, M., Clark, A. D., Wu, T., Jones, S. P., Waite, L. L., . . . Olson, N. A. (2021, Februari 17). Computational Fluid Dynamics Modeling of Cough Transport in an Aircraft Cabin. *bioRxiv*. Retrieved from <https://www.biorxiv.org/content/10.1101/2021.02.15.431324v1.abstract>
- Davis, A., Menard, D., Clark, A., Cummins, J., & Olson, N. (2021). *Comparison of cough particle exposure for indoor commercial and aircraft cabin spaces*. Boeing. Retrieved from [https://www.boeing.com/confident-travel/downloads/Boeing\\_Comparison\\_cough\\_particle\\_exposure\\_indoor\\_commercial\\_and\\_aircraft\\_cabin\\_spaces.pdf](https://www.boeing.com/confident-travel/downloads/Boeing_Comparison_cough_particle_exposure_indoor_commercial_and_aircraft_cabin_spaces.pdf)
- Duguid, J. (1946). The size and the duration of air-carriage of respiratory droplets and droplet-nuclei. *J Hyg(44)*, 471-479.
- Duguid, J. P. (1945). The numbers and the sites of origin of the droplets expelled during expiratory activities. *Edinburgh Medical Journal*.
- ECDC. (2020, July 1). *COVID-19 Aviation Health Safety Protocol: Guidance for the management of airline passengers in relation to the COVID-19 pandemic*. Retrieved from European Centre for Disease Prevention and Control : <https://www.ecdc.europa.eu/en/publications-data/covid-19-aviation-health-safety-protocol>
- Eldin, C. (2020). Probable aircraft transmission of Covid-19 in-flight from the Central African Republic to France. *Elsevier Public Health Emergency Collection*.
- EUROCONTROL. (2019a, May 15). *Taxi times - Winter 2018-2019*. Retrieved from Library: <https://www.eurocontrol.int/publication/taxi-times-winter-2018-2019>
- EUROCONTROL. (2019b, December 19). *Taxi times - Summer 2019*. Retrieved from Library: <https://www.eurocontrol.int/publication/taxi-times-summer-2019>
- Fabian, P., Brain, J., Houseman, A., Gem, J., & Milton, D. (2011). Origin of Exhaled Breath Particles from Health and Human Rhinovirus-infected subjects. *Journal of Aerosol medicine and pulmonary drug delivery*, 137-147.
- Gorbalenya, A. E., Baker, S. C., Baric, R. S., de Groot, R. J., Drosten, C., Gulyeva, A. A., & ... (2020). The species Severe acute respiratory syndrome-related coronavirus: classifying 2012-nCoV and naming it SARS-CoV-2. *Nature Microbiology*, 536-544.

- Government of the Netherlands. (2021). *Negative COVID-19 test results and declaration required*. Retrieved April 21, 2021, from Coronavirus COVID-19: <https://www.government.nl/topics/c/coronavirus-covid-19/visiting-the-netherlands-from-abroad/mandatory-negative-test-results-and-declaration>
- Gupta, J., Lin, C.-H., & Chen, Q. (2011). Transport of expiratory droplets in an aircraft cabin. *Indoor Air*, 21(1), 3-11.
- Haas, C. (2020, August 14). *Action Levels for SARS-CoV-2 in Air: Preliminary Approach*. Retrieved from <https://files.osf.io/v1/resources/erntm/providers/osfstorage/5f371de025e5dc00c4c9558f?action=download&direct&version=1>
- Hertzberg, V. S., & Weiss, H. (2016). On the 2-Row Rule for Infectious Disease Transmission on Aircraft. *Annals of Global Health*.
- Hoehl, S. (2020). Assessment of SARS-CoV-2 Transmission on an International Flight and Among a Tourist Group. *JAMA Network Open*.
- Hu M, L. H. (2021). Risk of Coronavirus Disease 2019 Transmission in Train Passengers: an Epidemiological and Modeling Study. *Clin Infect Dis*, 72(4). doi:10.1093/cid/ciaa1057
- IATA. (2021). *COVID-19: Air Travel, Public Health Measures and Risk - A Brief Summary of Current Medical Evidence (Version 1 - 24 April 2021)*. Retrieved from <https://www.iata.org/globalassets/iata/programs/covid/restart/covid-public-health-measures-evidence-docmk-26042021.pdf>
- Kampf, G., Brüggemann, Y., Kaba, H., Steinmann, J., Pfaender, S., Scheithauer, S., & Steinmann, E. (2020, December). Potential sources, modes of transmission and effectiveness of prevention measures against SARS-CoV-2. *Elsevier Public Health Emergency Collection*, 106(4), 678-697.
- Khanh et al. (2020). Transmission of Severe Acute Respiratory Syndrome Coronavirus 2 During Long Flight. *Emerging Infectious Diseases*.
- Kinahan, S. M. (2021). Aerosol tracer testing in Boeing 767 and 777 aircraft to simulate exposure potential of infectious aerosol such as SARS-CoV-2. doi:10.1101/2021.01.11.21249626
- La Rosa, G., Bonadonna, L., Lucentini, L., Kenmoe, S., & Suffredini, E. (2020). Coronavirus in water environments: Occurrence, persistence and concentration methods - a scoping review. *Water Research*.
- Liu, L., Wei, J., Li, Y., & Ooi, A. (2017). Evaporation and dispersion of respiratory droplets from coughing. *Indoor Air*, 179-190.
- Lu, J. G. (2020). COVID-19 Outbreak Associated with Air Conditioning in Restaurant, Guangzhou, China, 2020. *Emerging infectious diseases*, 26(7), 1628–1631. doi:10.3201/eid2607.200764
- Luo, K., Lei, Z., Hai, Z., Xiao, S., Rui, J., Yang, H., . . . Chen, T. (2020). Transmission of SARS-CoV-2 in Public Transportation Vehicles: A Case Study in Hunan Province, China. *Open Forum Infect Dis*, 7(10), ofaa430.
- Lytras, T. (2020). High prevalence of SARS-CoV-2 infection in repatriation flights to Greece from three European countries. *Journal of Travel Medicine*.
- Marcus, L. (2021). *Assessment of Risks of SARS-CoV-2 Transmission During Air Travel and Non-Pharmaceutical Interventions to Reduce Risk, Phase One Report: Gate-to-Gate Travel Onboard Aircraft*. Harvard T.H. Chan School of Public Health.
- Morawska, L. (2006). Droplet fate in indoor environments, or can we prevent the spread of infection? *Indoor Air*, 16(5), 335-347. doi:10.1111/j.1600-0668.2006.00432.x
- Mouchtouri, V. A., Bogogiannidou, Z., Dirksen-Fischer, M., Tsiodras, S., & Hadjichristodoulou, C. (2020). Detection of imported COVID-19 cases worldwide: Early assessment of airport entry screening, 24 January until 17 February 2020. *Tropical Medicine and Health*.
- Murphy, N. B. (2020). A large national outbreak of COVID-19 linked to air travel, Ireland, summer 2020. *Eurosurveillance*, 25(42). doi:10.2807/1560-7917.ES.2020.25.42.2001624
- NLR & RIVM. (2020). *CORSICA literature report: Key findings from literature review on the SARS-CoV-2 transmission in aircraft cabins (NLR-CR-2020-288)*. Amsterdam, the Netherlands: Royal Netherlands Aerospace Centre.
- NurseTogether. (2020, April 11). *File:Surgical face mask.jpg*. Retrieved from Wikimedia Commons: [https://commons.wikimedia.org/wiki/File:Surgical\\_face\\_mask.jpg](https://commons.wikimedia.org/wiki/File:Surgical_face_mask.jpg)
- Olsen, S. J., Chang, H.-L., Cheung, T. Y.-Y., Tang, A. F.-Y., Fisk, T. L., Ooi, S. P.-L., . . . Dowell, S. (2003). Transmission of the Severe Acute Respiratory Syndrome on Aircraft. *New England Journal of Medicine*, 349(25), 2416-2422. doi:10.1056/NEJMoa031349
- Oran, D. P., & Topol, E. J. (2021). The Proportion of SARS-CoV-2 Infections That Are Asymptomatic : A Systematic Review. *Annals of internal medicine*, M20-6976.

- Pang, J., Jones, S., Waite, L., Olson, N., Atmur, R., & Cummins, J. (2021, April 14). Probability and Estimated Risk of SARS-CoV-2 Transmission in the Air Travel System: A Systemic Review and Meta-Analysis. *medRxiv*. Retrieved from <https://www.medrxiv.org/content/10.1101/2021.04.08.21255171v1>
- Pavli, A. (2020). In-flight transmission of COVID-19 on flights to Greece: An epidemiological analysis. *Elsevier Public Health Emergency Collection*.
- Popa, A., Genger, J.-W., Nicholson, M. D., Penz, T., Schmid, D., Aberle, S. W., . . . et al. (2020). Genomic epidemiology of superspreading events in Austria reveals mutational dynamics and transmission properties of SARS-CoV-2. *Science Translational Medicine*, eabe2555.
- R Core Team. (2019). *R: A language and environment for statistical computing*. Vienna, Austria: R Foundation for Statistical Computing. Retrieved from <https://www.R-project.org/>.
- Ren, R., Zhang, Y., Li, Q., McGoogan, J. M., Feng, Z., Gao, G., & Wu, Z. (2021). Asymptomatic SARS-CoV-2 Infections Among Persons Entering China From April 16 to October 12, 2020. *JAMA*, 325(5), 489-492.
- Rijksoverheid. (2020a, June 12). *Advies luchtvaart COVID-19*. Retrieved from <https://www.rijksoverheid.nl/documenten/rapporten/2020/06/12/advies-luchtvaart-covid-19>
- Rijksoverheid. (2020b, June 12). *Nederlandse luchtvaart neemt maatregelen voor verantwoord vliegen in coronatijd*. Retrieved from Website of Dutch national government: <https://www.rijksoverheid.nl/onderwerpen/luchtvaart/nieuws/2020/06/12/nederlandse-luchtvaart-neemt-maatregelen-voor-verantwoord-vliegen-in-coronatijd>
- Rijksoverheid. (2021, April 22). *Negatieve COVID-19-testuitslagen verplicht bij vertrek naar Nederland*. Retrieved from Rijksoverheid.nl: <https://www.rijksoverheid.nl/onderwerpen/coronavirus-covid-19/reizen-en-vakantie/verplichte-negatieve-covid-19-testuitslagen>
- Rijksoverheid. (n.d.). *Maatregelen tegen verspreiding coronavirus in ov*. Retrieved from <https://www.rijksoverheid.nl/onderwerpen/coronavirus-covid-19/vervoer/openbaar-vervoer>
- RIVM. (2020a, November 27). *OMT 89*. Retrieved from <https://www.rivm.nl/omt89>
- RIVM. (2020b, November 30). *Grootschalig testen van personen zonder klachten - Achtergronddocument bij advies n.a.v. 89e OMT*. Bilthoven, the Netherlands: RIVM.
- RIVM. (2021a, May 5). *Face masks and gloves*. Retrieved from <https://www.rivm.nl/en/coronavirus-covid-19/face-masks-and-gloves>
- RIVM. (2021b). *Advies n.a.v. 100e OMT*. Bilthoven, the Netherlands: RIVM.
- RIVM. (n.d.). *COVID-19*. Retrieved from <https://www.rivm.nl/coronavirus-covid-19>
- Roosien, R. J., Peerlings, B., & Jabben, J. (2020). *Inventarisatie van de aanwezigheid van HEPA-filters in vliegtuigen op Nederlandse luchthavens*. Amsterdam, the Netherlands: NLR - Koninklijk Nederlands Lucht- en Ruimtevaartcentrum.
- Schijven, J., Vermeulen, L., Swart, A., Meijer, A., Duizer, E., & de Roda Husman, A. (2021, July 5). Quantitative microbial risk assessment for airborne transmission of SARS-CoV-2 via breathing, speaking, singing, coughing and sneezing. *Environmental Health Perspectives*, 129(4). doi:10.1101/2020.07.02.20144832
- Schwarz et al. (2020). Lack of COVID-19 transmission on an international flight. *CMAJ*.
- SeatGuru. (2020a). *Short-haul Economy Class Comparison Chart*. Retrieved October 14, 2020, from [https://www.seatguru.com/charts/shorthaul\\_economy.php](https://www.seatguru.com/charts/shorthaul_economy.php)
- SeatGuru. (2020b). *Long-haul Economy Class Comparison Chart*. Retrieved October 14, 2020, from [https://www.seatguru.com/charts/longhaul\\_economy.php](https://www.seatguru.com/charts/longhaul_economy.php)
- Shen, Y., Li, C., Dong, H., Wang, Z., Martinez, L., Sun, Z., & et al. . (2020). Community Outbreak Investigation of SARS-CoV-2 Transmission Among Bus Riders in Eastern China. *JAMA Intern Med*, 180(12), 1665-1671.
- Speake, H., Phillips, A., Chong, T., Sikazwe, C., Levy, A., Lang, J., . . . McEvoy, S. P. (2020). Flight-Associated Transmission of Severe Acute Respiratory Syndrome Coronavirus 2 Corroborated by Whole-Genome Sequencing. *Emerging Infectious Diseases*.
- Sze To, G. N. (2009). Experimental Study of Dispersion and Deposition of Expiratory Aerosols in Aircraft Cabins and Impact on Infectious Disease Transmission. *Aerosol Science and Technology*, 43(5), 466-485. doi:10.1080/02786820902736658
- Sze To, G., & Chao, C. (2010). Review and comparison between the Wells-Riley and dose-response approaches to risk assessment of infectious respiratory diseases. *Indoor Air*, 20(1), 2-16. doi:10.1111/j.1600-0668.2009.00621.x

- Tanabe, S.-i., Kobayashi, K., Nakano, J., Ozeki, Y., & Konishi, M. (2002, July). Evaluation of thermal comfort using combined multi-node thermoregulation (65MN) and radiation models and computational fluid dynamics (CFD). *Energy and Buildings*, 34(6), 637-646. doi:10.1016/S0378-7788(02)00014-2
- Volz, E., Hill, V., McCrone, J. T., Price, A., Jorgensen, D., O'Toole, A., . . . et al. (2021). Evaluating the Effects of SARS-CoV-2 Spike Mutation D614G on Transmissibility and Pathogenicity. *Cell*, 184(1), 64-75 e11.
- Wang, Z., Galea, E., Grandison, A., Ewer, J., & Jia, F. (2021). Inflight Transmission of COVID-19 Based on Aerosol Dispersion Data. *Journal of Travel Medicine*. doi:10.1101/2021.01.08.21249439
- WHO. (2020). *Evidence to recommendations: COVID-19 mitigation in the aviation sector - Interim guidance*. Retrieved from <https://www.who.int/publications/i/item/evidence-to-recommendation-covid-19-mitigation-in-the-aviation-sector>
- Wolfram Research, Inc. (2021). *Mathematica. Version 12.3*. Champaign, Illinois: Wolfram Research, Inc. Retrieved from <https://www.wolfram.com/mathematica>
- Wood, S. N. (2006). *Generalized Additive Models: An Introduction with R*. Chapman and Hall/CRC Press. Retrieved from <https://cran.r-project.org/web/packages/gamm4/index.html>
- World Health Organization. (2021). *WHO R&D Blueprint COVID-19 new variants: Knowledge gaps and research*. World Health Organization.
- Yang et al. (2020). In-flight Transmission Cluster of COVID-19: A Retrospective Case. *Infectious Diseases*.
- Zhou, B., Thao, T. T., Hoffmann, D., Taddeo, A., Ebert, N., Labroussaa, F., . . . et al. (2021). SARS-CoV-2 spike D614G change enhances replication and transmission. *Nature*, 592(7852), 122-127.
- Zhou, P., & et al. (2020). A pneumonia outbreak associated with a new coronavirus of probable bat origin. *Nature*, 270-273.

# Appendix A Summary of CORSICA literature report

This appendix contains the English (Appendix A.1) and Dutch (Appendix A.2) summaries of the CORSICA literature report (NLR & RIVM, 2020), used for guiding the measurement and simulation research documented in this final report.

## Appendix A.1 English

### Problem area

The coronavirus, COVID-19, has large consequences for aviation. Measures to combat COVID-19 have brought international aviation almost to a complete standstill in March 2020. RIVM advised on the safety on board of aircraft in relation to SARS-CoV-2 and the associated safety protocols put in place by Dutch airlines, based on guidelines by EASA and ICAO. RIVM deems it plausible that the ventilation system on board of aircraft, with a high air exchange rate and vertical air flows, limits possible transmission of SARS-CoV-2 on board of aircraft. Although the number of flights, following a short recovery during the summer, is still limited and little cases of SARS-CoV-2 contamination on board of aircraft are known at the moment, there are concerns about the contamination risk on board. Expanding the knowledge about the relevant factors and the effectiveness of currently implemented measures, can contribute to decision and policy making by travellers, airlines and authorities.

### Description of work

Royal Netherlands Aerospace Centre (NLR) and the National Institute for Public Health and the Environment (RIVM) have been tasked by the Ministry of Infrastructure and Water Management to conduct fact-based and objective research, consisting of simulations and measurements, on the SARS-CoV-2 contamination risk on board of aircraft. NLR primarily addresses aviation aspects and project coordination and RIVM is responsible for virology, exposure and health related aspects.

This report contains the results of the literature research and serves as input for the subsequent simulations and measurements. The final report will be published mid-December 2020.

### Results and conclusions

The literature research has identified the factors relevant for the contamination of SARS-CoV-2 on board of aircraft, distinguishing between cabin conditions, the contamination source, transmission through the cabin and the exposure of a recipient. Additionally, literature on documented cases of SARS-CoV-2 on board of aircraft and currently applied mitigation measures has been reviewed.

Following the most recent RIVM research, a range of  $<1 - 2000 \mu\text{m}$  will be assumed for particle size. This span both larger as well as smaller droplets (so-called aerosols). It is assumed that all passengers and crew in the cabin wear non—medical face masks. Based on available literature, an inhalation filtering efficiency of 30% and an exhalation filtering efficiency of 60% are currently assumed.

Three relevant routes for virus transmission have been investigated: transmission by means of larger droplets (e.g. following sneezing or coughing), transmission by means of aerosols (exhaled by breathing) and contact transmission.

The relative importance of these routes is subject of discussion in literature and is difficult to determine, although literature seems to note little cases of contact transmission. The simulations and measurements will therefore address the first two routes. For transmission by means of larger droplets, the use of mouth masks, good sneezing and coughing hygiene and gravity effects seem most relevant; for transmission by means of aerosols, air flows play a large role. These air flows are not only influenced by the ventilation system, but also by the physical presence and heat of passengers in the cabin.

In the next phase of this research, simulations and measurements will be used to complement theoretical knowledge with practical results thereby determine the contamination risk of SARS-CoV-2 on board of aircraft. The optimal combination of simulations and measurements will too be determined in that phase. To enable validation of the findings, the simulation work will start with a base scenario of the most common circumstances (cruise flight), for which data from literature is available. Later, additional scenarios are to be added. Measurements provide the most realistic representation of reality. Depending on the strategy, measuring cabin conditions and measuring actual transmission can both be considered. To ensure the highest level of realism, actual aircraft types rather than generic models will be considered. Based on the commonality at Schiphol, the Boeing 737 and Airbus A320 are identified as representative single-aisle aircraft. For the larger twin-aisle aircraft, the Boeing 777 and 787 are evident choices.

### **Applicability**

This report contains the results of the literature research and serves as input for the subsequent simulations and measurements in the CORSICA project. The research is limited to SARS-CoV-2 transmission on board of large aircraft used for commercial passenger transport.

## **Appendix A.2 Nederlands**

### **Probleemstelling**

Het coronavirus, COVID-19, heeft grote gevolgen voor de luchtvaart. De genomen maatregelen in de strijd tegen COVID-19 hebben de internationale luchtvaart in maart 2020 vrijwel volledig tot stilstand gebracht. Het RIVM heeft begin juni advies gegeven over de veiligheid aan boord van vliegtuigen in verband met COVID-19. Ook heeft het RIVM advies gegeven op de protocollen van de Nederlandse luchtvaartmaatschappijen. De basis voor de protocollen ligt in de EASA- en ICAO-richtlijnen. Het RIVM stelt in dit advies dat het plausibel is dat de ventilatiesystemen aan boord van vliegtuigen met hoge luchtverversing en verticale luchtstromen een beperking geeft op eventuele overdracht van SARS-CoV-2 aan boord. Hoewel er na een korte opleving gedurende de zomerperiode nog steeds weinig wordt gevlogen en er weinig gevallen van SARS-CoV-2 aan boord van vliegtuigen bekend zijn, zijn er tegelijkertijd zorgen over het risico op besmetting aan boord. Door de kennis over de relevante factoren en de effectiviteit van de genomen maatregelen aan te vullen, kan worden bijgedragen aan de besluit- en beleidsvorming door reizigers, luchtvaartmaatschappijen en autoriteiten.

### **Beschrijving van de werkzaamheden**

Het Koninklijk Nederlands Lucht- en Ruimtevaartcentrum (NLR) en het Rijksinstituut voor Volksgezondheid en Milieu (RIVM) hebben van het Ministerie van Infrastructuur en Waterstaat de opdracht gekregen om feitelijk en objectief onderzoek bestaande uit literatuuronderzoek, simulaties en metingen te doen naar de besmettingsrisico's voor COVID-19 aan boord van vliegtuigen. Hierbij richt NLR zich primair op de luchtvaartaspecten en projectcoördinatie en het RIVM op virologie en blootstellings- en gezondheidsaspecten.

Dit rapport bevat de resultaten van het literatuuronderzoek en dient om input te geven aan de hierop volgende simulaties en metingen. Het eindrapport zal medio december 2020 worden opgeleverd.

## Resultaten en conclusies

Het literatuuronderzoek heeft de factoren in beeld gebracht die relevant zijn voor de verspreiding van SARS-CoV-2 aan boord van vliegtuigen, onderverdeeld in cabine-condities, de bron van besmetting, verspreiding door de cabine en blootstelling van een ontvanger. Tevens is gekeken naar reeds bekende besmettingsgevallen uit de literatuur en naar literatuur met betrekking tot reeds genomen mitigatiemaatregelen.

Voor de grootte van de virusdeeltjes wordt conform het meest recente RIVM-onderzoek een bandbreedte van  $<1 - 2000 \mu\text{m}$  aangehouden, deze omvatten zowel grotere druppels als kleinere druppels (zogenoemde aerosolen). Aangenomen wordt dat alle passagiers en bemanningsleden in de cabine niet-medische mondkapjes dragen. Op basis van beschikbare literatuur wordt voornamelijk een efficiëntie van 30% bij inademen en 60% bij uitademen voor deze maskers aangenomen.

Er zijn drie relevante routes voor virusverspreiding onderzocht: verspreiding via grotere druppels (o.a. door niezen of hoesten), verspreiding via aerosolen (in de adem) en besmetting via oppervlakten. Het relatieve belang van deze routes voor de virusverspreiding is onderwerp van discussie in de literatuur en is lastig te bepalen, al lijkt besmetting via oppervlakten volgens de literatuur weinig voor te komen. De simulaties en metingen zullen zich dan ook richten op de eerste twee routes. Bij verspreiding via grotere druppels lijken gebruik van mondkapjes, goede nies- en hoesthygiëne en zwaartekrachteffecten het meest relevant, bij aerosolen-verspreiding spelen de luchtstromen een grote rol. Deze luchtstromen worden niet alleen door het ventilatiesysteem beïnvloed, maar ook door de fysieke aanwezigheid en warmte van de passagiers in de cabine.

In de volgende fase van dit onderzoek worden simulaties en metingen gebruikt om de theoretische kennis aan te vullen met praktische resultaten en daarmee het besmettingsrisico van SARS-CoV-2 in vliegtuigen te bepalen. De optimale combinatie van simulaties en metingen wordt in dezelfde fase bepaald. Om validatie van de bevindingen mogelijk te maken wordt gestart met een basis-simulatiescenario onder de meest voorkomende omstandigheden (de kruisvlucht). Hiervoor is ook data uit de literatuur beschikbaar. Later worden andere scenario's toegevoegd. Metingen leveren de meest realistische benadering van de werkelijkheid. Afhankelijk van de gekozen aanpak kan zowel gekeken worden naar het meten van cabinecondities als naar daadwerkelijke verspreiding. Voor een zo hoog mogelijk realiteitsgehalte wordt uitgegaan van echte vliegtuigtypes in plaats van generieke modellen. Op basis van gangbaarheid op Schiphol zijn de Boeing 737 en Airbus A320 geïdentificeerd als representatief *single-aisle* vliegtuig. Voor de grotere *twin-aisle* toestellen zijn dat de Boeing 777 en 787.

## Toepasbaarheid

Dit rapport bevat de resultaten van het literatuuronderzoek en dient om input te geven aan de hierop volgende simulaties en metingen van project CORSICA. Het onderzoek beperkt zich tot SARS-CoV-2 besmetting aan boord van grote vliegtuigen die worden ingezet voor commercieel passagiersvervoer.

# Appendix B Technical appendices

## Appendix B.1 Research approach

### Appendix B.1.1 Risk of illness

Figure 28 describes how the risk of illness  $p_{ill}$ , estimated number of flights to first transmission (SA/TA-Est.NO1) and estimated number flights until individual gets ill (SA/TA-Est.NO2) as described in the report are determined based on type-specific QMRA output of the same indicators. These are in turn determined with input from measurement runs without a mask (A320/B737/B787-NoMask-N/Vol), breathing (A320/B787-X-Br-N/Vol) and speaking (A320/B787-X-Sp-N/Vol) CFD simulations using different index locations.

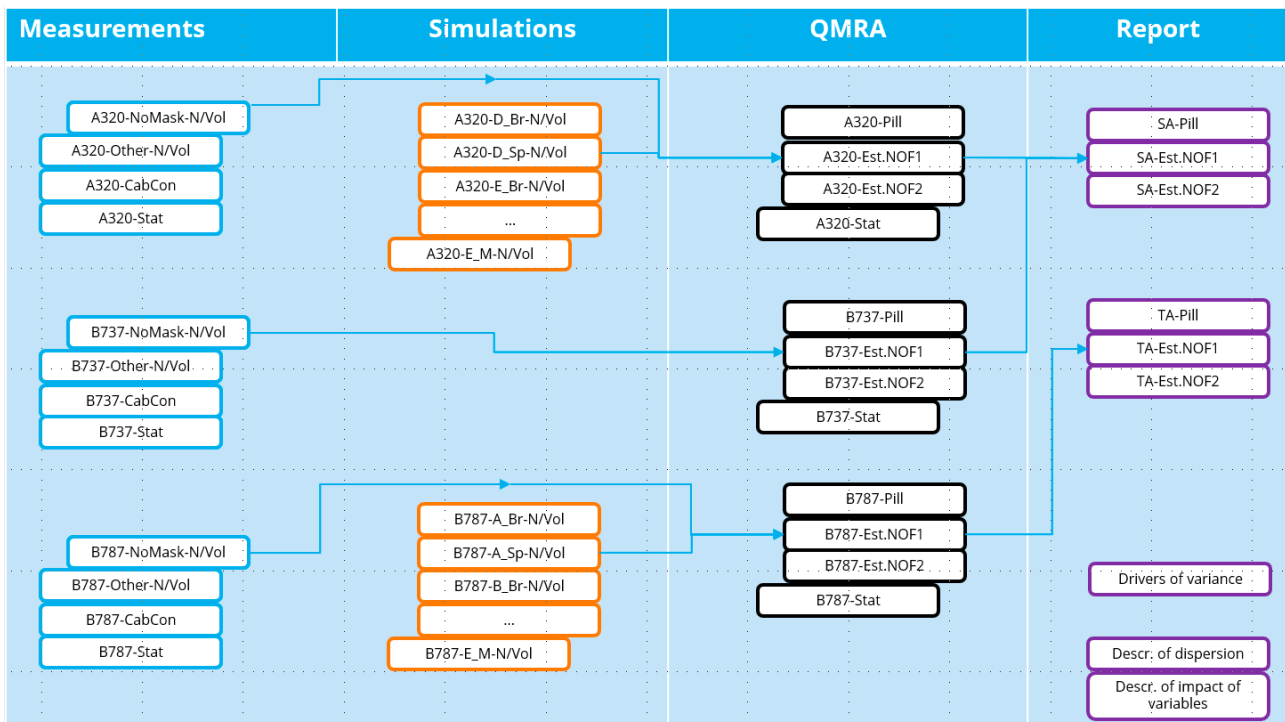


Figure 28: Data used for determining risk of illness, estimated no. of flights to first transmission and estimated no. flights until individual gets ill

## Appendix B.1.2 Drivers of variance

Figure 29 describes the data used to determine which measurement variables drive the risk of illness  $P_{ill}$ , estimated number of flights to first transmission (SA/TA-Est.NO1) using the statistical analysis as part of the QMRA and measurement data statistical analysis (both abbreviated with A320/B737/B787-Stat).

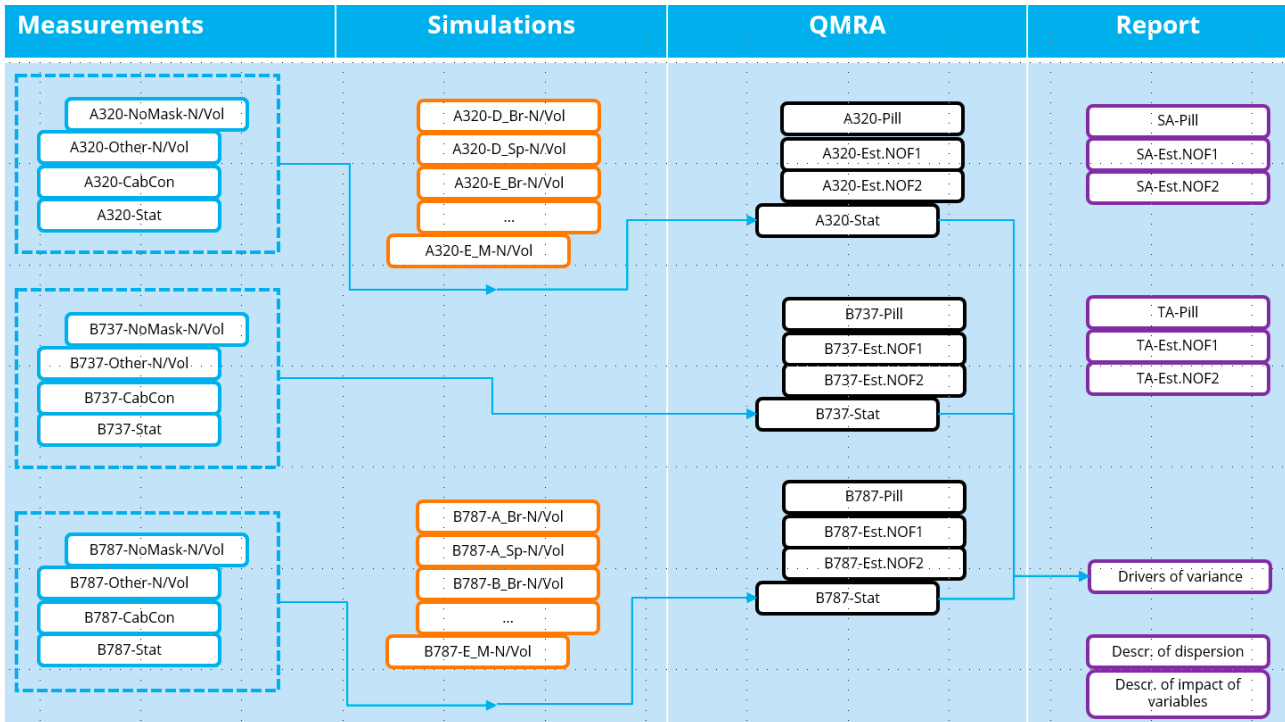


Figure 29: Data used for determining the main drivers of variation in risk of illness, estimated no. of flights to first transmission and estimated no. flights until individual gets ill

### Appendix B.1.3 Description of dispersion and impact of selected variables

Figure 30 illustrates the data used to describe the dispersion of aerosols (Descr. of dispersion) and the impact of the selected variables on aerosol dispersion (Descr. of impact of variables) using all available measurement and simulation data.

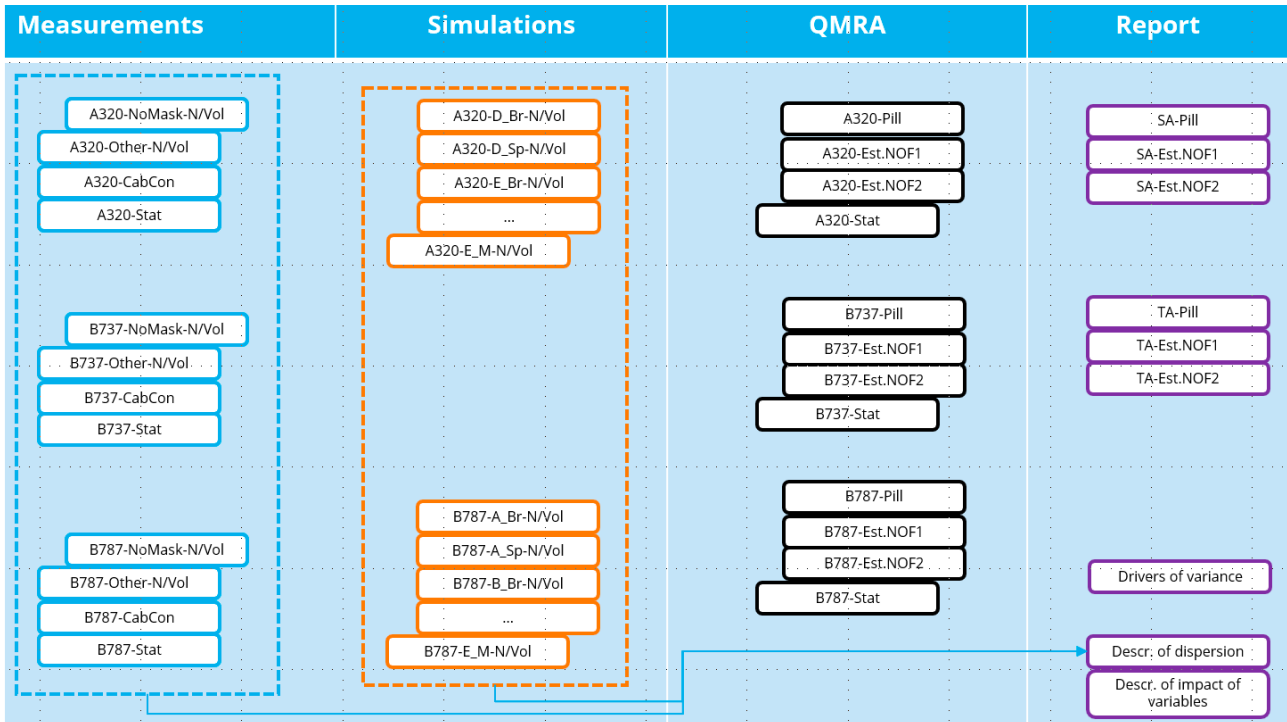


Figure 30: Data used for qualitatively describing the dispersion of aerosols and the impact of the selected variables on aerosol dispersion

## Appendix B.1.4 Cross-check measurements and simulations

Figure 31 illustrates how measurement data for runs without mask during cruise (A320/B787-NoMask-N/Vol) is cross-checked with CFD simulations of similar runs without a mask under similar conditions (A320/B787-E\_M-N/Vol).

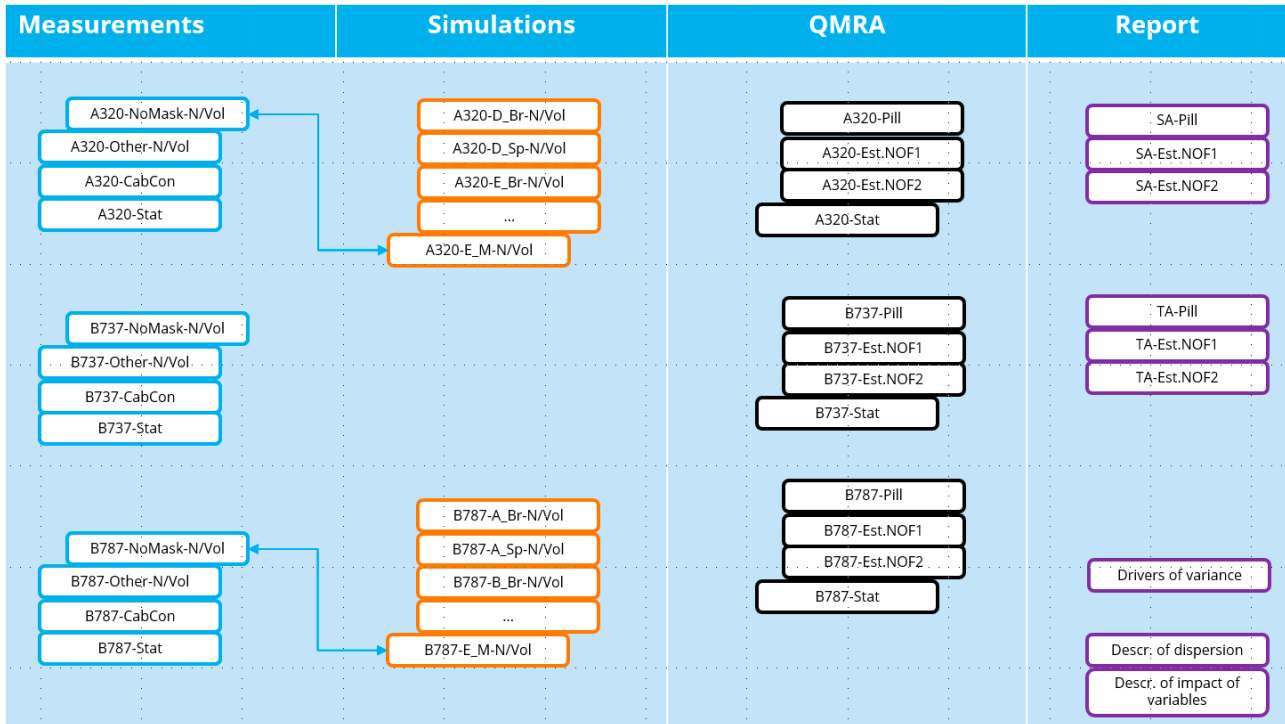


Figure 31: Data used for cross-check of measurements and simulations

## Appendix B.2 Measurement setup

### Appendix B.2.1 Equipment specification

Table 18: Instruments used for in-cabin measurements

Measurement	Instrument	Specifications
Temperature and relative humidity	EasyLog USB2 LCD +	Temperature: $-35 - 80\text{ °C} \pm 0.5\text{ °C}$ Relative hum.: $0 - 100\% \pm 2\%$ Sample frequency: 0.1 Hz
Surface temperature	FLIR E75 IR	Temperature: $0-50\text{ °C}$ , $\pm 0.1\text{ °C}$
Handheld flow meter	Testo 417 anemometer	Flow $0.3 - 20\text{ m/s}$ , $\pm 0.1\text{ m/s} + 1.5\%$ of measured value; 0.01 m/s
Air flow direction and speed	Gill Windmaster Pro 3D Anemometer	Speed: $0 - 65\text{ m/s} \pm 0.01\text{ m/s}$ Direction: $0 - 359.9^\circ \pm 0.2^\circ$ Sample frequency: 32 Hz
Spectrometer (APS)	TSI APS 3321	<p>Flow Rates*</p> <p>Aerosol Sample 1.0 L/min <math>\pm 0.1</math></p> <p>Sheath Air 4.0 L/min <math>\pm 0.1</math></p> <p>Total 5.0 L/min <math>\pm 0.2</math></p> <p>Atmospheric Pressure Correction</p> <p>Automatic correction between 400 and 1,030 mbar (full correction between 700 and 1,030 mbar)</p> <p>Laser Source 30-mW, 655-nm laser diode</p> <p>Detector Avalanche photodetector (APD)</p> <p>Front-panel Display <math>320 \times 240</math> pixels</p> <p>Operating Temperature 10 to <math>40^\circ\text{C}</math> (50 to <math>104^\circ\text{F}</math>)</p> <p>Operating Humidity 10 to 90% R.H., noncondensing</p> <p>Power 100 to 240 VAC, 50/60 Hz, 100 W, single phase or 24 VDC</p>
Particle matter sensor (PM)	Sensirion Particulate Matter Sensor SPS30	<a href="#">Particulate Matter Sensor SPS30   Sensirion</a>
Aerosol generator	Medspray Saliva-Aerosol	High Pressure (30 bar) Liquid Centrifugal Pump. Pressurized air requirement of 15 L/min at 2kPa
Source	Artificial saliva provided by Medspray	Water with 1%w/w glycerol and 2%w/w NaCl, designed to replicate human saliva. The total excipient concentration (what remains after evaporation) is 3%w/w.

## Appendix B.2.2 Measurement grid

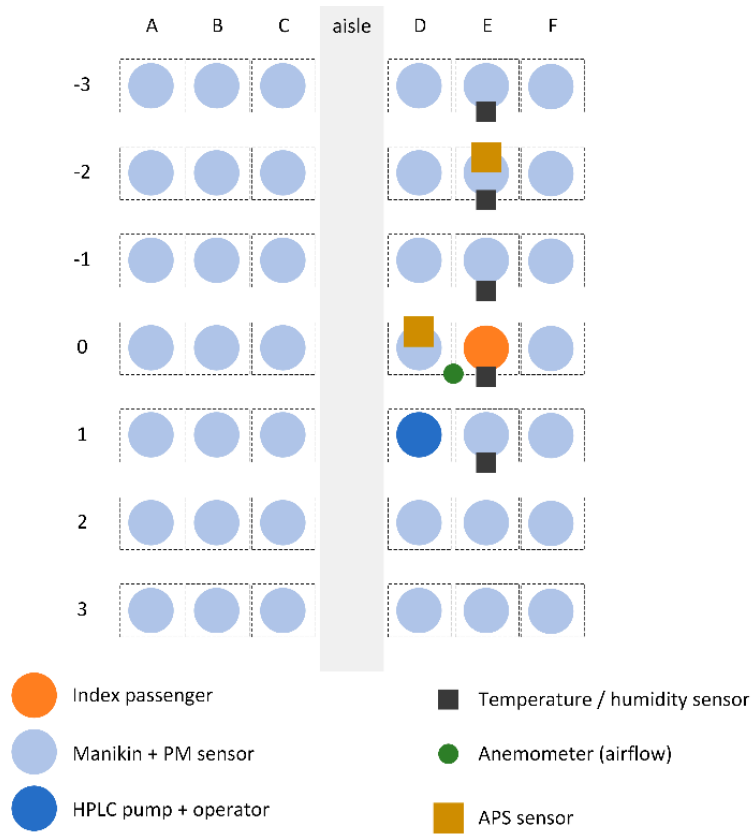


Figure 32: Measurement setup for Airbus A320 and Boeing 737-800

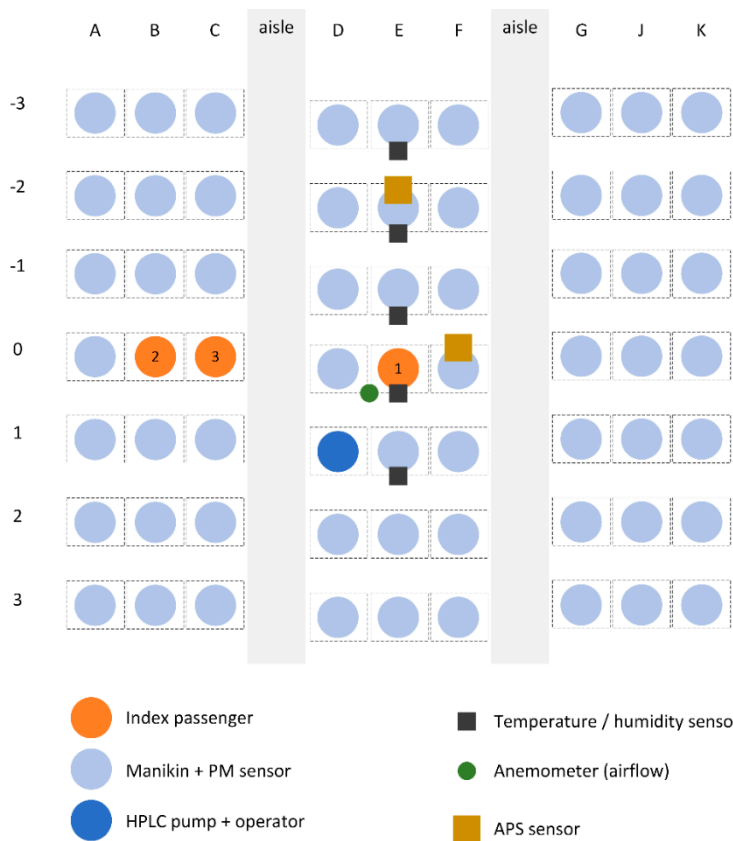


Figure 33: Measurement setup for Boeing 787-8, showing the three index locations tested (in different runs). Sensor locations were not varied between runs

### Appendix B.2.3 Measurement runs

The following tables provide an overview of the measurement runs included in the experimental campaign. Changes compared to the previous row are highlighted in a bold font.

Table 19: Airbus A320 measurement runs

#	Phase	Index seat	Heating blanket	Pack setting	Gasper use	Mask	Remarks
1	Ground	D	On	Normal	Closed	None	
2	Ground	D	On	Normal	Closed	<b>New</b>	
3	Ground	D	On	Normal	Closed	<b>Used</b>	
4	Ground	D	On	Normal	Closed	<b>None</b>	
5	Ground	D	<b>Off</b>	Normal	Closed	None	
6	Ground	D	Off	Normal	Closed	<b>New</b>	
7	Ground	D	Off	Normal	Closed	<b>Used</b>	
8	Ground	D	Off	Normal	Closed	<b>None</b>	
9	Ground	D	<b>On</b>	<b>High</b>	<b>All open</b>	<b>None</b>	
10	Ground	D	On	High	All open	<b>New</b>	Mask showed leakage
11	<b>Cruise</b>	D	<b>Off</b>	<b>Normal</b>	Middle open	<b>None</b>	
12	Cruise	D	Off	Normal	Middle open	None	
13	Cruise	D	Off	Normal	Middle open	<b>New</b>	
14	Cruise	D	Off	Normal	Middle open	<b>Used</b>	
15	Cruise	D	Off	Normal	Middle open	<b>New</b>	

#	Phase	Index seat	Heating blanket	Pack setting	Gasper use	Mask	Remarks
16	Cruise	D	Off	Normal	<b>All open</b>	<b>Used</b>	
17	Cruise	D	Off	<b>High</b>	All open	<b>New</b>	
18	Cruise	D	Off	High	All open	<b>Used</b>	
19	Cruise	D	Off	High	All open	<b>New</b>	
20	Cruise	D	Off	High	All open	New	
21	Cruise	D	Off	High	All open	<b>None</b>	
22	Cruise	D	Off	High	Closed	None	
23	Cruise	D	Off	High	Closed	<b>New</b>	
24	Cruise	D	Off	High	Closed	<b>Used</b>	
25	Cruise	D	Off	<b>Normal</b>	Closed	<b>None</b>	
26	Cruise	D	Off	High	Closed	<b>New</b>	

Table 20: Boeing 737-800 measurement runs

#	Phase	Index seat	Heating blanket	Pack setting	Gasper use	Mask	Remarks
1	Ground	D	On	Normal	Closed	<b>New</b>	
2	Ground	D	On	Normal	Closed	<b>Used</b>	
3	Ground	D	On	Normal	Closed	<b>New</b>	
4	Ground	D	On	Normal	Closed	<b>None</b>	
5	Ground	D	On	Normal	Closed	None	
6	Ground	D	On	Normal	<b>Middle open</b>	<b>New</b>	
7	Ground	D	On	Normal	Middle open	<b>Used</b>	
8	Ground	D	On	Normal	Middle open	<b>New</b>	
9	Ground	D	<b>Off</b>	Normal	Middle open	<b>None</b>	
10	Ground	D	Off	Normal	Middle open	<b>New</b>	
11	Ground	D	Off	Normal	Middle open	<b>Used</b>	
12	Ground	D	Off	Normal	Middle open	<b>New</b>	Grid disturbed
13	Ground	D	Off	Normal	Middle open	<b>None</b>	
14	Ground	D	Off	Normal	<b>Closed</b>	<b>New</b>	
15	Ground	D	Off	Normal	Closed	<b>Used</b>	Toilet flush
16	Ground	D	Off	Normal	Closed	<b>New</b>	
17	Ground	D	Off	Normal	Closed	<b>None</b>	
18	Ground	D	Off	Normal	<b>All open</b>	<b>New</b>	Taxiing, APU-power
19	<b>Cruise</b>	D	Off	Normal	<b>Closed</b>	<b>New</b>	
20	Cruise	D	Off	Normal	Closed	Used	
21	Cruise	D	Off	Normal	Closed	<b>New</b>	
22	Cruise	D	Off	Normal	Closed	<b>Used</b>	
23	Cruise	D	Off	Normal	Closed	<b>New</b>	
24	Cruise	D	Off	Normal	Closed	<b>None</b>	
25	Cruise	D	Off	Normal	Closed	None	90% aerosol spray
26	Cruise	D	Off	Normal	<b>Middle open</b>	<b>New</b>	
27	Cruise	D	Off	Normal	Middle open	<b>Used</b>	
28	Cruise	D	Off	Normal	Middle open	<b>New</b>	
29	Cruise	D	Off	<b>High</b>	Middle open	<b>Used</b>	
30	Cruise	D	Off	High	Middle open	<b>New</b>	
31	Cruise	D	Off	High	<b>All open</b>	New	

Table 21: Boeing 787-8 measurement runs

#	Phase	Index seat	Heating blanket	Pack setting	Gasper use	Mask	Remarks
1	Ground	E	On	Normal	Closed	New	
2	Ground	E	On	Normal	Closed	Used	
3	Ground	E	On	Normal	<b>Middle open</b>	<b>New</b>	
4	Ground	E	On	Normal	Middle open	<b>Used</b>	
5	Ground	E	On	Normal	Middle open	<b>New</b>	
6	Ground	E	<b>Off</b>	Normal	Middle open	New	
7	Ground	E	Off	Normal	Middle open	<b>Used</b>	
8	Ground	E	Off	Normal	Middle open	<b>New</b>	Engine runup
9	Ground	E	Off	Normal	Middle open	<b>None</b>	
10	Ground	E	Off	Normal	Middle open	<b>New</b>	
11	Ground	E	Off	Normal	Middle open	<b>None</b>	
12	<b>Cruise</b>	E	Off	Normal	Middle open	<b>New</b>	
13	Cruise	E	Off	Normal	Middle open	<b>Used</b>	
14	Cruise	E	Off	Normal	Middle open	<b>New</b>	
15	Cruise	E	Off	Normal	Middle open	<b>None</b>	
16	Cruise	E	Off	Normal	Middle open	<b>New</b>	
17	Cruise	E	Off	Normal	Middle open	<b>None</b>	
18	Cruise	E	Off	Normal	Middle open	None	
19	Cruise	E	Off	Normal	<b>All open</b>	<b>New</b>	
20	Cruise	E	Off	Normal	All open	<b>Used</b>	
21	Cruise	E	Off	Normal	All open	<b>New</b>	Grid disturbed
22	Cruise	E	Off	Normal	All open	<b>None</b>	SPS's fail
23	Cruise	E	Off	Normal	All open	None	
24	Cruise	B	Off	Normal	All open	<b>New</b>	
25	Cruise	B	Off	Normal	All open	<b>Used</b>	
26	Cruise	B	Off	Normal	All open	<b>New</b>	
27	Cruise	C	Off	Normal	All open	New	

## Appendix B.3 Cabin environmental conditions

The following figures present the results of the temperature and relative humidity measurements per aircraft and flight phase.

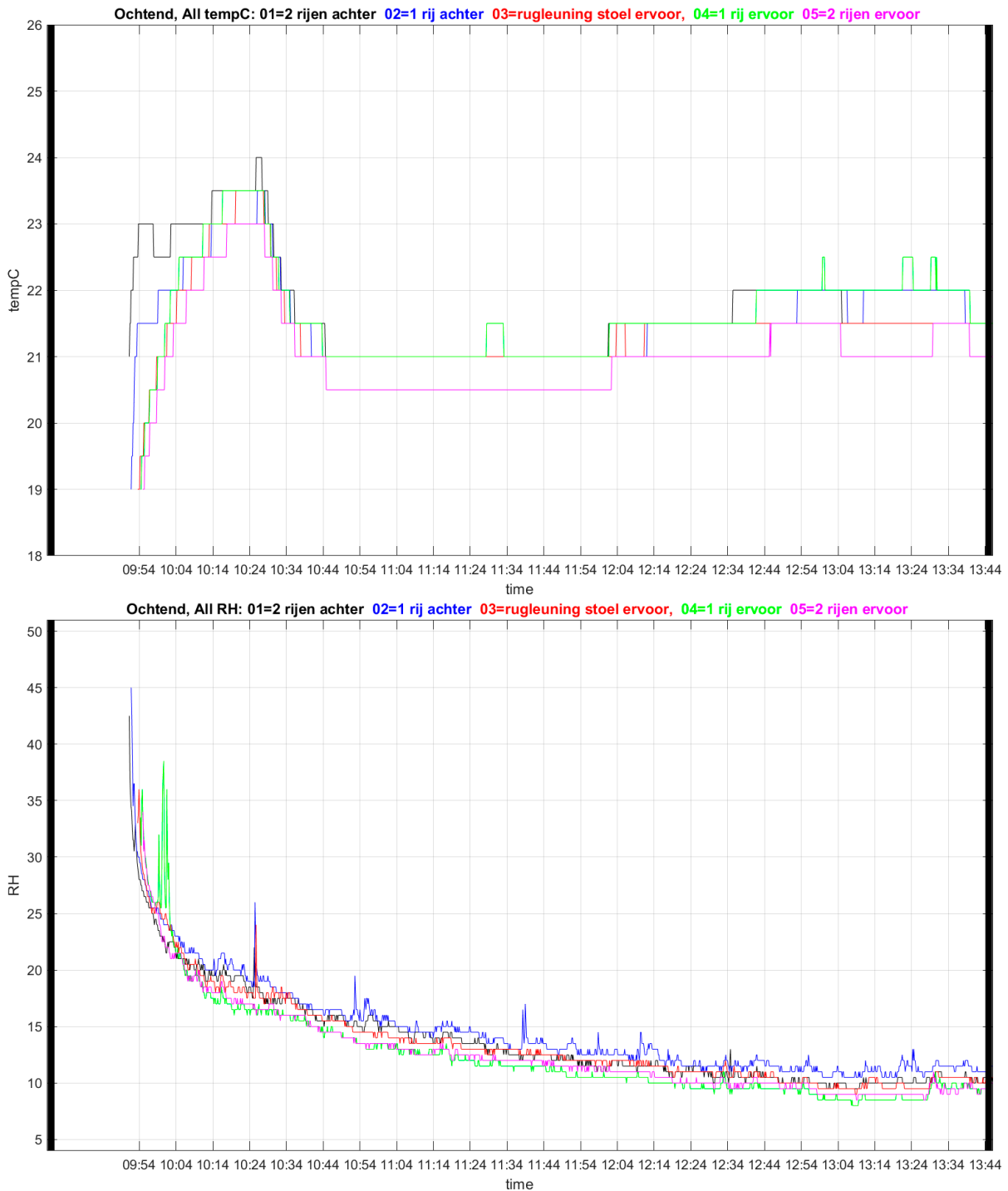


Figure 34: Airbus A320, cruise flight. Particle dispersion measurement runs were performed between 10:28 and 13:27

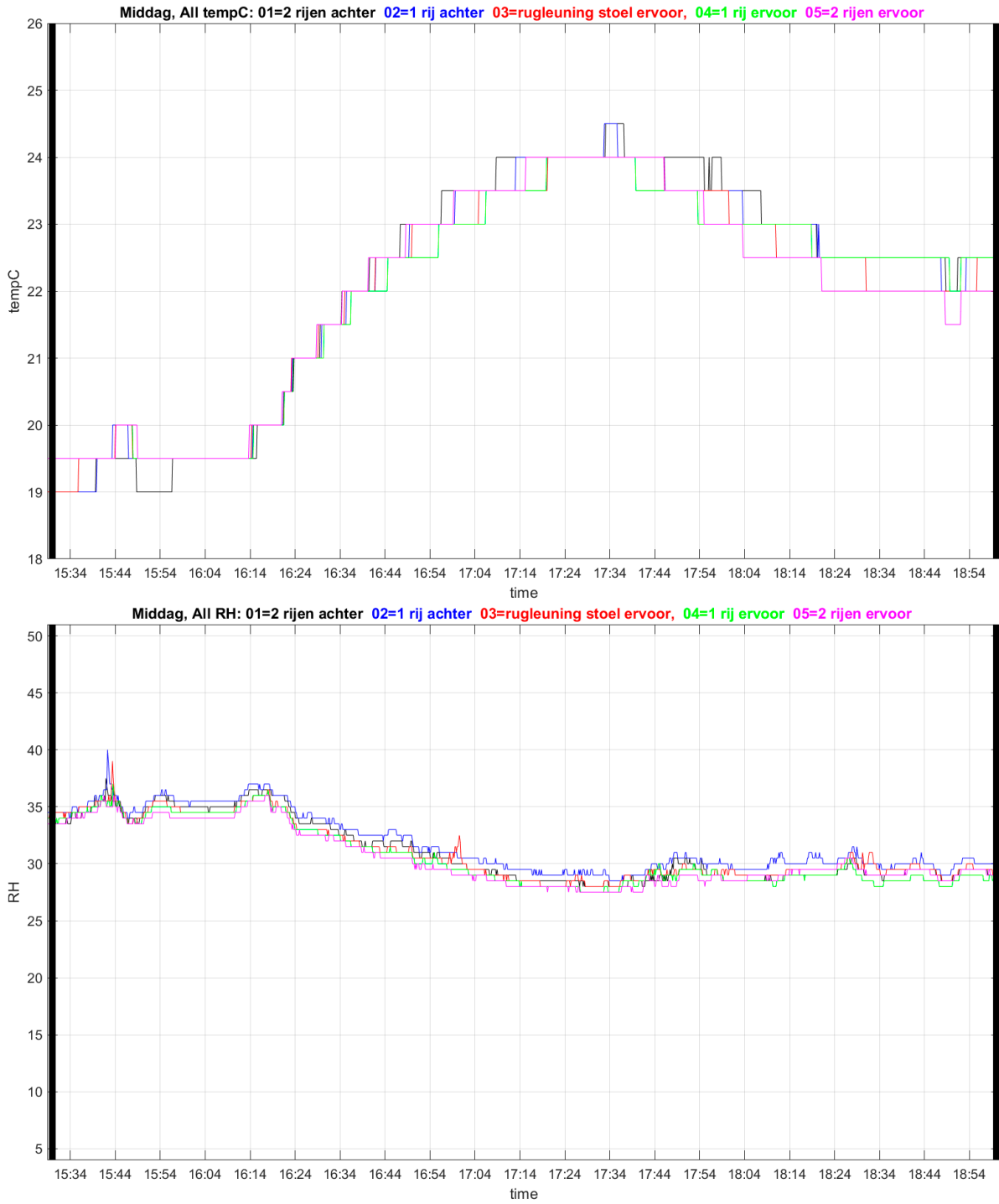


Figure 35: Airbus A320, ground. Particle dispersion measurement runs were performed between 16:57 and 18:55

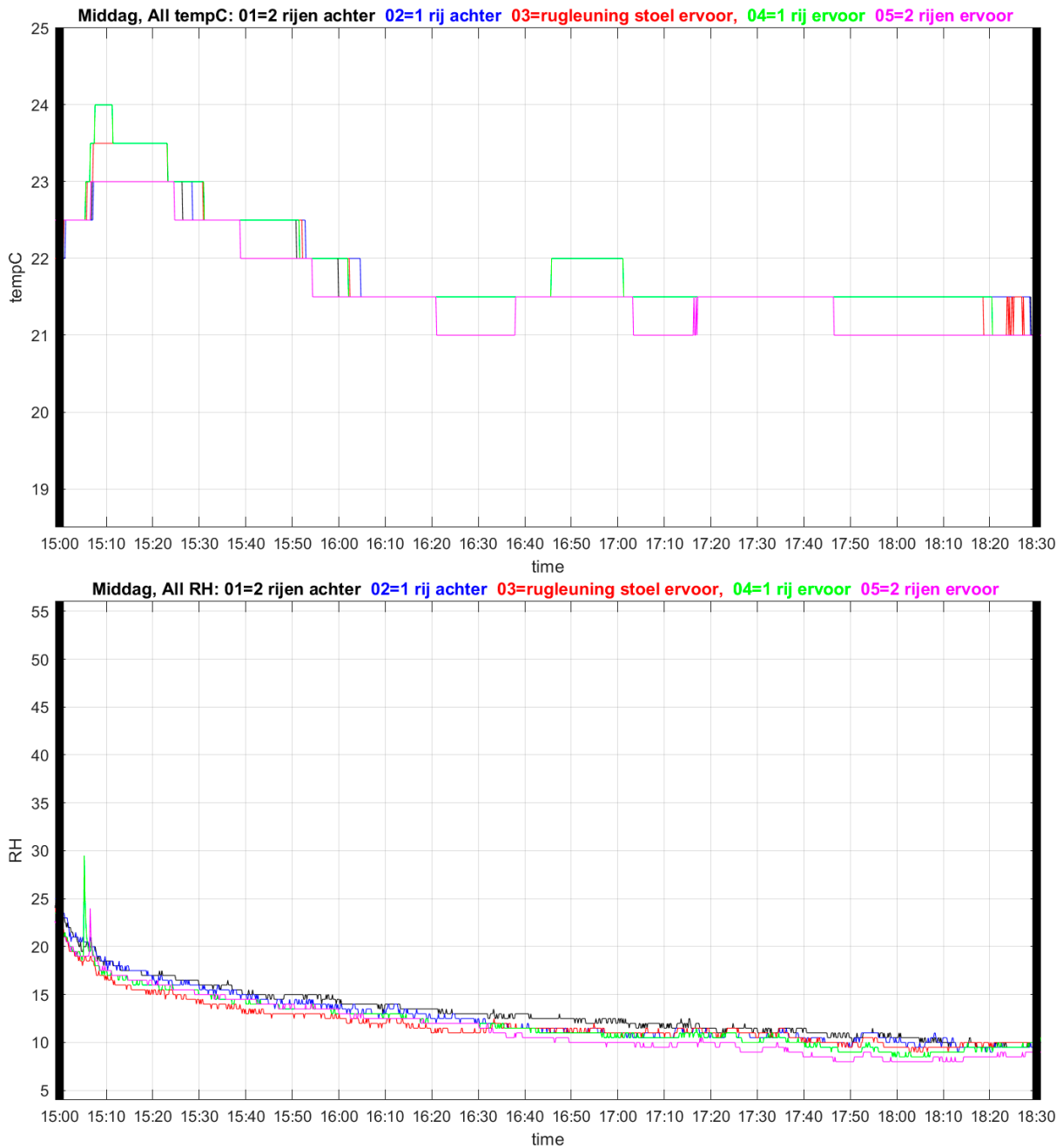


Figure 36: Boeing 737-800 (B737), cruise flight. Particle dispersion measurement runs were performed between 15:10 and 18:06

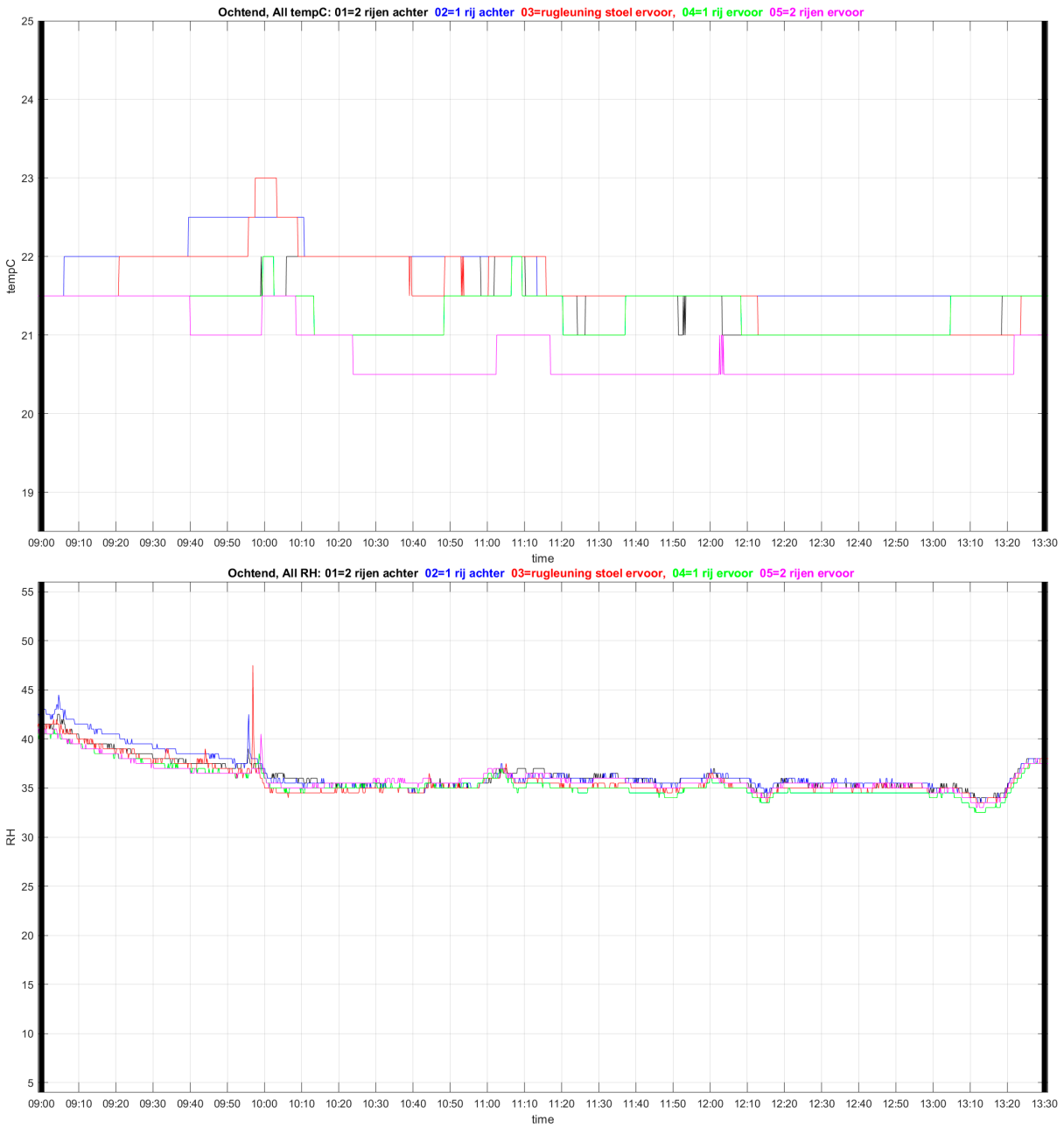


Figure 37: Boeing 737-800 (B737), ground. Particle dispersion measurement runs were performed between 09:07 and 13:18

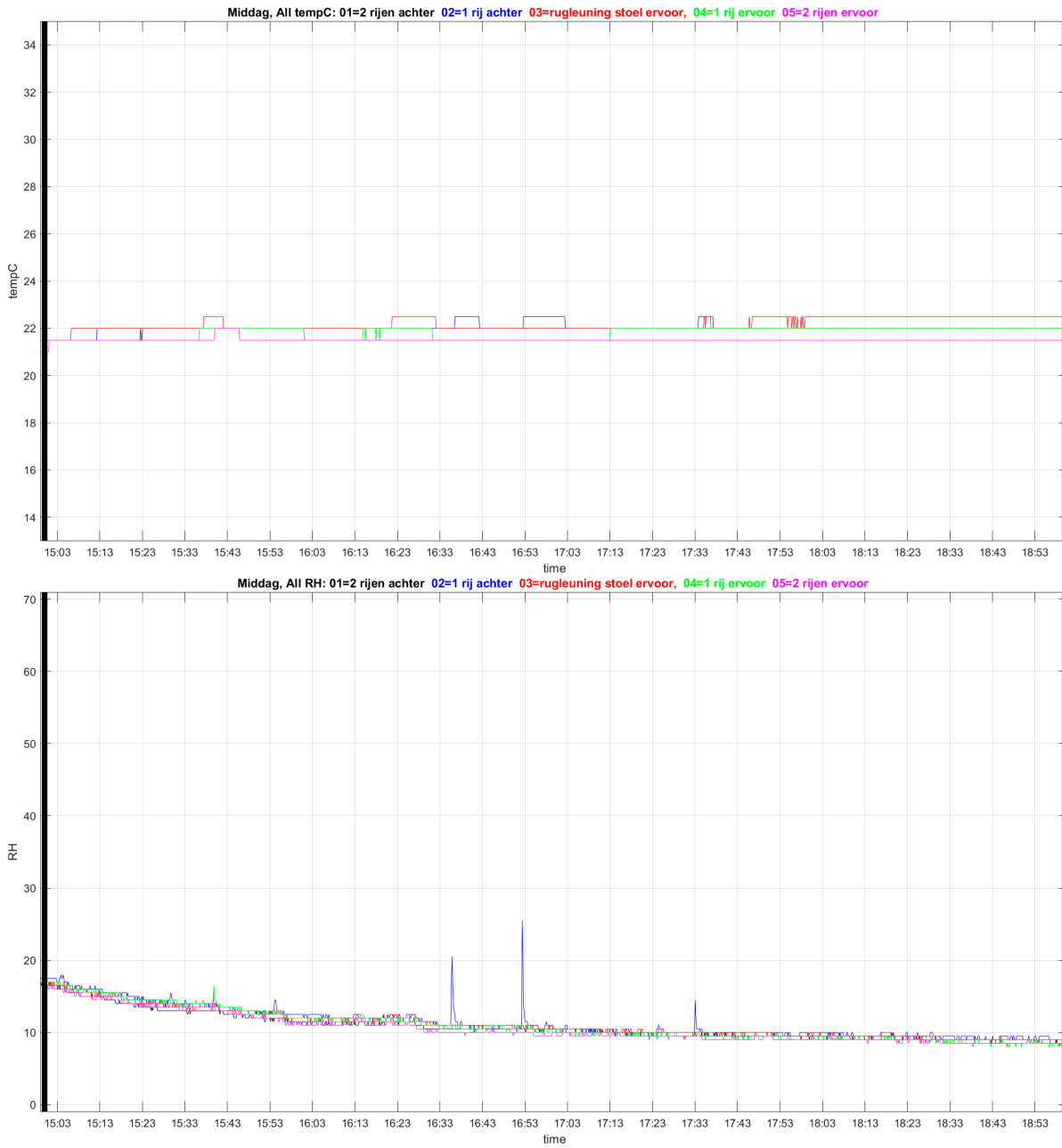


Figure 38: Boeing 787-8 (B787), cruise flight. Particle dispersion measurement runs were performed between 15:05 and 18:57

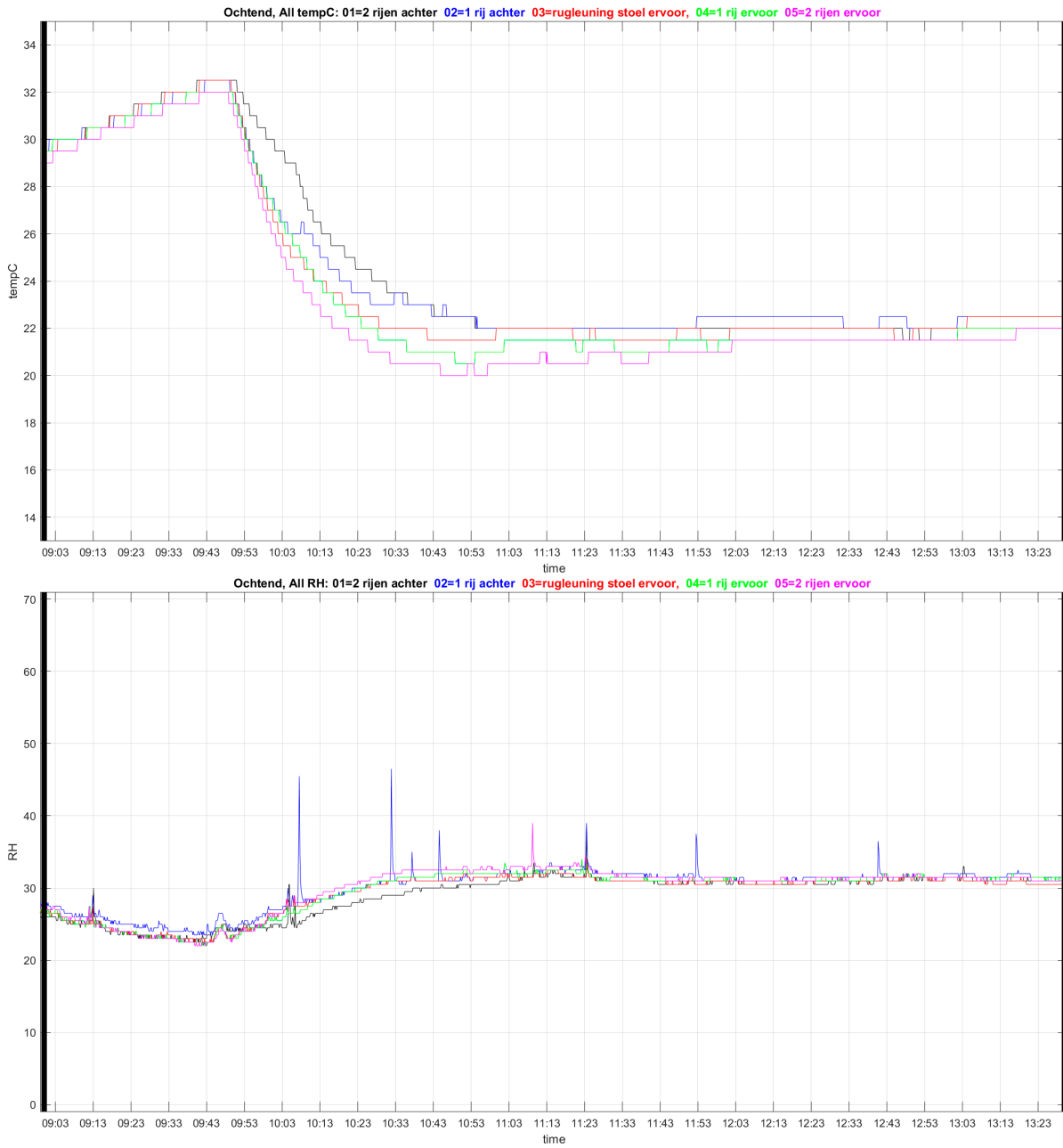


Figure 39: Boeing 787-8 (B787), ground. Particle dispersion measurement runs were performed between 09:19 and 12:58

## Appendix B.4 Source specification

### Appendix B.4.1 Source used in measurements and CFD simulations (cross-check only)

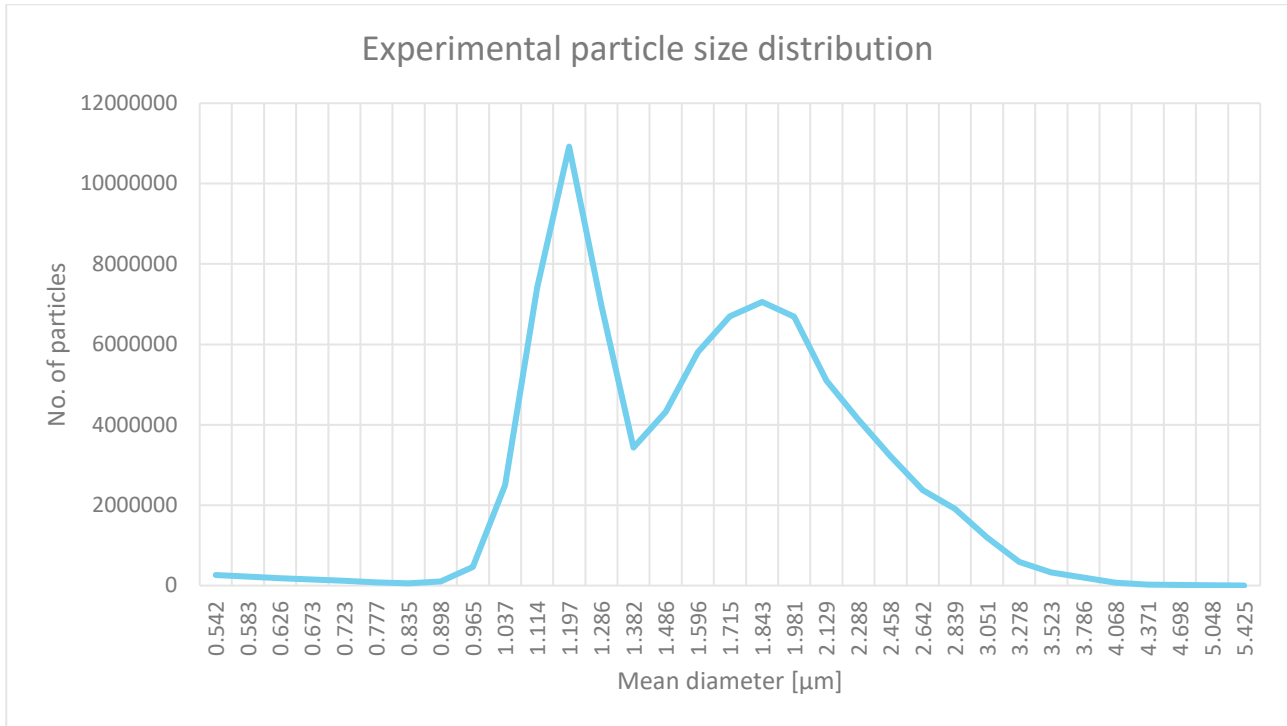


Figure 40: Number of particles sorted by diameter after evaporation of experimental source provided by Medspray

## Appendix B.4.2 Sources used in CFD simulation

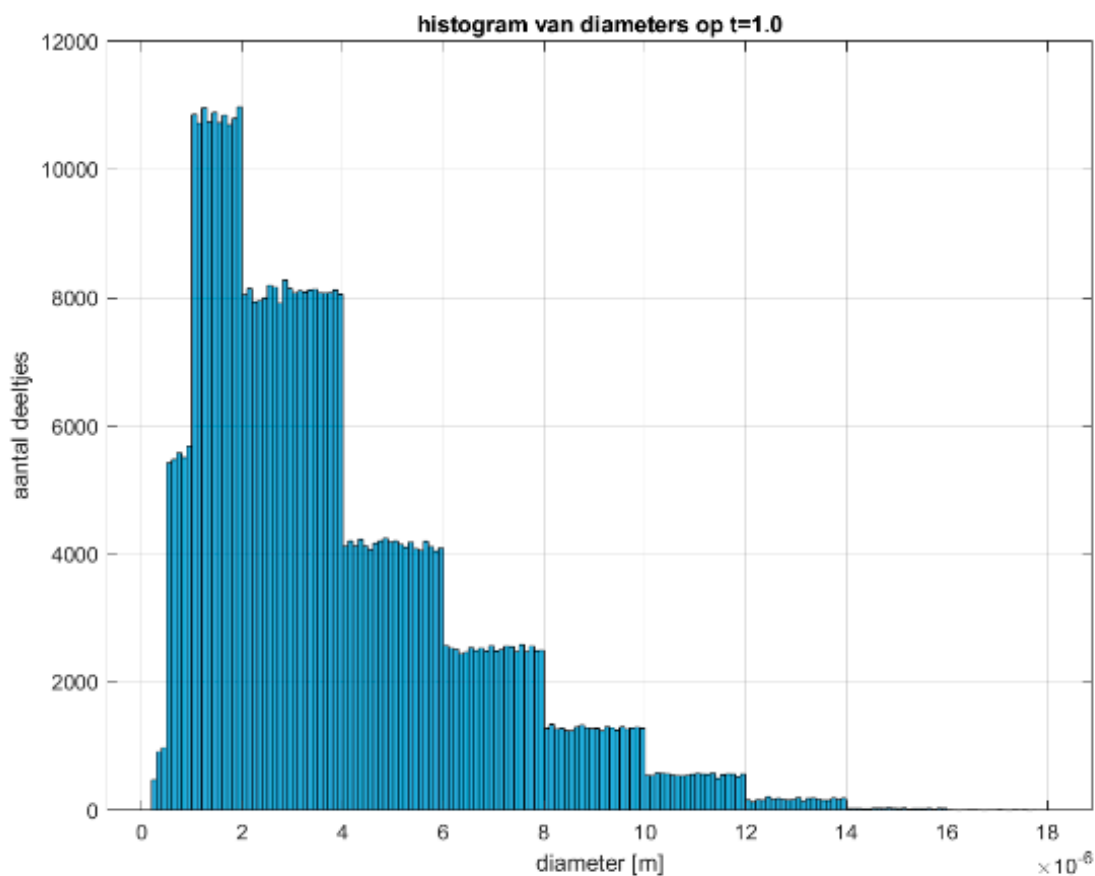


Figure 41: Aerosol size distribution (in number of particles) as used in CFD simulation to mimic speaking

Table 22: Aerosol size distribution (in number of particles and volume) as used in CFD simulation to mimic speaking

Bin	Mean diameter [μm]	Lower limit [μm]	Upper limit [μm]	Total number of particles in bin (uniformly distributed)	% of total volume
1	1.5	1	2	242298	0.46%
2	3	2	4	361749	5.53%
3	5	4	6	186408	13.24%
4	7	6	8	113957	22.04%
5	9	8	10	58656	24.14%
6	11	10	12	26172	19.59%
7	13	12	14	8567	10.44%
8	15	14	16	1642	2.97%
9	17	16	18	574	1.56%

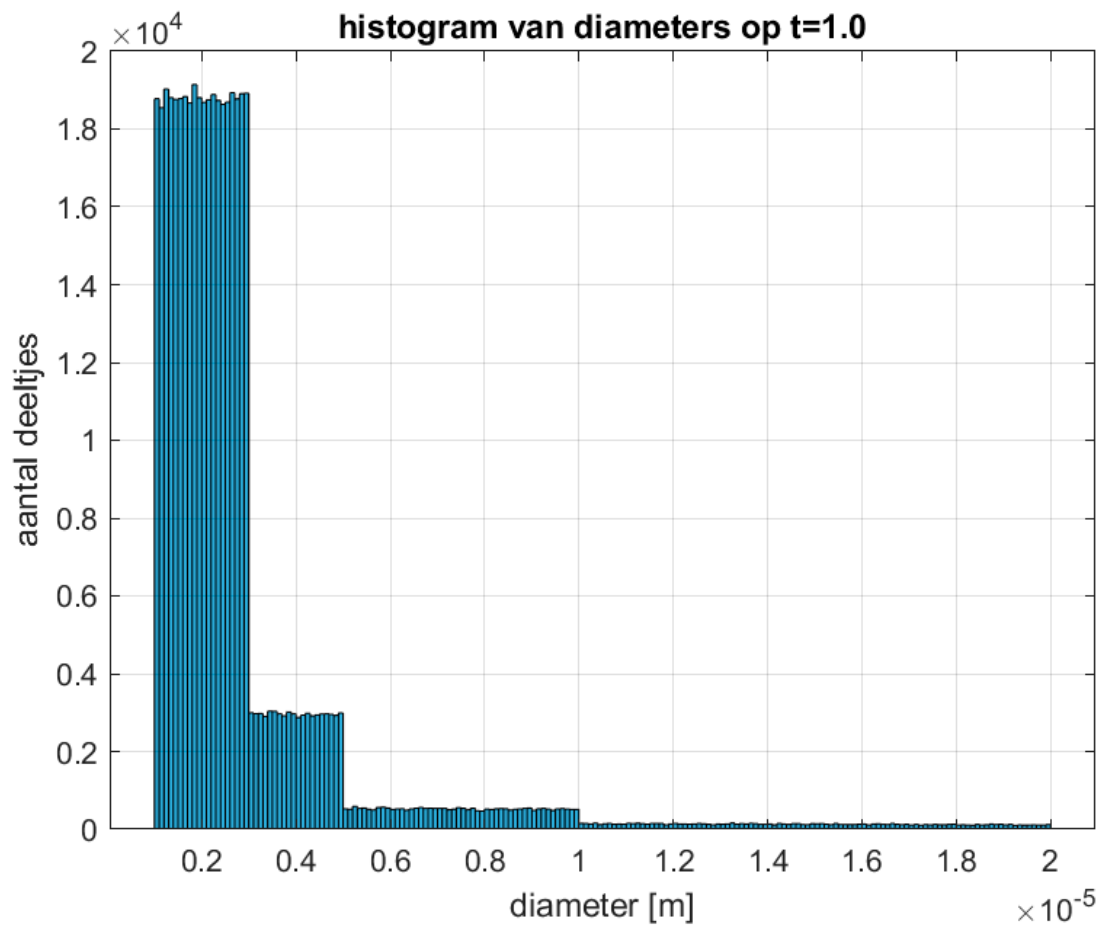


Figure 42: Aerosol size distribution (in number of particles) as used in CFD simulation to mimic breathing

Table 23: Aerosol size distribution (in number and volume of particles) as used in CFD simulation to mimic breathing

Bin	Mean diameter [ $\mu\text{m}$ ]	Lower limit [ $\mu\text{m}$ ]	Upper limit [ $\mu\text{m}$ ]	Total number of particles in bin (uniformly distributed)	% of total volume
1	2.0	1.0	3.0	787.963	4.31%
2	4.0	3.0	5.0	124.884	5.46%
3	7.5	5.0	10.0	55.784	16.09%
4	15.0	10.0	20.0	31.369	72.37%

# Appendix B.5 Aerosol dispersion

## Appendix B.5.1 Selected results of measured aerosol dispersion



Figure 43: Aerosol distribution with no mask (left) and with mask (right) on index during cruise in A320

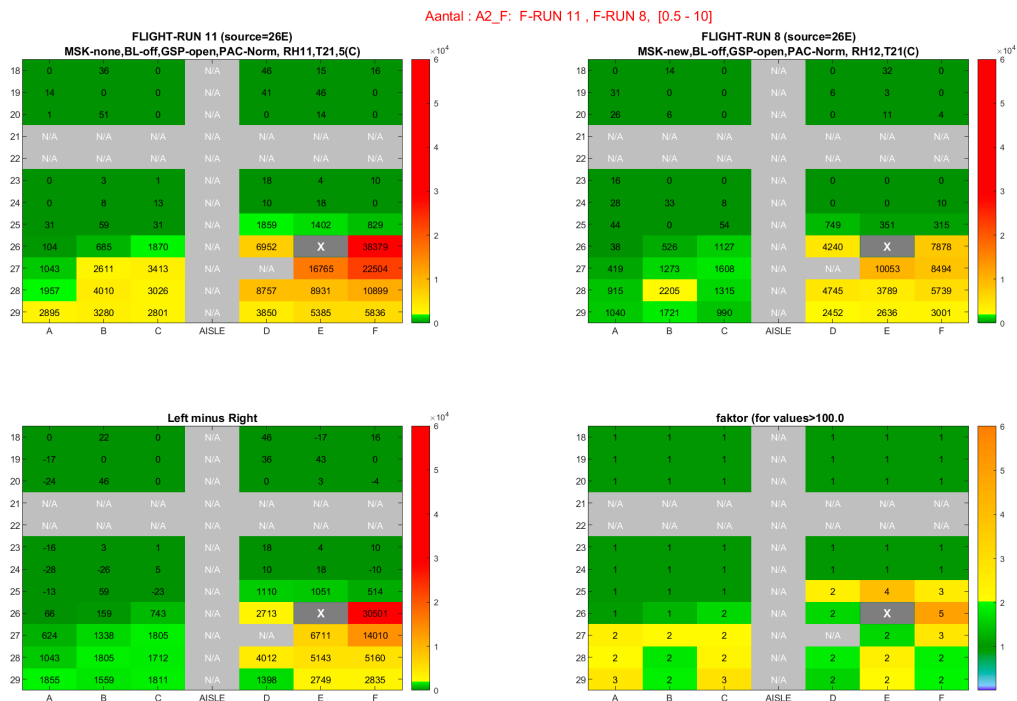


Figure 44: Aerosol distribution with no mask (left) and with mask (right) on index during cruise in B737

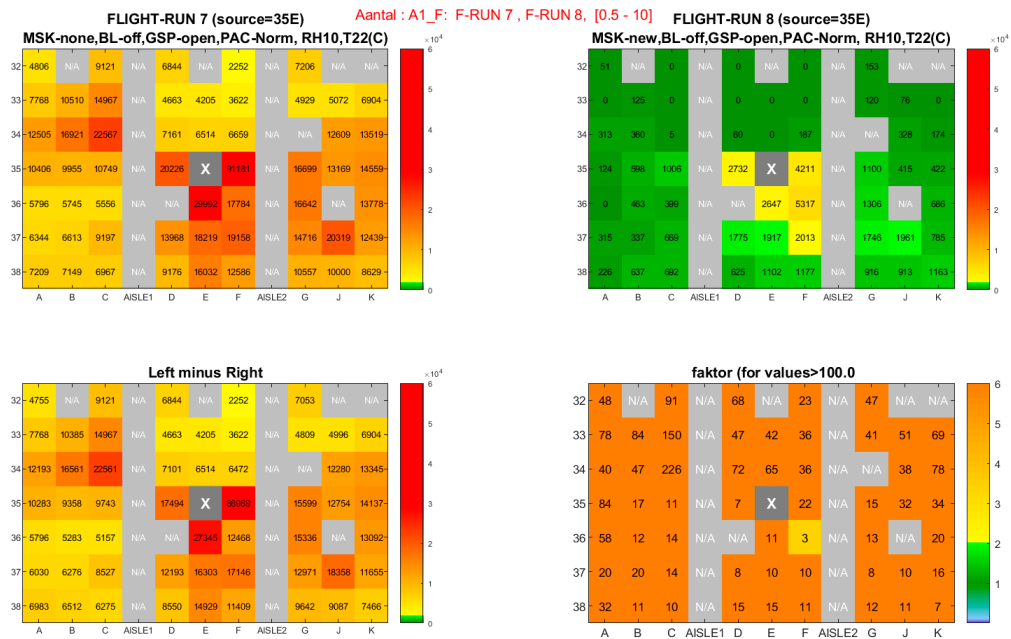


Figure 45: Aerosol distribution with no mask (left) and with mask (right) on index during cruise in B787

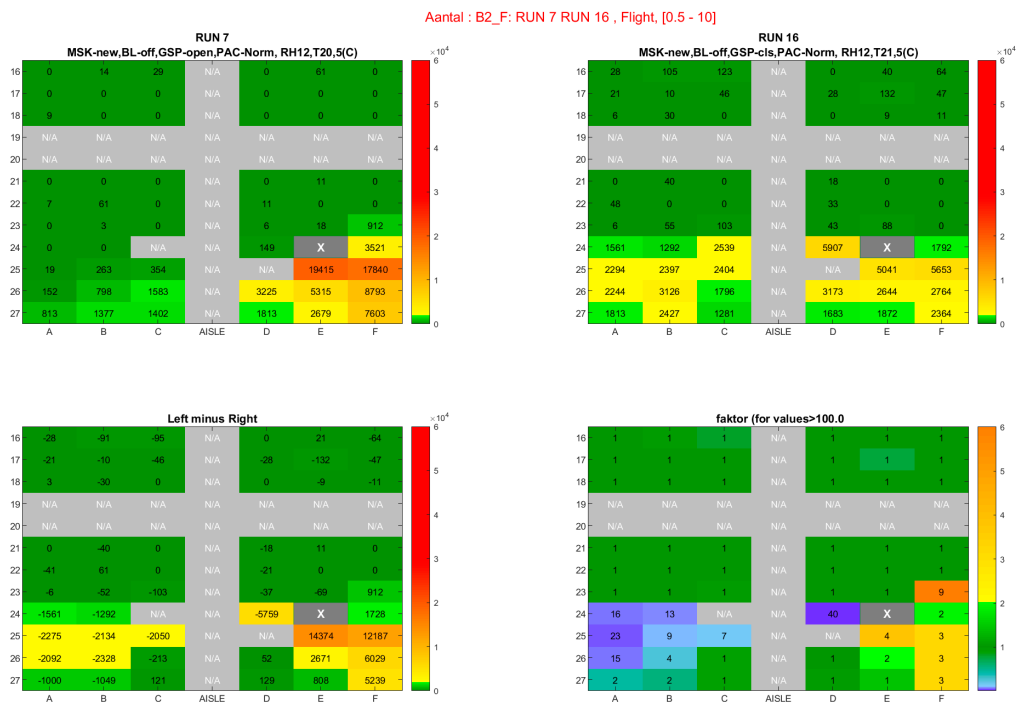


Figure 46: Aerosol distribution with gasper open (left) and gasper closed (right) in combination with mask on index during cruise in A320

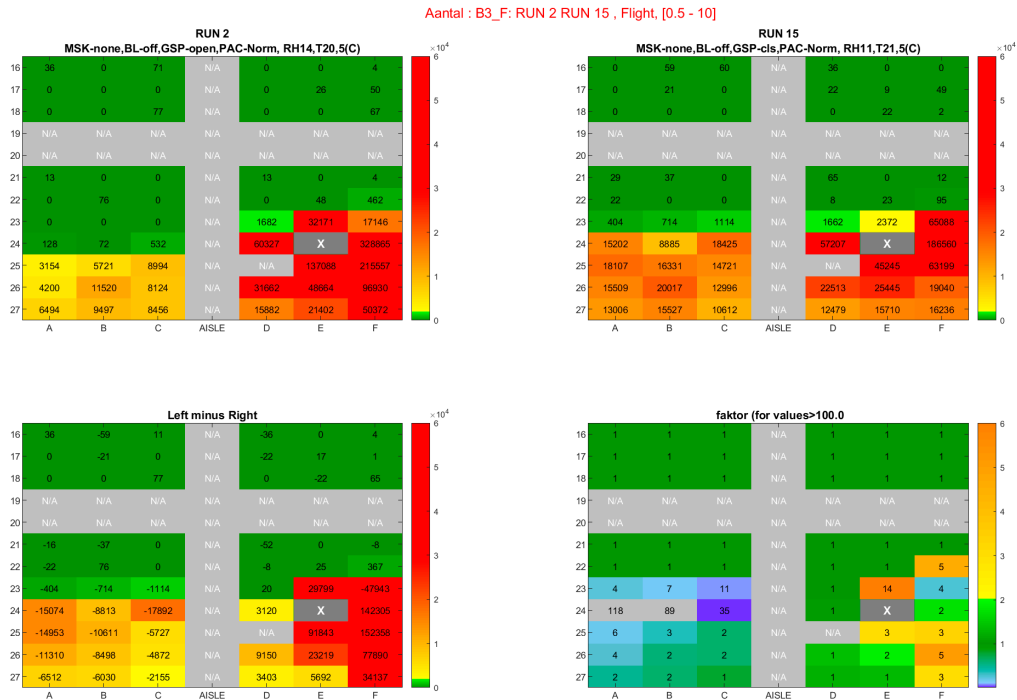


Figure 47: Aerosol distribution with gasper open (left) and gasper closed (right) in combination with no mask on index during cruise in A320

## Appendix B.5.2 Selected results of measured particle size distribution and spread

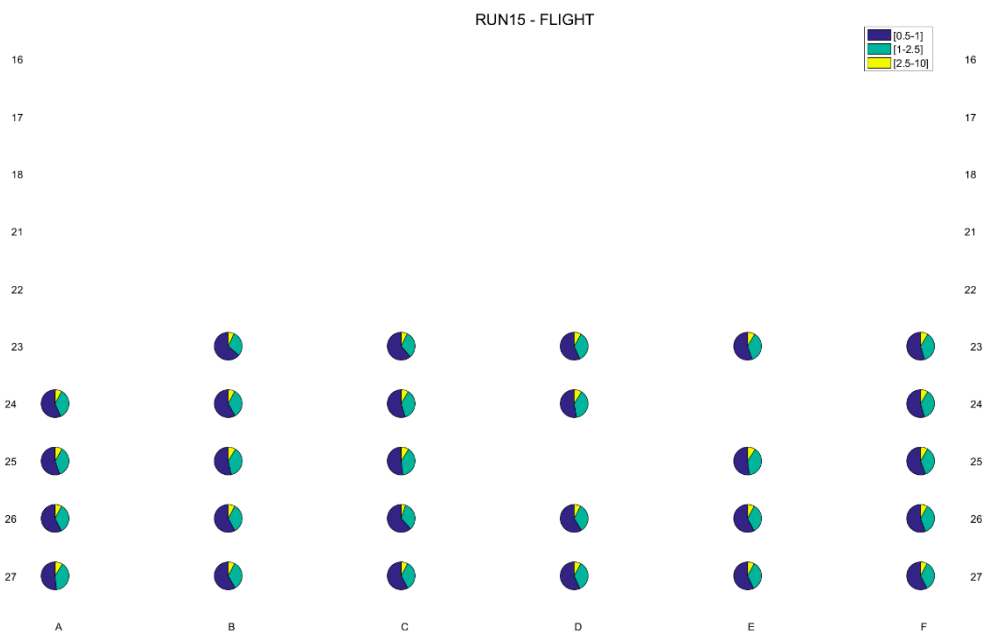


Figure 48: Pie charts plotted on each seat, showing particle size distributions throughout the cabin, as measured by the PM sensors

Figure 48 shows the particle size distributions throughout the cabin as measured with the PM sensors. Deviations between seat positions are relatively small, meaning that particle size does not change significantly after insertion. Other measurements showed similar results.

### Appendix B.5.3 Particle size distribution in experimental setting

Using the APS sensors, the particle size distributions have been determined for scenario's where a mask or no mask was used. This has been done for all aircraft in flight, as these showed minimal disturbance due to small particles that existed in the background concentrations while measuring on ground.

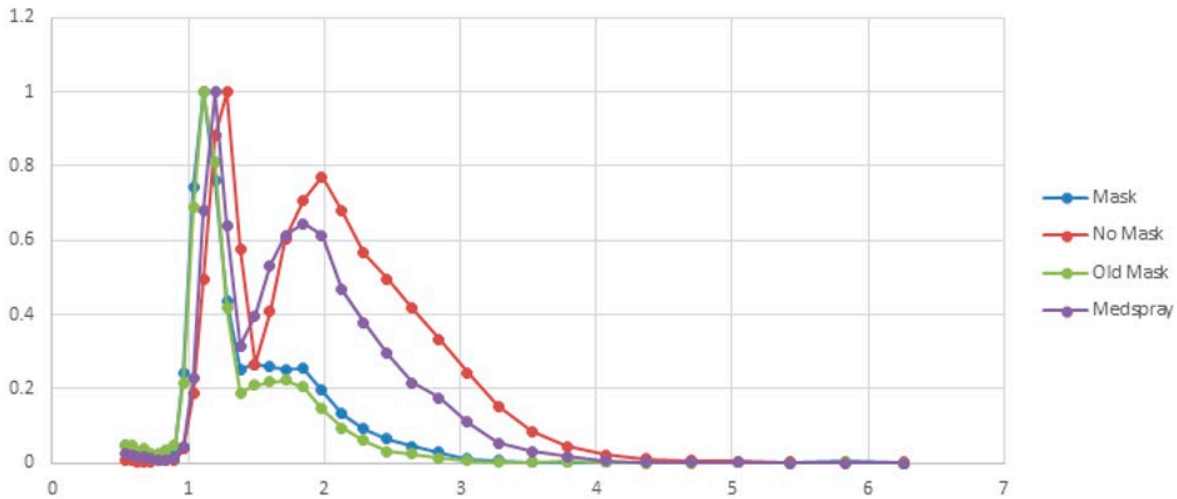


Figure 49: Normalized particle size distribution averages for the A320 flight measurements

Figure 49 shows that the no-mask distribution corresponds well with the Medspray distribution. Because the APS was close to the source, it is expected that some evaporation will take place, so that the no-mask and Medspray distribution will overlap more precise. It is expected that the distribution may change due to certain size particles behaving differently (sticking to surfaces, gravity, aerodynamics, etc), however this has not been measured. When comparing the curve for no mask with the mask curve, it can be seen that the mask has a substantial reduction effect. This effect is greater for larger particles ( $>1.5\mu\text{m}$ ). The measurements of the size distributions in the B737 and B787 showed a higher relative second peak, but also showed substantial reductions.

### Appendix B.5.4 Selected results of simulated aerosol dispersion

Single-aisle

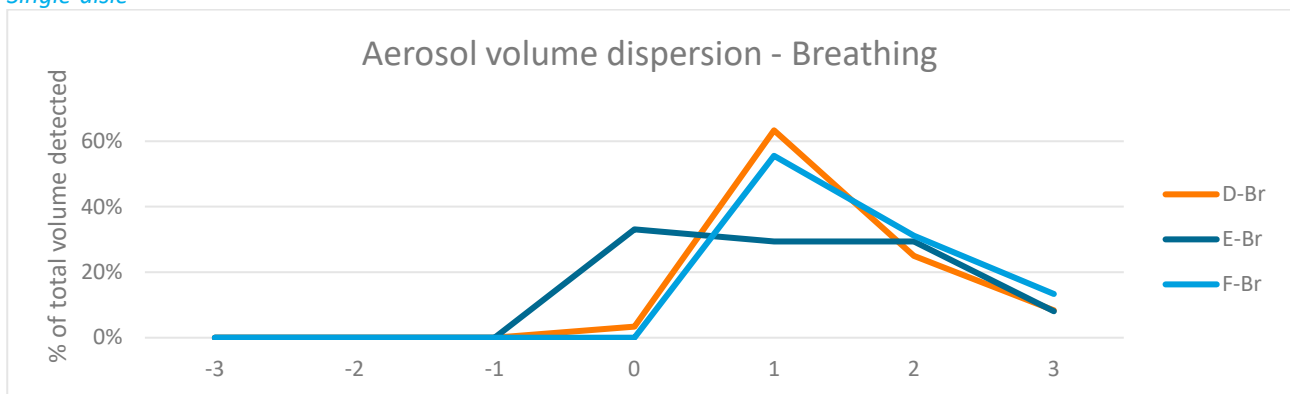


Figure 50: Simulated particle dispersion in A320 for breathing index on seats D, E and F

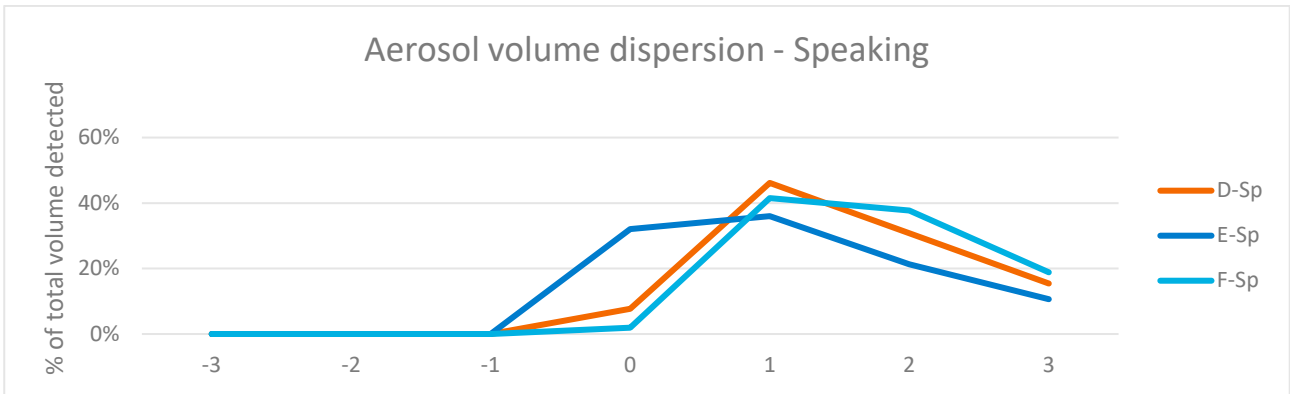


Figure 51: Simulated particle dispersion in A320 for speaking index on seats D, E and F

Table 24: Mean volume per seat as percentage of total volume likely to be inhaled by passengers

Mean volume per seat (% of total emitted)			
D-Breathe	0.60	D-Speak	0.33
E-Breathe	0.27	E-Speak	0.38
F-Breathe	0.45	F-Speak	0.27

Twin-aisle

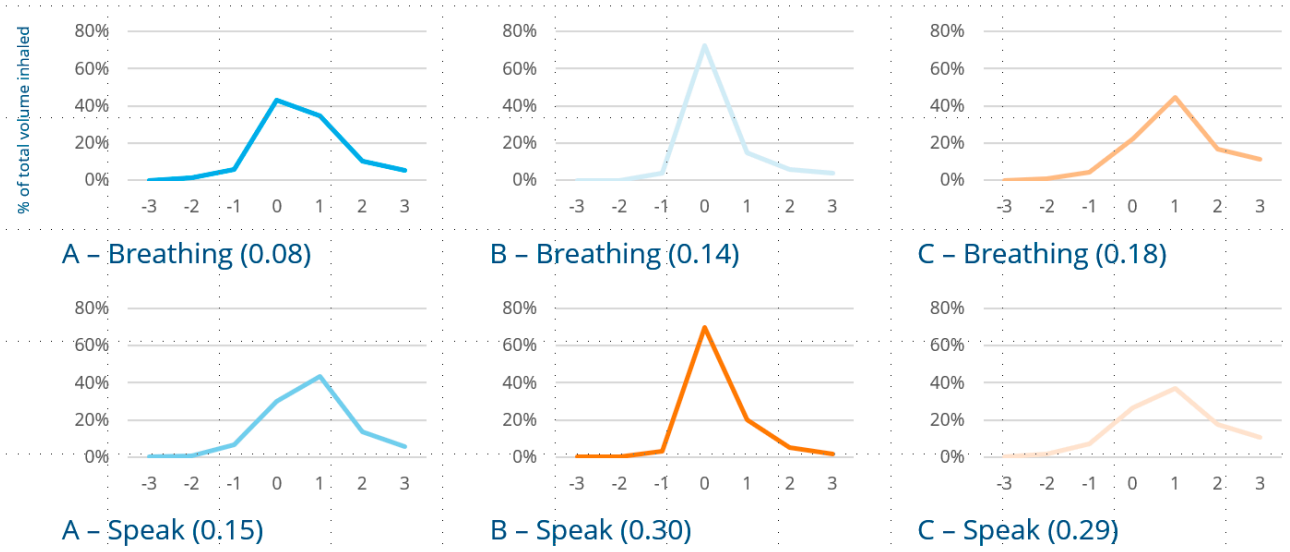


Figure 52: Simulated particle dispersion in B787 for breathing or speaking index on seats A, B and C, mean volume per seat as % of total emitted in between brackets

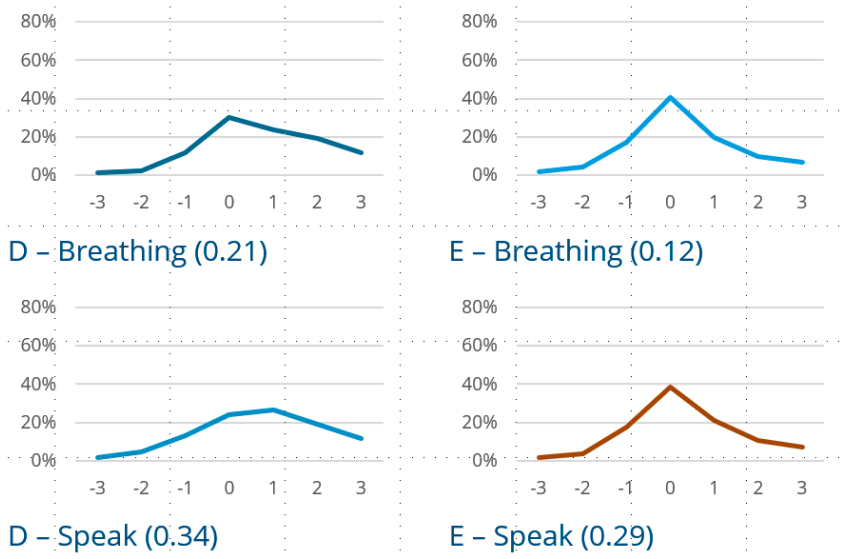


Figure 53: Simulated particle dispersion in B787 for breathing or speaking index on seats D and E, mean volume per seat as % of total emitted in between brackets

## Appendix B.6 Exposure evaluation

### Appendix B.6.1 Exposure evaluation on the basis of transmission experiments: method

In the aerosol transmission experiments artificially produced aerosol was released with a constant rate in runs of approximately 3 minutes. The particle size distribution of the generated aerosol was controlled and calibrated to, after initial evaporation to the final size, resemble aerosol particles exhaled by humans under typical speaking conditions (Asadi, et al., 2019). It was assumed that after initial evaporation, no further evaporation during the experiments took place, which is in line with observations in literature (Liu, Wei, Li, & Ooi, 2017). Air concentrations of transmitted aerosol [# particles/cm<sup>3</sup>] were measured by SPS at different seat locations distributed over 7 rows around the source. The measured particle number concentrations in air were divided over five different size classes, namely [0.3 µm – 0.5 µm; 0.5 µm – 1.0 µm; 1.0 – 2.5 µm; 2.5 µm – 4.0 µm; 4.0 µm – 10.0 µm]. The PM sensors had a native measurement range of 0.3 to 2.5 µm, other size bins were extrapolations using software as discussed in section 5.1.1, Table 2. Particle counts per cm<sup>3</sup> air in each of these diameter classes were determined in samples of approximately 1 second duration, for a period of 5 to 10 minutes after the start of the emission of aerosol.

To extrapolate transmission data from experiment to realistic exposure scenarios, the transmission data was converted to the fraction of the emitted aerosol that may be inhaled by a passenger at each seat. This was done as follows:

- 1) Measured particle count concentrations  $c_N$  per size bin were converted to aerosol volume concentration  $c_V$ . The particle counts in each size class were converted to total volume  $\Delta V(d)$  in that particle class by multiplication of the number of particles  $N$  in the particle class with the average particle volume in that class:

$$\Delta V(d) = N \frac{\pi}{6} \langle d^3 \rangle \quad 1$$

The average particle volume  $\frac{\pi}{6} \langle d^3 \rangle$  is the mean of the particle volumes at the class boundaries  $d_{\min}$  and  $d_{\max}$ :

$$\frac{1}{2} \times \left( \frac{\pi}{6} d_{\min}^3 + \frac{\pi}{6} d_{\max}^3 \right) \quad 2$$

Using the aerosol volume in each particle class,  $c_V$  was calculated from  $c_N$  as

$$c_V = \sum_{i=1}^5 c_N(d_i) \times \Delta V(d_i) \quad 3$$

- 2) From  $c_V$  at a seat, the dose of aerosol volume  $d_{\text{vol}}$  that may be inhaled by a passenger at that seat at time  $t$  follows from:

$$d_{\text{vol}}(t) = q_i \times c_V(t) \quad 4$$

with  $q_i$  the inhalation rate of the passenger.

- 3) The total aerosol volume potentially inhaled during an experimental run  $d_{\text{vol,exp}}$  followed from integration over the run duration  $t_{\text{run}}$ :

$$d_{vol,exp} = q_i \times \int_0^{t_{run}} c_V(t') dt' \quad 5$$

Integration was performed in Mathematica (Wolfram Research, Inc., 2021) by use of an interpolating function on the measurement data and numerical integration of this interpolating function over the entire experimental run duration.

- 4) The volume dose  $d_{vol,exp}$  was normalized by dividing with the total volume of aerosol released in the run  $V_{emission}$ . This resulted in a dimensionless quantity *frac*, the fractional transfer, that represents the fraction of aerosol released that may be inhaled by a passenger at a seat.

$$frac = q_i \times \frac{1}{V_{emission}} \int_0^{t_{run}} c_V(t') dt' \stackrel{def}{=} q_i \times T_{seat} \quad 6$$

$V_{emission}$  was estimated to be 25  $\mu\text{L}$  on the basis of the following assumptions:

To produce aerosol, 700  $\mu\text{L}$  liquid was used in the experimental runs. Losses due to residues adhering to the experimental setup were estimated at 11  $\mu\text{L}$  so that the total volume of liquid dispersed was 689  $\mu\text{L}$ . This volume was expected to be reduced to about 1/27 of its initial value due to evaporation of the volatile components (water) (Liu, Wei, Li, & Ooi, 2017).

The quantity *frac* was evaluated for each seat, for all experimental runs. It should be noted that *frac* includes two factors: the inhalation rate  $q_i$  and the ‘transfer’  $T_{seat}$ . The inhalation rate  $q_i$  is, in principle a scenario assumption that may vary in different exposure scenarios.  $T_{seat}$  is a factor that is uniquely determined in the experiment.

The calculated *frac* was used to extrapolate the experimental measurements of aerosol dispersion by assuming that *frac* represents dispersion under realistic conditions at all times. So that, in any scenario in which an infectious index passenger emits aerosol volume  $V_{src}$ , an exposed passenger will inhale *frac* (at his seat):

$$d_{vol} = frac \times V_{src} = frac \times fmask \times q_{src} \times t_{exp} \quad 7$$

Where, for convenience, the emission was expressed as a constant rate  $q_{src}$  during an exposure time  $t_{exp}$  (which was selected in different risk assessment scenarios). In equation 7 *fmask* represents the total effect of mask wearing by both index passenger and exposed passenger. For mask removal efficiencies *fmask\_exhale* for exhalation and *fmask\_inhale* for inhalation, *fmask* follows as

$$fmask = (1 - fmask_{inhale})(1 - fmask_{exhale}) \quad 8$$

From the inhaled volume of aerosol  $d_{vol}$  the virus dose followed by multiplying with the virus concentration  $c_{virus}$  in the aerosol.  $c_{virus}$  was estimated from data on the virus concentration in human sputum  $c_{sputum}$  by assuming that the aerosol particle shrank to 1/27<sup>th</sup> of its original volume due to evaporation losses, while maintaining the same virus content, so that

$$c_{virus} = 27 \times c_{sputum} \quad 9$$

Finally, exposure to virus was expressed as viral load  $d_{virus}$ , the number of virus copies inhaled in the exposure period.

$$d_{virus}(seat) = c_{virus} \times d_{vol}(seat) \quad 10$$

## Appendix B.6.2 Exposure evaluation on the basis of transmission simulations: method

Transmission simulations determined the volume of aerosol particles that arrived in a sample volume  $V_{box}$  at different seats during simulation.

In total 7 rows were simulated for 2 aircraft configurations (A320 and B787), minus the seat of the index passenger. This amounted to 41 modelled seat locations for the A320 and 62 seat locations for the B787. Simulation tracked individual particles and the time they resided in the sample volume  $V_{box}$ . Particles with similar residence time were aggregated, their total volume  $\Delta V_{aerosol}$  and residence time  $t_{res}$  were provided as simulation output, resulting in a series of tuples  $\{\Delta V_{aerosol}, t_{res}\}$  for different values of the residence time.

Similar to the evaluation of exposure from the experimental measurements, the simulation results were converted to the dimensionless factor *frac*, that expresses translocation per seat as the fraction of aerosol volume emitted that may be inhaled by a passenger at the seat. For the simulation results, this was done as follows:

- 1) At each seat, total aerosol volume concentration in air  $c_V$  was calculated as :

$$c_V = \frac{1}{V_{box}} \sum_i t_{residence,i} \times \Delta V_{aerosol,i} \quad 11$$

In the simulation the sample volume  $V_{box}$  was chosen as a box of volume  $(0.3 \times 0.3 \times 0.3) = 0.027 \text{ m}^3$ .

- 2) From  $c_V$  at a seat, the total dose of aerosol volume  $d_{vol}$  that may be inhaled by a passenger at that seat during the simulation period was calculated:

$$d_{vol} = q_i \times c_V \quad 12$$

Where  $q_i$  the inhalation rate of an exposed person.

- 3) Finally, *frac*, the fraction of the emitted aerosol inhaled was obtained by normalizing with the total volume of aerosol particles simulated,  $V_{emission}$ .

$$frac = \frac{d_{vol}}{V_{emission}} \quad 13$$

$V_{emission}$  was  $8.9 \times 10^{-11} \text{ m}^3$ .

Using the fractional transfer *frac* calculated from the simulation, exposure evaluation was conducted as described in section 2.2.1.

## Appendix B.6.3 Simulation of exposure scenarios

Doses in various exposure scenarios were calculated on the basis of the fractional transfers '*frac*' derived either from experiment or from simulation.

In each exposure evaluation, fractional transfers were selected from the measurement run or the simulation that most closely represented the exposure scenario settings. Fractional transfers were available for all the monitored and simulated seats, typically seats in 7 rows including the index location. SPS measurements were conducted for 7 rows in each plane: the row containing the index location plus an additional 3 rows in each direction. For the A320 and B737, each featuring 6 seats per row, this amounted to a total of 40 monitored seats per experimental run. For the B787 with 9 seats per row, the total number of measured seats came down to 59.

Simulations were performed for 7 rows with 6 seats, giving a total of 42 sample locations, each with their respective estimate of the transfer, *frac*. In each simulation, exposure and risk of sickness were evaluated for all individual sample locations. Variation in exposure conditions was accounted for by representing exposure factors with probability distributions and conducting a Monte Carlo simulation.

This resulted in a set of dose samples, one for each seat.

## Appendix B.6.4 Exposure evaluation on the basis of transmission experiments: parameters

### *Particle size distribution exhaled aerosol*

Emission of aerosol particles by an infectious index passenger is characterized by a mass rate of emitted aerosol  $m(t)$  and the particle diameter distribution  $P(d)$  of the emitted aerosol. For the  $P(d)$ , a non-parametric distribution function is used, represented in Schijven et al. (2021). This distribution is based on data published in Asadi et al. (2019), representing emission during speaking. Appendix B.4 contains the particle size distributions used in this study.

### *The load of infectious virus particles in the aerosol particles*

Aerosol particles emitted by an infectious index passenger are assumed to contain a certain viral load  $L(d, t)$  which will depend on particle size (larger particles contain more virions) and time (virions may degrade in time when released in air). Here, we follow the assumptions made in Schijven et al. (2021), where virus load in expired aerosol particles is assumed to be independent of time, and equal to the concentration in nasopharyngeal swabs. Observed SARS-CoV-2 concentrations in nasopharyngeal swabs (nose / throat swabs) span a wide range, from  $10^2$  to  $10^{11}$  RNA copies / mL (corresponding to a range of Ct values from 40 to 10.5) (Schijven, et al., 2021). The median is at  $10^{7.5}$  RNA copies / mL. To represent the variation in virus load, we assume here a distribution of the  $\log_{10}$  transformed concentrations, given as a normal distribution with median 7.53 and standard deviation of 1.28.

### *Inhalation rate*

The inhalation rate of exposed passengers is subject to inter-individual variability. In model simulations of the inhaled dose and the risk assessment, it is assumed to be represented by a log normal distribution  $N(\text{Log}_{10}(6.8); 0.050)$  l/min (Schijven, et al., 2021; Fabian, Brain, Houseman, Gem, & Milton, 2011).

### *Filter efficiency mask*

The use of facial masks will reduce both emission and inhalation of aerosol particles. Particle filtering efficiency will depend on the type of mask and how well it fits the face. Also, filtering efficiency will generally depend on aerosol particle size. Also, filtering efficiency will be different for inhalation of aerosol particles and exhalation. In the exposure estimate a simplified assumption on the inhalation filtering efficiency is made: as proposed in NLR & RIVM (2020) filtering is assumed to be constant at 30% for inhalation (i.e. 30% of all particles is intercepted, irrespective of the

particle's size), and 60% for exhalation. This will amount to a total reduction of dose of 28% when both index passenger and exposer passenger wear a mask. Evaluated exposure is proportional to this assumption.

Table 25: Viral modelling parameters, based on Schijven et al. (2021)

Model parameter	Symbol	Dimension	Default	Range	Distribution	Reference
<b>Virus properties</b>						
Concentration in aerosol at onset of symptoms	$c_{sputum}$	/ml		$10^2$ - $10^{11}$	Log <sub>10</sub> of Ca, N[7.53,1.28]	(Schijven, et al., 2021)
Intact fraction	$f$	-	1/80			RIVM
Infectious fraction (exponential dose response)	$r$	-	1/18			(Haas, 2020) (Schijven, et al., 2021)
<b>Contagious person</b>						
Aerosol volume emission rate	$q_{src}$	pL/minute			Simulated data	(Schijven, et al., 2021)
<b>Mask efficiency</b>						
Inhalation removal efficiency	$f_{mask\_inhale}$		0.3			(NLR & RIVM, 2020)
Exhalation removal efficiency	$f_{mask\_exhale}$		0.6			(NLR & RIVM, 2020)
<b>Exposed persons</b>						
Exposure time	$t_{exp}$	minute				
Inhalation rate (tidal breathing)	$q_i$	l/minute			N(Log <sub>10</sub> (6.8); 0.050]	(Schijven, et al., 2021; Fabian, Brain, Houseman, Gem, & Milton, 2011)

## Appendix B.7 Calculation of risk

### Appendix B.7.1 Risk evaluation

Risk of illness of a person was calculated as a probability of that person developing COVID as a result of inhalation of a dose  $d_{virus}$  :

$$P_{illness} = 1 - \exp(-rf d_{virus}) \quad 14$$

$f$  is the fraction of plaque forming units (PFU) in virus RNA copies

$r$  is a dose-response parameter

Finally, risk was expressed as

$$P_{illness} = \frac{1}{[number\ of\ passengers]} \quad 15$$

Where *[number of passengers]* is the size of the group of passengers in which one secondary case is expected.

The Monte Carlo simulation of the doses at the seats surrounding the index passenger results in a sample of 10,000 potential doses for each seat. This distribution represents the range of doses of inhaled RNA copies that are deemed plausible under realistic flight conditions. The sample is expected to represent actual exposure in realistic conditions. To infer risks after exposure,  $p_{illness}$  was evaluated for all samples of the virus dose for all considered seats. From the resulting distribution of the probability of illness, the mean and 95<sup>th</sup> percentiles were determined. The mean represents the average probability per passenger on illness on a flight with an infectious index passenger on board.

## Appendix B.8 Statistical modelling and analysis

### Appendix B.8.1 Method

Estimated mean risks  $p_{ill}$  after 1 hour of exposure per exposed passenger (manikin) and per run (experiment) were subjected to statistical analysis as dependent variable in R (version 3.6.0 (2019-04-26)) (R Core Team, 2019) for analysing the effects of a number of variables. Values of  $p_{ill}$  equal to zero were excluded, because in those cases no SPS-sensor data were available. In the statistical analysis, mean pill values were log10 transformed.

Of the A320 data, run 1 under cruise conditions was excluded. In this run, a double amount of aerosol was generated with an interruption. Of the B787 data, ground runs 1 and 2 were excluded, because conditions were not representative: engines were not running. The A320 data and B737 data were categorized as single-aisle aircraft and the B787 as twin-aisle aircraft. Table 26 summarizes the data that were used in the statistical analysis.

Generalized Additive (Mixed) Models were fitted using packages *\*gam4\** (version 0.2-6, (Wood, 2006)). As fixed categorical effects, *\*aircraft\** (single and two aisle), *\*gc\** (ground/cruise), *\*mask\** (No/Yes), *\*heating\** (Y/N, only during ground conditions), *\*gasper\** (closed/open, affects air flow, only during ground conditions) were entered into the models. *\*distance\**, *\*oc\** (cabin air temperature) and *\*rh\** (relative humidity) were modelled with smooth additive effects, while *\*angle\** was modelled with a cyclic spline (0-360 degrees). *\*Run\** was entered as random intercept in the GAM Mixed models (GAMM). GAMM models were fitted with restricted maximum likelihood. Significance and p-values were based on t-tests used the Satterthwaite's method. An effect of *\*blankets\** was not investigated because this effect could not be distinguished from *\*heating\**. Similarly, an effect of *\*pack\** was not investigated because this effect could not be distinguished from *\*gasper\**.

Table 26: Summary of data used for the statistical analysis

		Single aisle		Twin aisle	
		Cruise	Ground	Cruise	Ground
Runs	N	28	27	16	9
Total	N	1119	1076	908	620
Mask no	N	280	397	280	89
Mask yes	N	839	679	628	531
Heating off	N	1119	596	908	325
Heating on	N	0	480	0	295
Gasper closed	N	480	638	0	118
Gasper open	N	639	438	908	502
Distance (m)	Mean	2.0	2.0	2.2	2.1
	Min	0.48	0.48	0.48	0.48
	Max	3.4	3.4	5.0	3.6
Temperature (°C)	Mean	21.4	21.9	21.8	22.0
	Min	20.5	20.5	21.5	20.3
	Max	23.5	24.0	22.5	26.1
Relative humidity (%)	Mean	12.1	33.3	10.8	29.4
	Min	8.1	27.7	8.5	22.7
	Max	17.8	40.5	16.0	32.5
$p_{ill}$ , mask no	Mean	$2.7 \times 10^{-3}$	$3.7 \times 10^{-3}$	$3.0 \times 10^{-3}$	$2.6 \times 10^{-3}$
	Min	$2.3 \times 10^{-5}$	$3.6 \times 10^{-5}$	$8.8 \times 10^{-5}$	$1.2 \times 10^{-3}$
	Max	$3.1 \times 10^{-2}$	$2.4 \times 10^{-2}$	$1.7 \times 10^{-2}$	$1.1 \times 10^{-2}$

		Single aisle		Twin aisle	
		Cruise	Ground	Cruise	Ground
$p_{ill}$ , mask yes	Mean	$4.9 \times 10^{-4}$	$8.5 \times 10^{-4}$	$7.2 \times 10^{-4}$	$8.1 \times 10^{-4}$
	Min	$1.3 \times 10^{-5}$	$2.3 \times 10^{-5}$	$3.4 \times 10^{-5}$	$4.1 \times 10^{-4}$
	Max	$6.5 \times 10^{-3}$	$4.8 \times 10^{-3}$	$3.3 \times 10^{-2}$	$2.3 \times 10^{-2}$

## Appendix B.8.2 Results

The adjusted  $R^2$  of the GAMM model was 73%. Figure 54 depicts boxplots of  $\log_{10}p_{ill}$  according type of aircraft (single-aisle/twin-aisle), gasper (open/closed) and heating (on/off). It shows a wider distribution of risks in the single-aisle aircraft compared to the twin-aisle aircraft. Table 27 summarizes the categorical fixed on  $\log_{10}p_{ill}$ . The categorical as well as the smoothed fixed effects were all highly significant. Generally, risks were reduced when the source wore a mask, the overall effect was highly significant and amounted to a risk reduction factor of 3.7 ( $10^{0.5733}$ ). Temperature and relative humidity also significantly affected risks. Generally, risks increased with increasing temperature and increasing humidity (Figure 55). Figure 55 also shows an initial faster decline of risk with increasing distance. In the single-aisle aircraft the smooth effect of angle suggests that the net transport of aerosols was more backwards and to the left, whereas in the twin-aisle aircraft this directional effect was less. During ground conditions, the overall effect of opening gaspers was an increase in risks by a factor of 1.5 that of heating the blankets that were covering the passengers to mimic body heat decreased risks by a factor of 1.7 (Table 27).

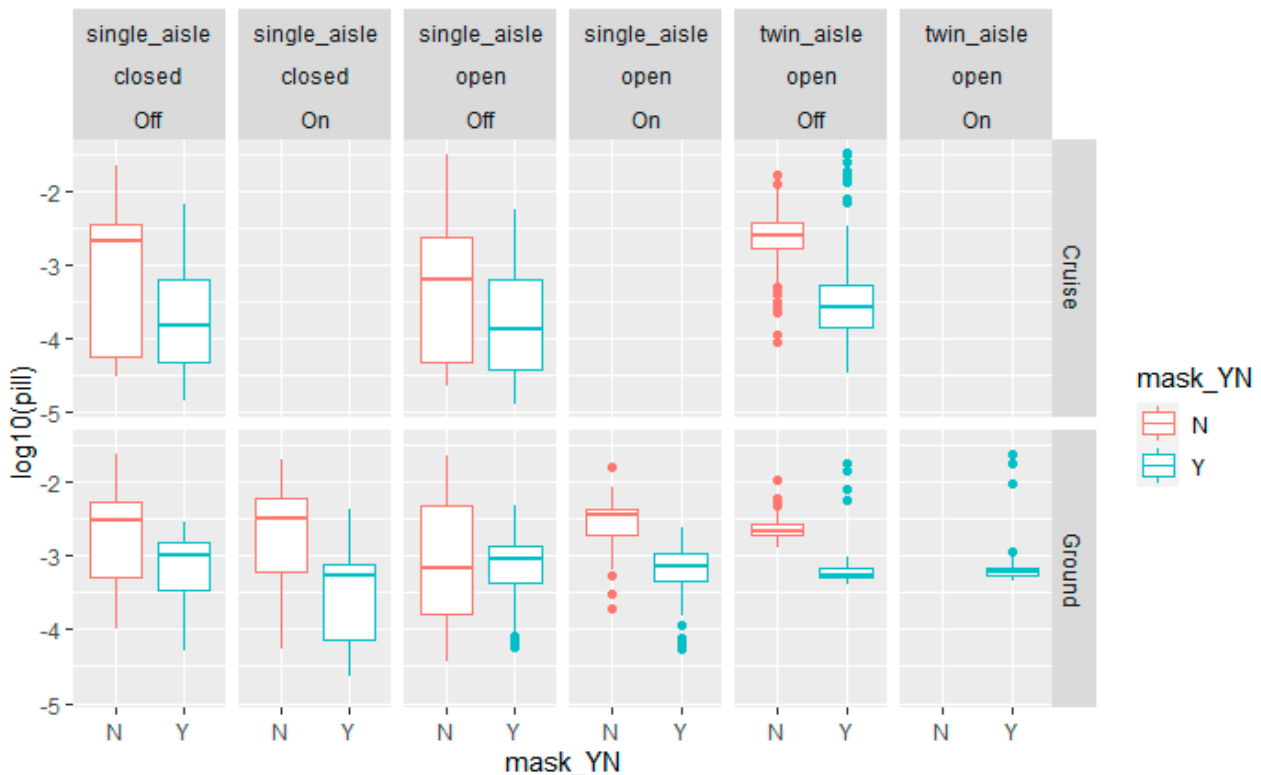


Figure 54: Boxplots of  $\log_{10}p_{ill}$  per exposed passenger according to type of aircraft (single-aisle/twin-aisle), gasper (open/closed) and heating (on/off). Middle line is median, boxes encompass the quartiles and the whiskers the 95% interval

Table 27: Categorical fixed effects

Term	Estimate	Std. Error	p.value
<b>All data without considering effects of gasper and heating.</b>			
mask yes	-0.5733	0.0143	0
twin_aisle aircraft	0.5099	0.0185	0
Ground	-1.6467	0.1514	0
twin_aisle aircraft * Ground	-0.0719	0.0280	0.01
<b>Data at ground conditions considering effects of gasper and heating.</b>			
mask_yes	-0.5837	0.0143	0
twin_aisle aircraft	0.3913	0.0189	0
gasper open	0.1739	0.0202	0
heating on	-0.2365	0.0267	0

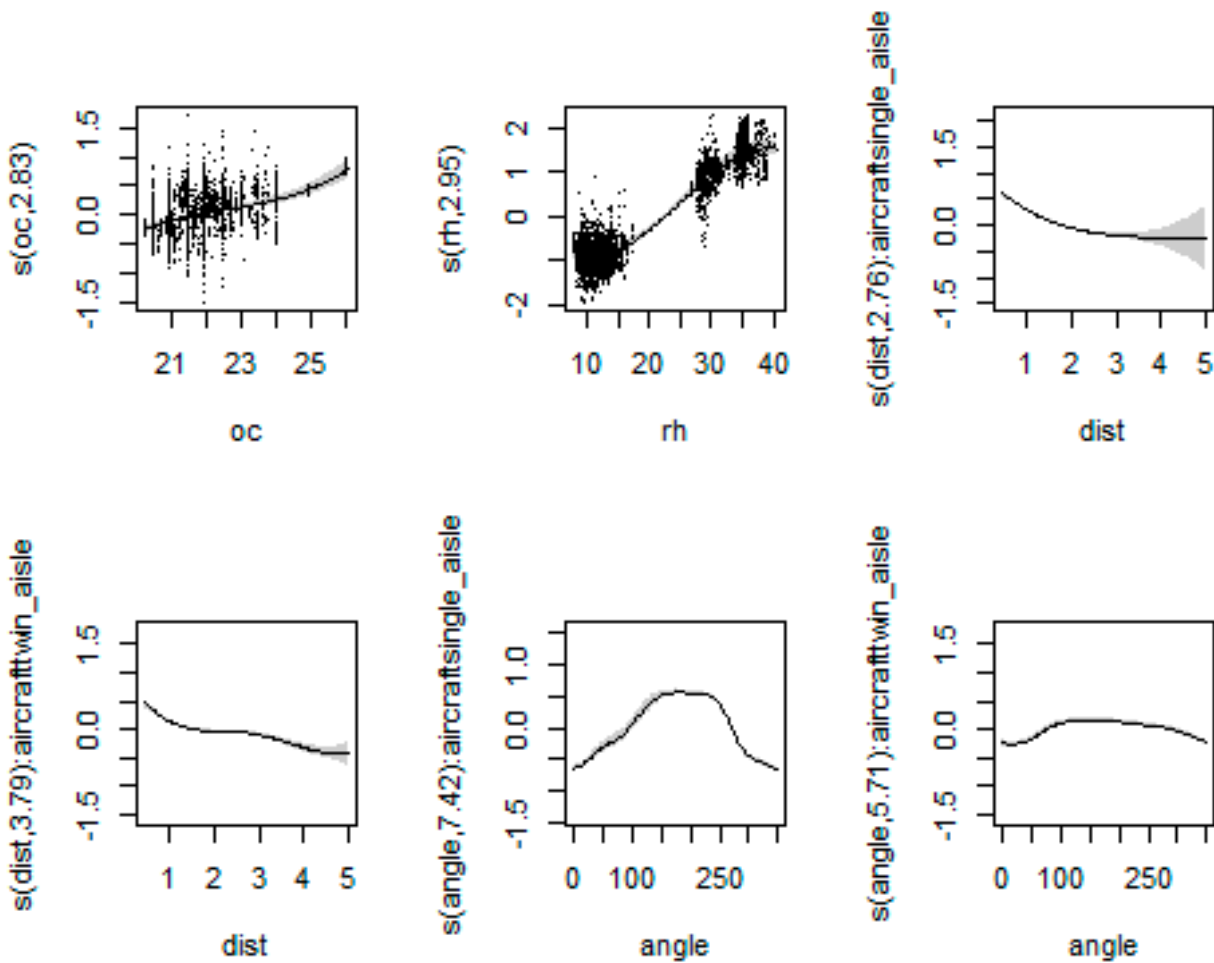


Figure 55: Splines plots (smooth effects) of temperature ( $oc$ ), relative humidity ( $rh$ ), distance from the index person ( $dist$ ) and the angle relative to the index person ( $0^\circ$  is towards the front,  $90^\circ$  is to the right). The y-axis the adjusted  $\log_{10}P_{ill}$ , which is a relative measure. A value of 0, implied no effect of temperature, relative humidity, distance or angle



Dedicated to innovation in aerospace

## Royal NLR - Netherlands Aerospace Centre

Royal NLR operates as an objective and independent research centre, working with its partners towards a better world tomorrow. As part of that, NLR offers innovative solutions and technical expertise, creating a strong competitive position for the commercial sector.

NLR has been a centre of expertise for over a century now, with a deep-seated desire to keep innovating. It is an organisation that works to achieve sustainable, safe, efficient and effective aerospace operations.

The combination of in-depth insights into customers' needs, multidisciplinary expertise and state-of-the-art research facilities makes rapid innovation possible. Both domestically and abroad, NLR plays a pivotal role between science, the commercial sector and governmental authorities, bridging the gap between fundamental research and practical applications. Additionally, NLR is one of the large technological institutes (GTIs) that have been collaborating over a decade in the Netherlands on applied research united in the TO2 federation.

From its main offices in Amsterdam and Marknesse plus two satellite offices, NLR helps to create a safe and sustainable society. It works with partners on numerous programmes in both civil aviation and defence, including work on complex composite structures for commercial aircraft and on goal-oriented use of the F-35 fighter. Additionally, NLR helps to achieve both Dutch and European goals and climate objectives in line with the Luchtvaartnota (Aviation Policy Document), the European Green Deal and Flightpath 2050, and by participating in programs such as Clean Sky and SESAR.

For more information visit: [www.nlr.org](http://www.nlr.org)

### Postal address

PO Box 90502  
1006 BM Amsterdam, The Netherlands  
e) [info@nlr.nl](mailto:info@nlr.nl) | [www.nlr.org](http://www.nlr.org)

### Royal NLR

Anthony Fokkerweg 2  
1059 CM Amsterdam, The Netherlands  
p) +31 88 511 3113

Voorsterweg 31  
8316 PR Marknesse, The Netherlands  
p) +31 88 511 4444